IOSUD – "DUNAREA DE JOS" UNIVERSITY OF GALAȚI

Doctoral School of Fundamental Sciences and Engineering

DOCTORAL THESIS
- SUMMARY -

OBTAINING AND CHARACTERIZING HETEROAROMATIC COMPOUNDS WITH BIOACTIVE PROPERTIES USING CLASSICAL METHODS OR THOSE BELONGING TO GREEN CHEMISTRY

PhD student,

Andreea Veronica DEDIU (BOTEZATU)

Scientific coordinator,

Prof. univ. Dr. chem. habil. Rodica Mihaela DINICĂ

Series C: Chemistry No. 8

GALAȚI

2023

IOSUD – "DUNAREA DE JOS" UNIVERSITY OF GALATI

Doctoral School of Fundamental Sciences and Engineering

UNIVERSITAS
GALATIENSIS

DOCTORAL THESIS

- SUMMARY -

OBTAINING AND CHARACTERIZING HETEROAROMATIC COMPOUNDS WITH BIOACTIVE PROPERTIES USING CLASSICAL METHODS OR THOSE BELONGING TO GREEN CHEMISTRY

PhD student,

Andreea Veronica DEDIU (BOTEZATU)

President	Prof. univ. Dr. Eng. Gabriela-Elena BAHRIM "Dunarea de Jos" University of Galati
Scientific coordinator	Prof. univ. Dr. Chem. habil. Rodica Mihaela DINICĂ "Dunarea de Jos" University of Galati
Scientific referents	Prof. univ. Dr. Chem. Sabine CHIERICI Grenoble Alpes University, Grenoble, France
	Prof. univ. Dr. Chem. habil Paizs CSABA "Babes-Bolyai" University, Cluj, Romania
	Prof. univ. Dr. Chem. Ionel MANGALAGIU, "Alexandru Ioan Cuza" University, Iasi, Romania

Series C: Chemistry No. 8

GALAŢI

2023

The series of doctoral theses publicly presented in UDJG starting with October 1, 2013 are:

Fundamental field ENGINEERING SCIENCES

Series I 1**: Biotechnology**
Series I 2**: Computers and Information Technology**
Series I 3: **Electrical Engineering**
Series I 4**: Industrial Engineering**
Series I 5: **Materials Engineering**
Series I 6**: Mechanical Engineering**
Series I 7**: Food Engineering**
Series I 8: **Systems Engineering**
Series I 9**: Engineering and Management in Agiculture and Rural Development**

Fundamental field SOCIAL SCIENCES

Seria E 1: **Economie**
Seria E 2: **Management**
Seria E 3: **Marketing**
SSEF Series: **Science of Sport and Physical Education**
SJ Series: **Law**

Fundamental field HUMANITIES

Series U 1: **Philology- English**
Series U 2: **Philology - Romanian**
U Series 3**: History**
Series U 4: **Philology - French**

Fundamental field MATHEMATICS AND NATURAL SCIENCES

C Series: **Chemistry**

Fundamental field BIOMEDICAL SCIENCES

M Series: **Medicine**
Series F: **Pharmacy**

ACKNOWLEDGEMENTS

„I am among those who believe that science has great beauty...
I was taught that the road to progress is neither fast nor easy." (Marie Curie)

The scientific foundation and elaboration of this doctoral thesis would have been impossible without the help, support, and guidance of special people who, through high professional degrees and dedication, contributed to my introduction to the wonderful world of scientific research in the field of chemistry and my professional training.

First of all, I am very grateful to my scientific mentor and supervisor, Prof. univ. dr. chem. habil. Rodica Mihaela Dinică, for her guidance, support, work, dedication, and encouragement at each stage of the doctoral internship that led to achieving this important goal in my professional activity. I thank you for the offered opportunity, for sharing knowledge, and valuable scientific advice, for supporting my research objectives, for integrating me into various scientific activities, but also for opening new research directions for the future.

With special consideration, I thank the members of the public support committee, Prof. univ. dr. chim. Sabine Chierici, Prof. univ. dr. chem. habil. Paizs Csaba, Prof. univ. dr. chem. Ionel Mangalagiu, and the president of the doctoral committee, Prof. dr. eng. Gabriela-Elena, Bahrim for the honor of reviewing this doctoral thesis.

Special consideration and acknowledgements to the members of the doctoral thesis guidance committee, Prof. dr. habil. Geta Cârâc, Assoc. prof. Bianca Furdui, and Prof. dr. eng. Gabriela-Elena Bahrim, for her patience, help, advice, evaluation of scientific content and elaboration of this doctoral thesis.

To my special colleagues during my PhD, Anna Busuioc, Mihaela Cudălbeanu, Maria Mihăilă and Fănică Bălănescu, I sincerely acknowledge for their trust, friendship, help and invaluable support. I am grateful for the wonderful laboratory group with great goals in research, mutual support, and experience of fruitful collaboration.

I express my gratitude to the entire team of the Faculty of Sciences and Environment for everything they taught me and for their continuous support in carrying out the experimental activities. Special thanks to the team of the Faculty of Food Science and Engineering for their support in conducting experimental research. Thanks to all the teams of "Dunarea de Jos" University with whom I had the honor to collaborate.

Also, thanks to all researchers and PhD students from French-speaking countries who have benefited from Eugen Ionescu (AUF) scholarships within the Department of Chemistry, Physics and Environment, for their collaboration and trust.

I thank project PN-III-P1-1.1-MC2019-1608 for the funding that made it possible to carry out the Research Internship at the Department of Molecular Pharmacochemistry (DPM), of the "Grenoble Alpes" University, Grenoble, France. Special thanks to the DPM team, especially Prof. dr. chem. Martine Demeunynck, for the opportunity to carry out the mobility internship and share knowledge that has been of real use to me in scientific research. Special gratitude for the help given in carrying out biological anticancer activities to Mrs.CS Fernanda Marques, "Centro de Ciências e Tecnologias Nuclears (C2TN), Instituto Superior Técnico", "Universidade de Lisboa", Portugal.

With great gratitude and love, I dedicate this thesis to the family members who were by my side, surrounded me with affection and supported me in every way. I thank my parents and sister who were very important to me and supported me unconditionally. I thank my husband and daughter, Daria, with whom I shared every moment of joy, fatigue, and success in recent years, who supported me with affection and patience.

Sincere thanks to everyone for their support during these beautiful years to complete this doctoral thesis!

To my teachers and mentors, respectfully,
To my family, with love,
Chem. Andreea Veronica DEDIU (BOTEZATU)

Content

INTRODUCTION

Compounds with a pyridine core have attracted attention for potential applications in various fields such as biochemistry, materials science, medicine or molecular biology, due to their different chemical structures, physical and electrical properties such as electrochromic or fluorescent [1,2].

Pyridine and its derivatives exhibit a wide range of biological activities, such as antitumor, antiparasitic, antimicrobial, anti-inflammatory, antidiabetic, antiviral, and antipyretic [3,4].

Although several synthetic routes have been developed to obtain these important compounds, most of them present many disadvantages such as expensive catalysts, toxic reagents and solvents, high temperatures, low reaction yields, or multiple steps in the synthetic process.

Therefore, due to the applications of compounds with a pyridine nucleus, a research direction of great interest is the development of new or improved synthesis methods for obtaining them, with various substrates and with better reaction yields.

Attention to environmental issues, such as pollution problems and the need for new sources of energy and raw materials, has increased significantly in recent years. Traditional industrial chemistry processes are usually focused on optimizing reaction efficiency and chemical yield. Due to increasingly stringent legislative regulations and growing awareness in the scientific community of the problems arising from the intensive production of toxic and polluting waste, it is now well-known that the production of waste and/or the use of hazardous chemicals must be taken into consideration when estimating the efficiency of a process.

About 30 years ago, a new approach to chemistry began to emerge, which is now called "green chemistry" and is characterized by the design of reaction products and processes that reduce or eliminate the use or generation of hazardous substances [5]. This perspective requires a prediction of environmental impact when designing a chemical compound or the process by which it will be manufactured on a large scale. In the context of *green chemistry*, new tools are being developed that harmoniously combine design, process, toxicology, and finished materials considerations with experimentally demonstrated examples of successful commercial process implementation.

Attempts are being made to develop methods that produce low amounts of waste, involve low energy consumption and low costs. The development of efficient catalytic systems and the use of alternative reaction media are powerful tools to achieve the goal of both economically and environmentally sustainable chemistry.

This PhD thesis describes some examples of how the use of an unconventional catalytic system coupled with suitable reaction media can provide a significant improvement in results along with a decrease in the risk of environmental pollution.

Incorporating *green chemistry* is essential for implementing sustainable and environmentally friendly processes, and this PhD thesis represents an important step in catalyzing this vision.

In this context, the doctoral thesis had as its main purpose the use of unconventional methods for the synthesis of nitrogen heterocyclic compounds and their comparison with classical methods, aiming at the evaluation of some of their biologically active properties.

The fulfilment of the main purpose of the doctoral thesis was achieved by pursuing the following specific scientific objectives:

- the development of new methods of synthesis, conventional and unconventional, of nitrogen heterocyclic compounds with structural diversity

(quaternary pyridinium salts, indolizines, pyridinium-indolizine hybrids, metal complexes);

- characterization of the structure of compounds synthesized by classical and non-conventional methods;

- evaluation of the toxicity of some studied compounds, from the class of quaternary pyridinium salts and the class of indolizines, on the germination of wheat seeds (*Triticum aestivum*);

- investigating the cytotoxicity of some indolizine compounds on the model microorganism, the yeast *Saccharomyces cerevisiae*, during the multiplication and alcoholic fermentation processes.

- investigation of some biologically active properties of heterocyclic compounds with nitrogen (quaternary pyridinium salts, indolizines, pyridinium-indolizine hybrids, metal complexes) such as antimicrobial, antioxidant, anticancer, antineurodegenerative and anti-inflammatory.

- *in silico* evaluation of some N-heterocyclic compounds against Alzheimer's disease by determining the intra-molecular interactions as well as the binding affinity to the target molecule.

The doctoral thesis is divided into **two main parts** which are structured in **ten chapters**. The first part of the doctoral thesis highlights the recent studies in the specialized literature on the development of new derivatives of pyridinium salts and indolizines through classical or unconventional reactions.

The first chapter provides a general introduction to the development of new derivatives of pyridinium salts and indolizines by classical or unconventional reactions. The chapter is focused on the description, according to literature data, of the obtaining reactions for these classes of compounds and the catalytic conditions used, being focused on general aspects, the most interesting and recent applications of catalysis in classical or non-conventional media. "Green chemistry" has been used in recent years for the synthesis of a variety of nitrogen heterocycles and contributions to this field are covered in this chapter.

The second chapter describes a wide range of practical applications of nitrogen heterocyclic compounds that vary according to their chemical structure. Quaternary pyridinium salts and indolizines are highlighted as pharmaceutical and biologically active molecules but also have applications in materials science, bioimaging, chemistry, food industry and medicine.

Classical synthesis reactions are widely used for various organic transformations, and **Chapter 3** deals with the various classical reactions in organic solvents applied in the synthesis of quaternary pyridinium salts, indolizine derivatives and pyridinium-indolizine hybrids in this PhD thesis. Also, a new method for the synthesis of metal complexes incorporating N-heterocyclic ylides is presented. The compounds obtained by classical syntheses are characterized by modern analysis techniques, such as elemental analysis, IR analysis, NMR and MS.

Catalytic conditions are of high importance in many organic reactions, and therefore a description of the effect of non-conventional reaction conditions, such as ultrasound or microwave assistance in obtaining quaternary pyridinium salts, is presented in **Chapter 4**.

Chapter 5 presents "green chemistry" synthesis methods by using biocatalysis with plant enzymes, pure (commercial) enzymes as well as the unconventional I_2/H_2O_2 catalytic system. The methods used for the purification and structural characterization of the indolizine derivatives are also presented.

Quaternary pyridinium salts and indolizine compounds show various medical, biological, pharmaceutical and food applications among others. To select a potential drug or

germicide, the target compounds must be non-toxic or have low toxicity to beneficial microorganisms, plants, animals and humans. In this context, in **Chapter 6**, the original results obtained from the evaluation of the toxicity of these compounds, in the case of their potential use as drugs, toxicity which was carried out on plants and model microorganisms, are presented.

The selection of molecules through modern techniques of analysis and evaluation of drug-target molecule interactions can offer important advantages in pharmaceutical chemistry and pharmacotherapy. Therefore, in the context of the difficulty of treating numerous conditions, **Chapter 7** deals with different methods of evaluating the biologically active potential of heterocyclic nitrogen compounds and the original results obtained. Considering the potential of bipyridinium salts, indolizines and pyridinium-indolizine hybrids as antioxidants and cholinesterase inhibitors, **Chapter 8** describes the evaluation of the factors involved in cholinesterase inhibition by molecular docking calculations with the most relevant hybrid molecules, as well as the influence of their structures on binding modes to target molecules.

Chapter 9 reveals the general conclusions and original elements of this PhD thesis. The obtained results led to the synthesis and structural characterization of heterocyclic nitrogen compounds with structural diversity through classical and unconventional methods, which could contribute to the complex process of identifying potential drugs or germicides for a wide range of practical applications. Finally, **Chapter 10** presents the dissemination of the results obtained in this doctoral thesis.

CHAPTER 3. Preparation of N-heterocyclic compounds by classical catalysis

3.1. Introduction

The synthesis of the studied compounds from this thesis (quaternary pyridinium salts, indolizines, metal complexes) was carried out starting from three bipyridine compounds (Figure 3.1).

4,4'-bipyridine   1,2-di(pyridin-4-yl)ethane   1,3-di(pyridin-4-yl)propane
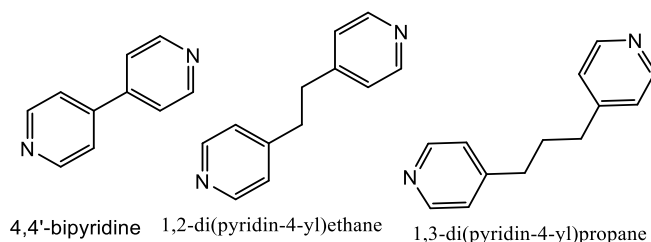
Figure 3.1. The chemical structure of bipyridine compounds used as starting reactants in synthesis reactions.

3.2. Specific scientific objectives

The specific scientific objective of this chapter was to synthesize heterocyclic nitrogen compounds (quaternary pyridinium salts, indolizines, pyridinium-indolizine hybrids, metal complexes) by conventional (classical) obtaining methods.

3.3. Synthesis of quaternary pyridinium salts

Quaternary pyridinium salts were conventionally prepared using methodology selected from the literature, with acetonitrile as the solvent, under reflux conditions by conventional heating and continuous stirring up to 48 h (Figure 3.3) [274,285]. Symmetrical bis-quaternary salts of bipyridinium S1a–e have been prepared using a conventional methodology reported in the literature [285], of 4,4'-bipyridyl and halogenated derivatives using a stoichiometric ratio 1:2 (Figure 3.4), in anhydrous acetonitrile at reflux. Bipyridinium bisquaternary salts S1a-e were obtained after 12-24 h of reaction with conventional heating to 80°C (Table 3.1). The

obtained ScPy were dried in the oven, stored in flasks at room temperature and used in subsequent analyses. The compounds obtained by chemical synthesis showed high yields (85-95% ± 1%) and high melting points (>300°C). The synthesis of bis-quaternary salts S2a-q was achieved by alkylation of 1,2-di(pyridine-4-yl)ethane with reactive halogenated reagents (Figure 3.5) in anhydrous acetonitrile by a conventional method reported in the literature [50,274].
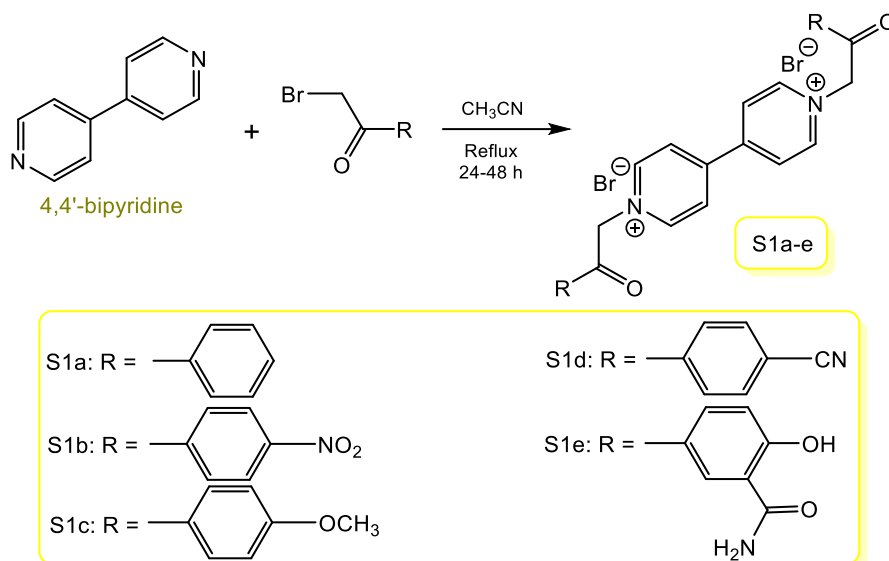
Figure 3.4. Conventional synthesis of bis-quaternary salts of bipyridinium S1a-e
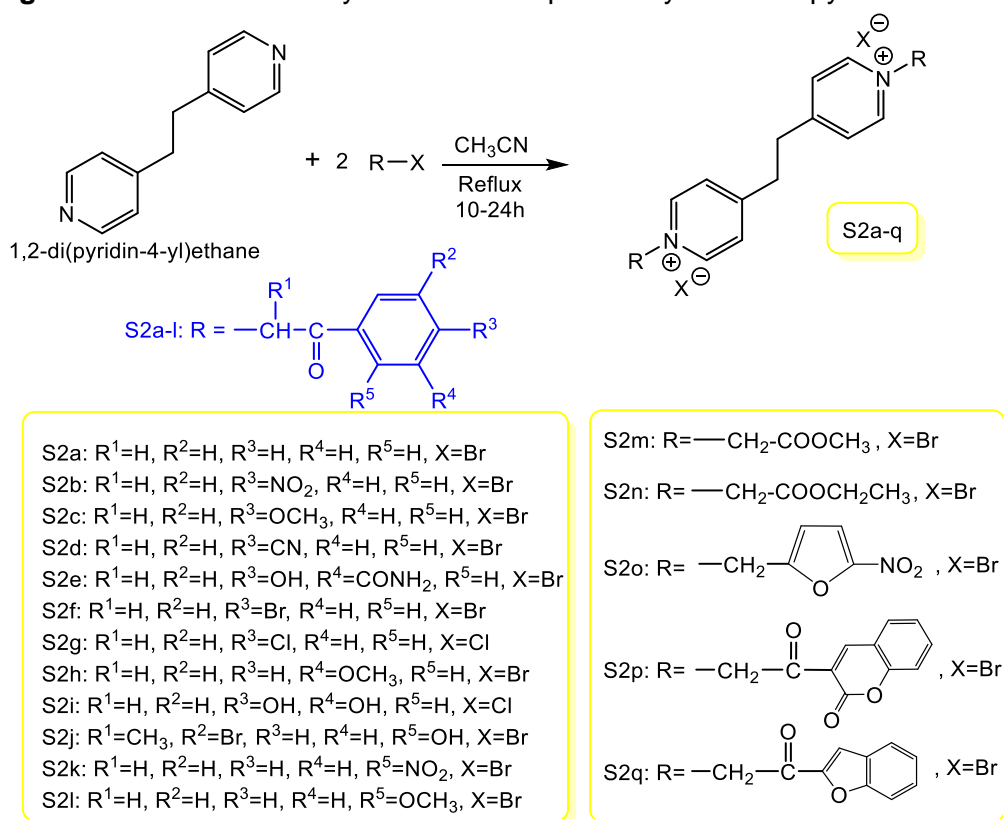
Figure 3.5. Conventional synthesis of bis-quaternary salts of bipyridinium S2a-q derived from 1,2-di(pyridine-4-yl)ethane

3.4. Synthesis of indolizine compounds

Pyridinium salts have the property of forming pyridinium ylides in a base medium, this property being important in the synthesis of other heterocyclic compounds by dipolar

cycloaddition reactions [36]. The indolizine compounds were prepared using the methodology shown in Figure 3.6, according to the classical synthesis methodology selected from the literature [22,36,279].

A series of indolizines has been prepared from 1 mmol bis-quaternary salt of bipyridinium (S1a-e) and 2 mmol of activated alkyne (ethyl propiolate). The reaction mixture was stirred continuously (500 rpm) and conventionally warmed (Figure 3.7).
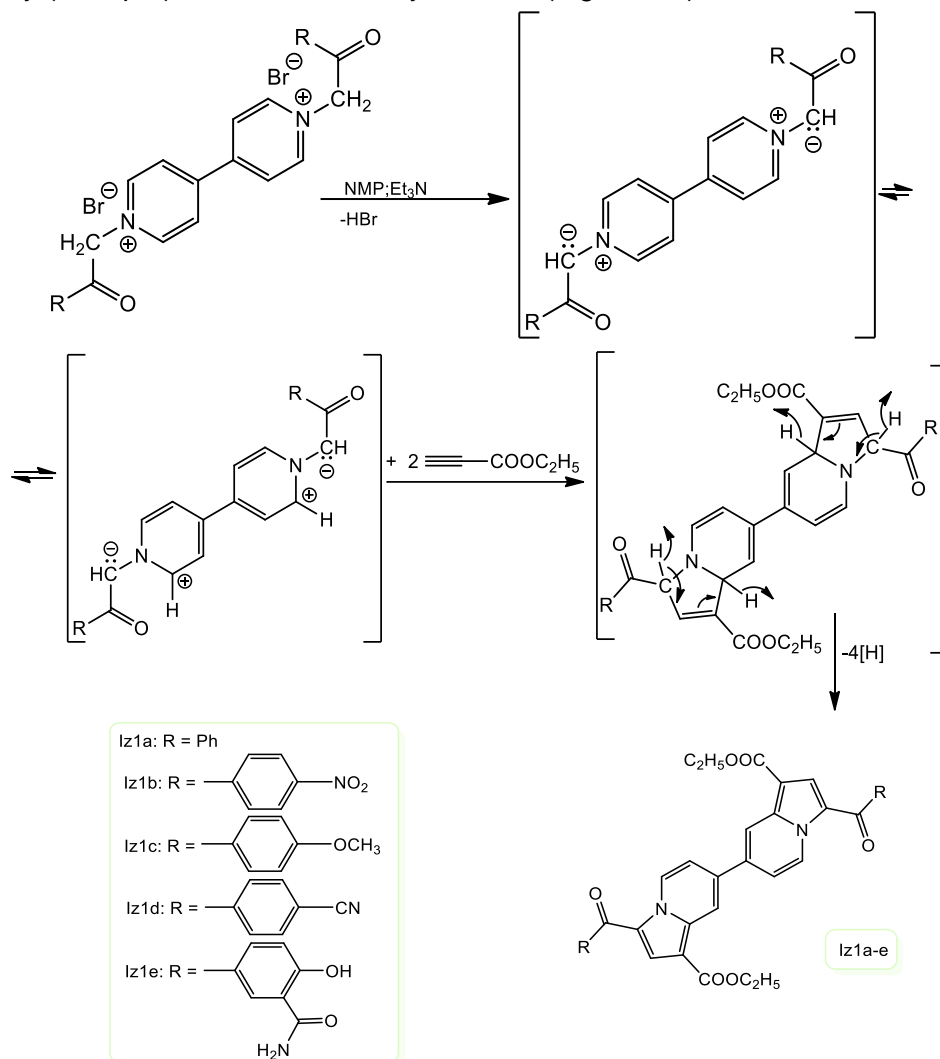
Figure 3.7. The general route of classical synthesis of bis-indolizines Iz1a-e from quaternary bipyridinium salts and the involved reaction mechanism

Another series of indolizine derivatives were generated from the reaction of 1 mmol of bipyridinium bis-quaternary salt (S2a-e) and 2 mmol of activated alkyne (ethyl propiolate), the reaction mixture was stirred continuously (500 rpm) for up to 24 hours and with conventional heating on the magnetic stirrer (Figure 3.8). The compounds were precipitated from the reaction medium with methanol, ethyl ether or water and then purified by recrystallization. Several non-symmetrical bipyridine monoindolizines have been prepared by methods already reported in the literature [287,351]. 4,4'-bipyridyl, 1,2-di(4-pyridyl)ethane and 1,3-bis(4-pyridyl)propane were used as substrates for the Iz1-f, Iz2-f, Iz-2g, Iz3-a and Iz3-b indolizines synthesis (Figure 3.9, Table 3.3). To prepare these compounds, 4,4'-bipyridine was first monoalkylated before cyclization with ethyl propiolate.
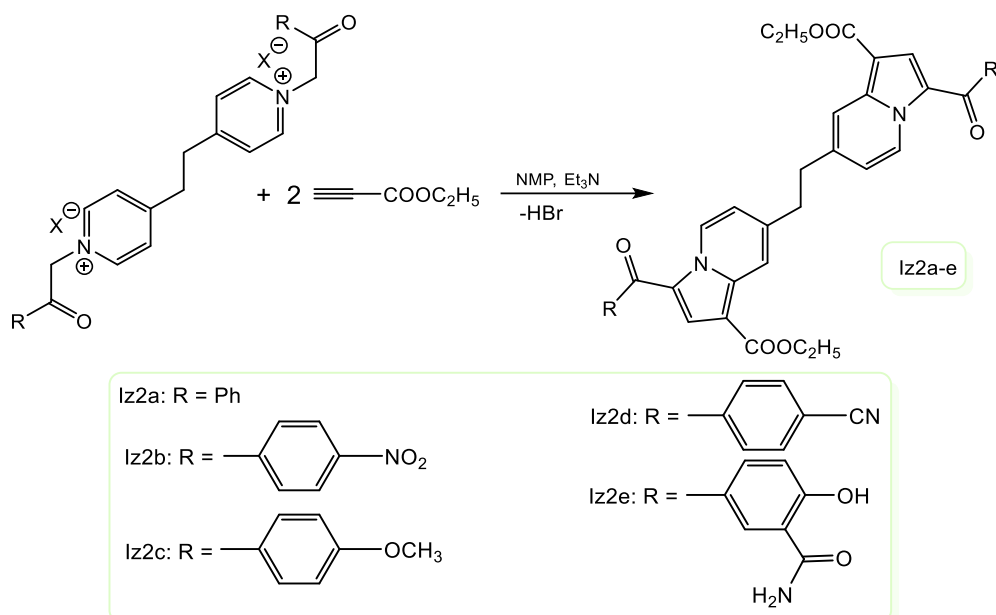
Figure 3.8. General route of classical synthesis of some bis- indolizines from ScPy derived from 1,2-di(pyridine-4-yl)ethane
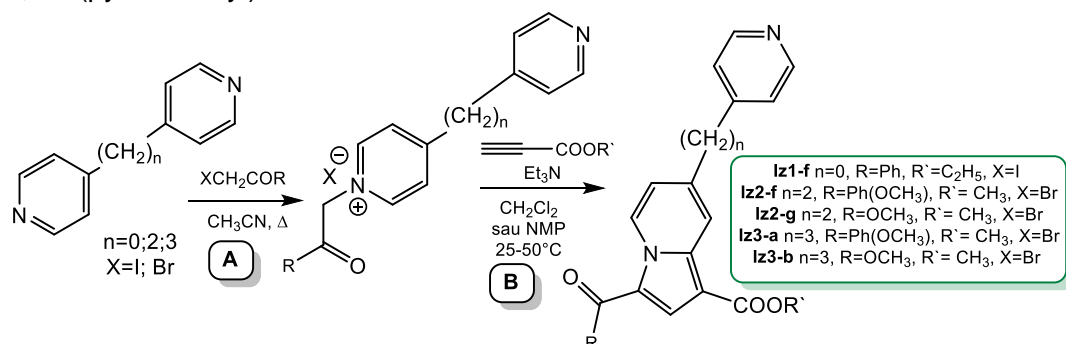
Figure 3.9. The general route of classical synthesis of mono-indolizines

3.5. Synthesis of N-alkylpyridinium-indolizine hybrids

To prepare several structurally diverse N-alkylpyridinium-indolizine hybrids (Iz-Py), the nature of both the original bipyridines and N-alkyl substitutes was varied. Two strategies were followed, both based on the formation of the indolizine nucleus by 1,3-dipole cycloaddition of alkynes with ylides formed *in situ* from appropriately substituted pyridine salts (Figure 3.10). As already reported [287,351] the compounds Iz-Py-1, Iz-Py-2 and Iz-Py-3 were obtained by controlled monomethylation of 4,4'-bipyridyl in acetone, followed by a second alkylation step with iodoacetophenone resulting in the unsymmetrical bispyridinium bis-alkylated salts, and then subjected to regioselective monocycloaddition with ethyl propiolate on the ylide-generating fragment (Figure 3.10.a). For the Iz-Py-1-Iz-Py-11 series, with 2 or 3 carbon atoms respectively between the two pyridine rings, the molecules differ mostly like the N-alkylpyridinium group (Figure 3.10.b). It has been experimentally found that the optimal synthesis protocol involves first generating the indolizine nucleus, and then quaternization of pyridinium-indolizine resulting from the use of various alkylating agents (Figure 3.11, Table 3.4). As already reported in the literature [287], the compounds Iz-Py-1, Iz-Py-2 and Iz-Py-3 were obtained by controlled monomethylation of 4,4'-bipyridine, followed by a second alkylation step with iodoacetophenone that generated the unsymmetrical bispyridinium bis-alkylated salts and then subjected to regioselective cycloadditions with ethyl propiolate on the ylide-forming fragment.
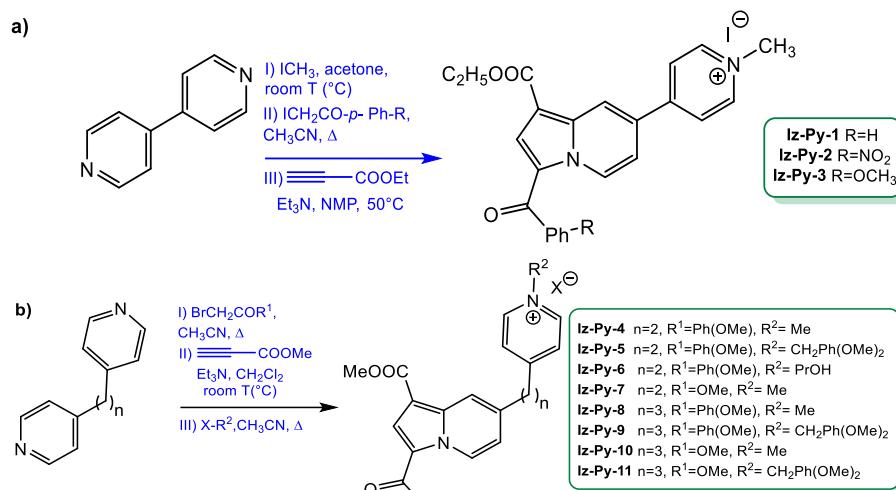
Figure 3.10. General routes of synthesis of a series of N-pyridinium-indolizine hybrids (**Iz-Py**)
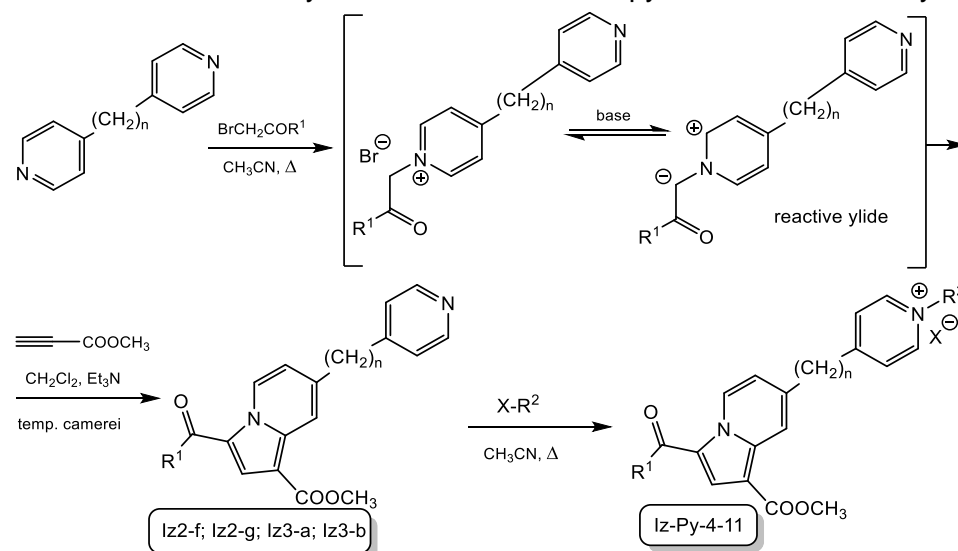
Figure 3.11. The general route of synthesis of N-alkylpyridinium-indolizine hybrids and the involved reaction mechanism

3.6. Synthesis of a new mixed lanthanum (III) complex incorporating a bipyridinium ylide

The proligand used for the synthesis of a mixed lanthanum(III) complex was the bis-quaternary salt of bipyridinium S1-a (Figure 3.12), which was prepared by the method described in subchapter **3.2** [50].
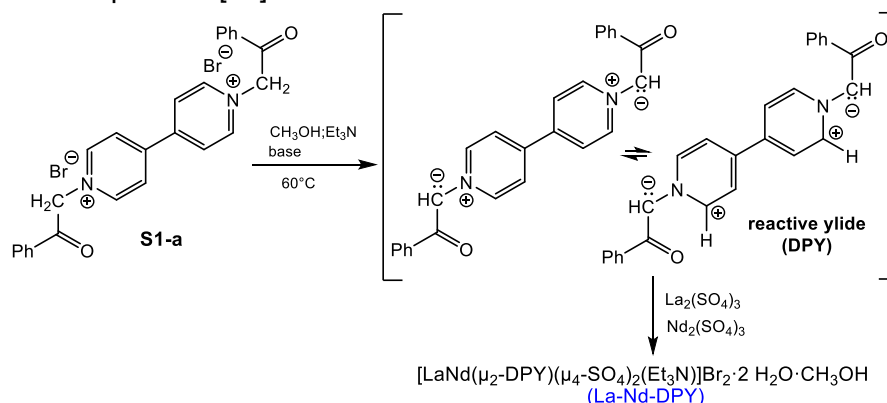
Figure 3.13. Synthesis of the mixed complex Ln (III) – ylide (La-Nd-DPY) from quaternary bipyridinium salt S1-a and the mechanism of generating reactive ylide in the basic medium

A mixed metal complex of La and Nd was synthesized by dissolving 0.5 mmol S1-a in a round-bottomed flask, adding 0.33 mmol lanthanum (III) sulfate to 20 mL of methanol, under heating at 60°C and stirring (300 rpm). Further, 1 mL triethylamine (Et₃N) was added and a colour shift from light yellow to purple was observed, the color turn being specific to the corresponding ylide formation reaction (Figure 3.13).

3.8. Results and discussion

Characterization of quaternary pyridinium salts

Bipyridinium bis-quaternary salts S1a-e and S2a-q have been synthesized according to the methodology presented in the literature [36,50,192,274], and the experimental analyses carried out confirmed their structure. These compounds were synthesized in anhydrous acetonitrile by conventional heating at reflux, under continuous stirring for 12-48 h.

The chemical structure and purity of the synthesized compounds have been demonstrated by elemental, spectrophotometric and chromatographic analyses.

The FT-IR spectra of the synthesized compounds have been investigated in the 4.000–400 cm^{-1} frequency range, and the observed bands confirm the proposed chemical structures (Figure 3.14 and Annexes A1–A12). In the FT-IR spectra of newly synthesized compounds S1d, S1e, S2d and S2e, bond-specific bands of the proposed chemical structures were also identified (Figure 3.14.a-d). The synthesized compounds were also characterized by proton and carbon NMR spectra, the signals specific to protons and carbon atoms in the chemical structures of the synthesized compounds being attributed according to data from the specialized literature [354–357].

Synthesis of indolizine compounds

The symmetrical bis-indolizines Iz1a-c and Iz2a-c were prepared from the corresponding quaternary salts of 4,4'-bipyridinium and 1,2-di(4-pyridinium) ethane. The synthesis reactions were based on the formation of the indolizine ring by 1,3-dipole cycloaddition of alkynes with *in situ* formed ylides from appropriately substituted pyridinium salts.

The chemical structure and purity of the synthesized compounds have been demonstrated by elemental, spectrophotometric and chromatographic analyses. FT-IR spectra of synthesized compounds Iz1a-e and Iz2a-e have been investigated in the 400–4.000 cm^{-1} frequency range, and the bands in the spectra obtained confirm the proposed chemical structures. The FTIR spectra of Iz1a-c compounds are shown in Figure 5.9 and for Iz1d-e and Iz2a-e compounds in Annexes A13-A19. The indolizine structures were further confirmed by ^{1}H-NMR.

Structural characterization of N-alkylpyridinium-indolizine hybrids

In this thesis, several N-alkylpyridinium-indolizine hybrids with structural diversity were prepared by varying the nature of both the original bipyridine and N-alkyl substituents. Two strategies were followed, both based on the formation of the indolizine ring by 1,3-dipole cycloaddition of alkynes with *in situ* formed ylides from appropriately substituted pyridinium salts. As already reported in the literature, compounds Iz-Py-1, Iz-Py-2 and Iz-Py-3 were obtained by controlled monomethylation of 4,4'-bipyridine, followed by a second alkylation step with iodoacetophenone that generated the unsymmetrical bispyridinium bis-alkylated salts, and then subjected to regioselective monocycloaddition with ethyl propiolate on the ylide-forming fragment. To prepare the pyridine analogue Iz1-f, 4,4'-bipyridine was first alkylated with iodoacetophenone before cyclization with ethyl propiolate.

The resulting monoindolizines of indolizinyl-pyridine type, Iz2-f, Iz-2g, Iz3-a and Iz3-b were isolated with yields of 12-51%. The final reaction step with various alkylating agents was performed in CH₃CN to result in pyridinium-indolizine salts Iz-Py-4-Iz-Py11 with good to excellent yields (50-100%). Three of the indolizinyl-pyridine intermediates, Iz2-g, Iz3-a, and

Iz3-b, were selected for biological evaluation as neutral analogues. The compounds showed high purity, as assessed by spectrophotometric, chromatographic, and elemental analyses, and were used without further purification. ^{1}H and ^{13}C NMR spectra are collected in Annexes A47-A71.

Synthesis of a mixed lanthanum (III) complex incorporating a bipyridinium ylide

In a recent study, sulfates of Ln(III) (Ln = La, Nd) to synthesize two new Ln(III) binuclear homo-metallic complexes incorporating a bipyridinium ylide [374]. To provide more applicative valences to some N-heterocyclic ligands, it was aimed in this thesis to create new coordination species containing both viologen and lanthanide compounds, as well as to evaluate their biological properties. The synthesis, characterization, and biological properties of the new mixed Ln (III) complex were carried out to obtain a complex with improved potential as an anticancer agent.

The new mixed-use complex of LN (III) was obtained with a yield of 60%. La-Nd-DPY has been isolated as a violet powder, stable in the presence of air and moisture, and soluble in DMSO and DMF, poorly soluble in alcohols, acetone, acetonitrile, and water. X-ray diffraction analysis on powder (PXRD- Eng. „Powder X-ray diffraction") revealed the amorphous nature of the complex. PXRD experimental models for both complex and initial compounds, recorded for comparative purposes in the 2θ = 15-90° range, are shown in Figure 3.17. However, various characterization tools such as Fourier transform infrared spectroscopy (FT-IR), elemental analysis, electrospray ionization mass spectrometry (ESI-MS), UV-Vis spectroscopy and thermogravimetric analysis (TGA) were used to propose the structure for La-Nd-DPY. Elemental analysis led to the hypothesis of the stoichiometric formula of the newly obtained complex, as being of the type $[LaNd(\mu_2\text{-}DPY)(\mu_4\text{-}SO_4)_2(Et_3N)]Br_2\cdot 2H_2O\cdot CH_3OH$.
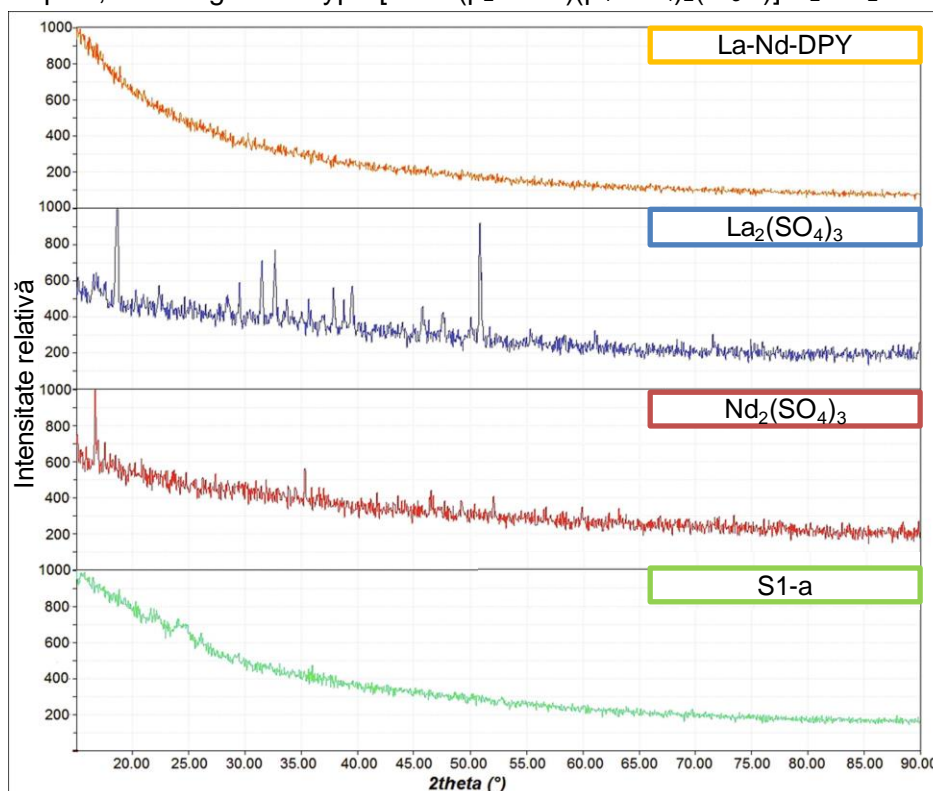
Figure 3.17. X-ray diffractograms on powder for samples indicated in the range 2θ=15-90°. La-Nd-DPY (orange), sulphate of La (III) (blue), sulphate of Nd (III) (red) and S1-a (green)

The IR spectrum of La-Nd-DPY mixed complex (Figure 3.18) shows weak and medium absorption bands in the region 1.640–1.440 cm^{-1}, which are attributed to the stretch vibrations of double bonds C=C and C=N of phenyl and pyridine structures respectively, in the structure of the ylide [41].

Thermogravimetric analysis (TGA) was used to assess the thermal stability of the obtained mixed complex Ln (III) and the main mass losses recorded when heating.

Analysis by liquid chromatography coupled with mass spectrometry (LC-MS) allowed the identification of fragments from the analyzed complex, with the appearance of intense characteristic peaks in the range 0–500 (m/z), corresponding to ylide structure, and less intense peaks after m/z 500, corresponding to lanthanide-based fragments (Figure 3.21, Table 3.5).
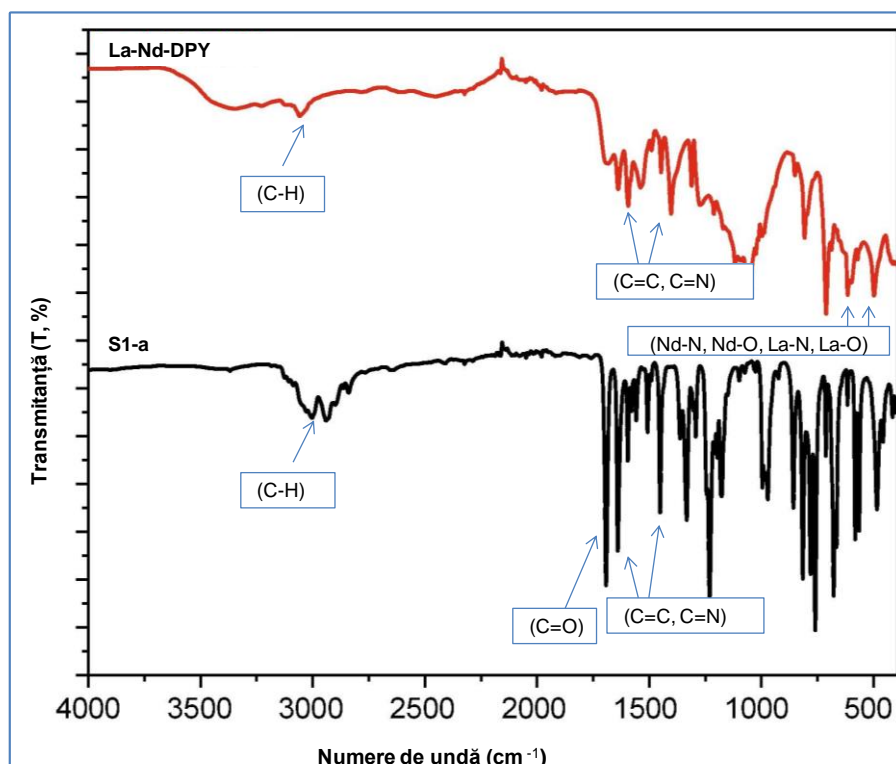
Figura 3.18. Overlay of IR spectra of quaternary bipyridinium salt S1-a (black) and La-Nd-DPY mixed complex (red)

All the results of the structural analyses described above allowed the proposal of a structural model for the La-Nd-DPY mixed complex in the form of a coordination polymer, whose monomer units consist of an organic N-heterocyclic DPY ligand (the ylide of compound S1-a), an ion La (III), an ion Nd(III), two sulfate groups and one triethylamine molecule (Figure 3.22.).
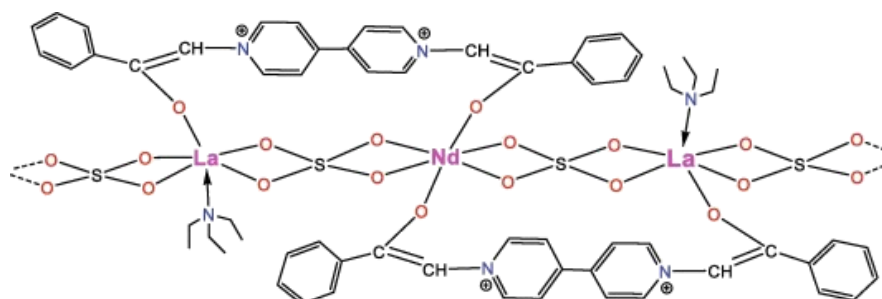
Figure 3.22. Proposed 1-D polymer structure for La-Nd-DPY

A literature review has not identified any other studies describing a linear chain model constructed with alternating Ln (III) ions joined by sulfate groups in a bischelated way. On the other hand, the six coordination of such Ln(III) ions, although still relatively rarely identified, join the group of lanthanide-based complexes presented so far in the literature [374,384–387]. Higher coordination requirements of ions La (III) and Nd (III) may be the probable cause for the polymer complex La-Nd-DPY.

The redox behavior of the La-Nd-DPY complex was evaluated by cyclic voltammetry experiments (CV), both in methanol (pH = 7.3) and DMSO (pH = 10.4), which reveals that the oxidation/reduction potentials of the mixed complex are shifted towards positive or negative values, being assigned to the corresponding ligand (Figure 3.23).
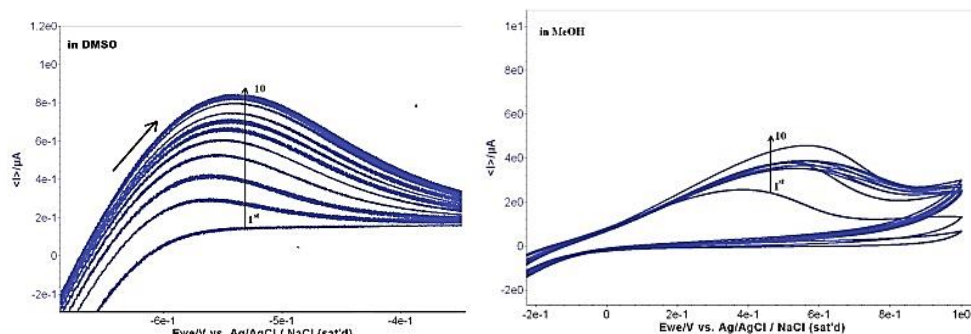
Figure 3.23. Cyclic voltammograms of the mixed Ln complex 10^{-6}M in DMSO and MeOH solutions, on the platinum working electrode; E = ±1 V/$_{EAg/AgClsat}$; scan rate 50 mVs^{-1}; 10 consecutive voltametric cycles.

The redox potentials assessed are within the relevant and accessible biological range. In cells that are proliferating, the reduction potential is approximately -0,24 V [53], while inside the tumor it can be up to 100 mV smaller. This means that biological reducing agents, i.e., redox group GSSG/2GSH or ascorbic acid, can reduce synthesized compounds [54], according to the results obtained, the process of biological reduction of the synthesized mixed complex can be carried out.

Scanning electron microscopy (SEM) showed that the new mixed complex develops in a morphology similar to the fibrillar network quite uniform and homogeneous, with porous characteristics, as can be seen at higher magnifications (Figure 3.24 A, B, C and D). This type of morphology is thus different from the homo-metallic La-DPY and Nd-DPY complexes, which exhibited multiform crystalline structures and morphologies (elongated micro- and nanoparticles, aggregate micro- and nanoparticles) [27]. EDX analysis, obtained at a selected point in the image with the highest magnification, confirmed the presence of both lanthanum ions (III) in the mixed complex.
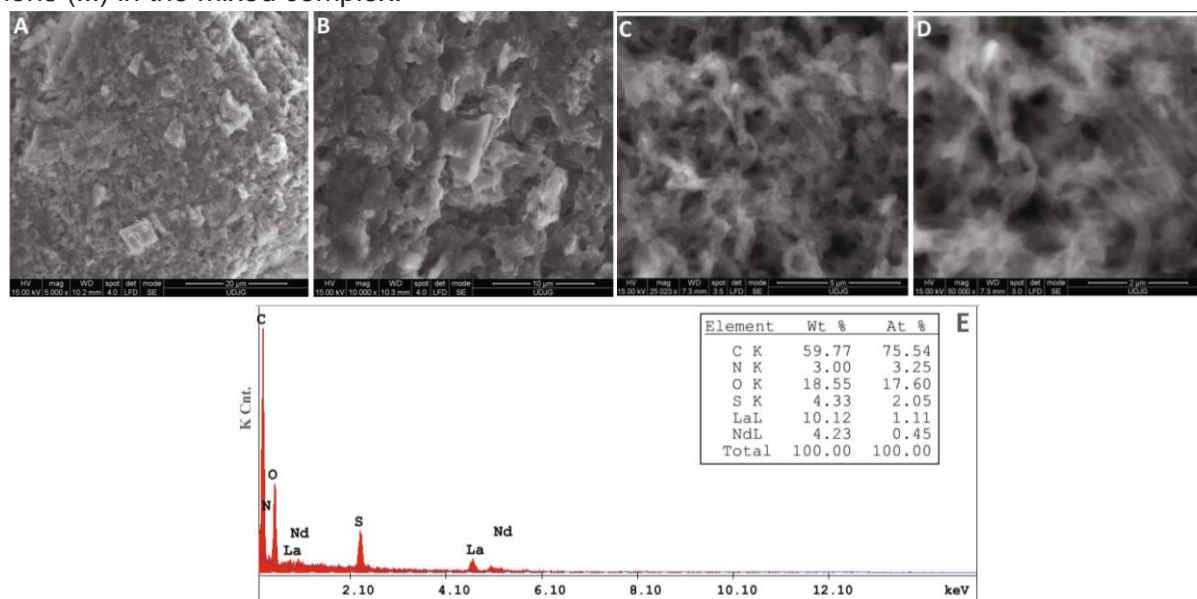
Figure 3.24. A-D: SEM images of the complex La-Nd-DPY; E: EDX spectrum obtained at a selected point from the 50,000x magnification image, together with elemental composition.

CHAPTER 4. Generation of symmetric bipyridinium quaternary salts by unconventional catalysis

4.2. Specific scientific objectives

The specific scientific objective of the research presented in this chapter was to generate heterocyclic compounds with nitrogen (bisquaternary salts of bipyridinium) by unconventional methods belonging to *green chemistry*.

4.4. Results and discussion

With conventional methods, it took 12 to 24 hours for the complete alkylation of 1,2-di(4-pyridyl)ethane with reactive halogenated derivatives in anhydrous solvent and reflux conditions. Irradiation with MW or US reduced reaction time and reaction products from the class of quaternary pyridinium salts were obtained in a much shorter time (a few minutes).

In Table 4.1, the results obtained in the classical synthesis and by the two *green methods* are compared, the yields obtained thus making obvious the remarkable advantage of these *unconventional* alternatives in terms of saving time, solvents and increasing reaction yield. *Green synthetic* alternatives successfully led to bisquaternary bipyridinium salts with very good yields, close to those of the classical method. In the classical method of synthesis, a much larger volume of solvent was used (150 acetonitrile anhydrous equivalents). In reactions with a synthesis efficiency of less than 90%, unreacted starting compounds were identified by thin-layer chromatography, but due to their solubility in the reaction medium, they were removed by washing the precipitate obtained with hot anhydrous acetonitrile. MW or US-assisted reactions were monitored after 5, 10 and 15 minutes.

**Table 4.1.** Comparative yields and reaction conditions for classical and unconventional synthesis, respectively

ScPy	Classic heating			Irradiation with MW (300 W)			Irradiation with US (35 Hz)		
	Time (min)	T (°C)	η (%)	Time (min)	T (°C)	η (%)	Time (min)	T (°C)	η (%)
S2a	1440	80.0	92	5-10	95.0	95	60	60.0	90
S2b	1440	80.0	95	5-10	95.0	95	60	60.0	95
S2c	1440	80.0	94	5-10	95.0	95	60	60.0	95
S2f	1.40	80.0	88	5-10	95.0	90	60	60.0	90
S2g	1440	80.0	94	5-10	95.0	94	60	60.0	95
S2h	1440	80.0	90	5-10	95.0	93	60	60.0	90
S2i	1440	80.0	82	5-10	95.0	85	60	60.0	85
S2j	1440	80.0	81	5-10	95.0	83	60	60.0	90
S2k	720	80.0	93	5-10	95.0	95	60	60.0	90
S2l	720	80.0	92	5-10	95.0	95	60	60.0	90
S2m	1440	80.0	98	5-10	95.0	98	60	60.0	98
S2n	1440	80.0	85	5-10	95.0	88	60	60.0	86
S2o	1440	80.0	85	5-10	95.0	87	60	60.0	90
S2p	720	80.0	90	5-10	95.0	92	60	60.0	93
S2q	720	80.0	76	5-10	95.0	77	60	60.0	80

It has been found that an increase in reaction time for MW or US assisted reactions no longer leads to an increase in reaction efficiency. Therefore, the optimal time frame of 5-10 minutes was considered, which was the best approach for the synthesis of such ScPy. It is important to underline that MW irradiation was particularly efficient, with only a few minutes required to obtain the desired products with excellent yields, while several hours of conventional heating in classical conditions would be required to generate the same results.

Also, US irradiation was effective, yields were excellent in all cases analyzed, and reaction times were reduced from 12-24 hours under conventional heating to just one hour of US-assisted synthesis, these results are also similar to those reported in the literature for other classes of compounds [149,400].

According to literature data, MW or US assisted syntheses in this thesis are proposed for the first time as methods for obtaining bisquaternary bis-pyridinium salts S2a-c and S2f-q, thus paving the way for the generation of ScPy by *green* methods with high yields. The infrared (FT-IR) spectra of the compounds obtained were analyzed in a frequency range between 4,000 and 400 cm^{-1}, and the identified bands confirmed the proposed chemical structures by comparison with the data obtained for classical synthesis control compounds (Figure 4.3). The synthesized compounds showed in the NMR spectra signals specific to protons and carbon atoms from the chemical structures of the proposed compounds, assigned according to data from the specialized literature [354–357] (Figure 4.4.a). ^{13}C-RMN spectra also confirmed the chemical structures of ScPy (Figure 4.4.b). The NMR spectra corresponding to the compounds are collected in Annexes A20 to A46.

(a)

(b)

(c)
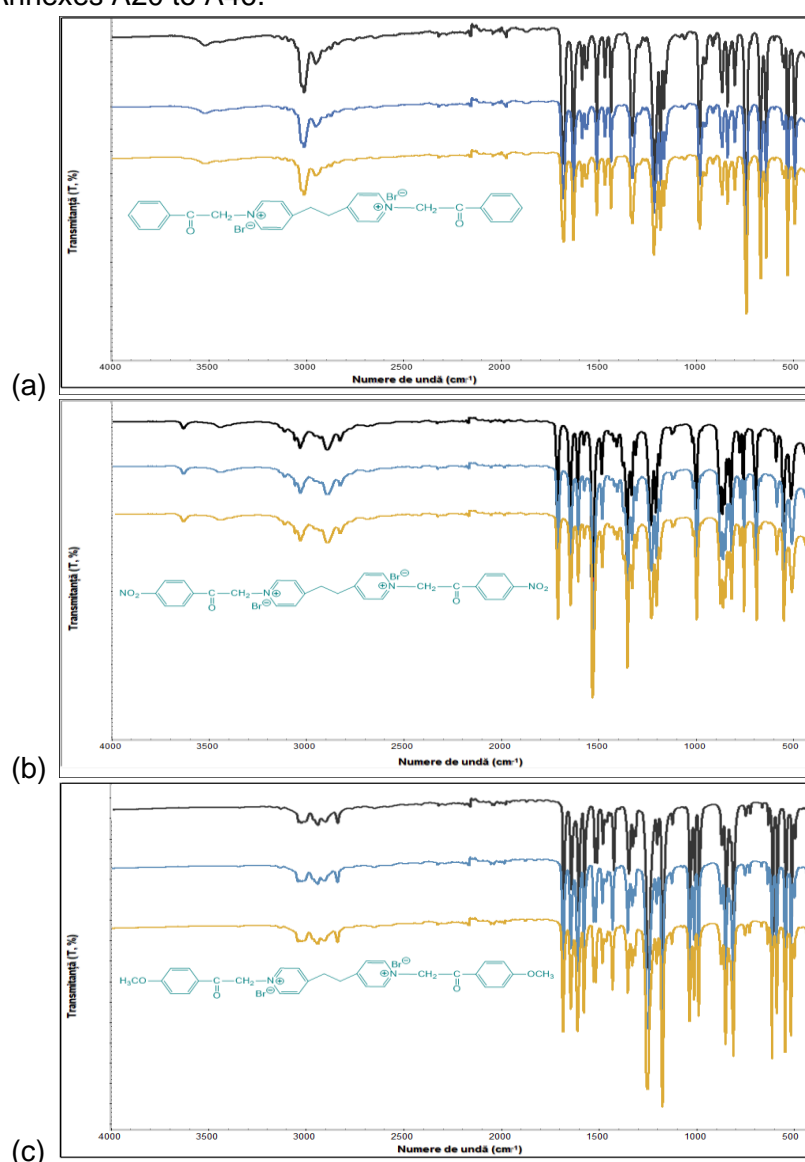
Figure 4.3. FTIR overlay spectrum of a) S2a, b) S2b, c) S2c: black-classical synthesis, brown-synthesis with US, blue-synthesis with MW.
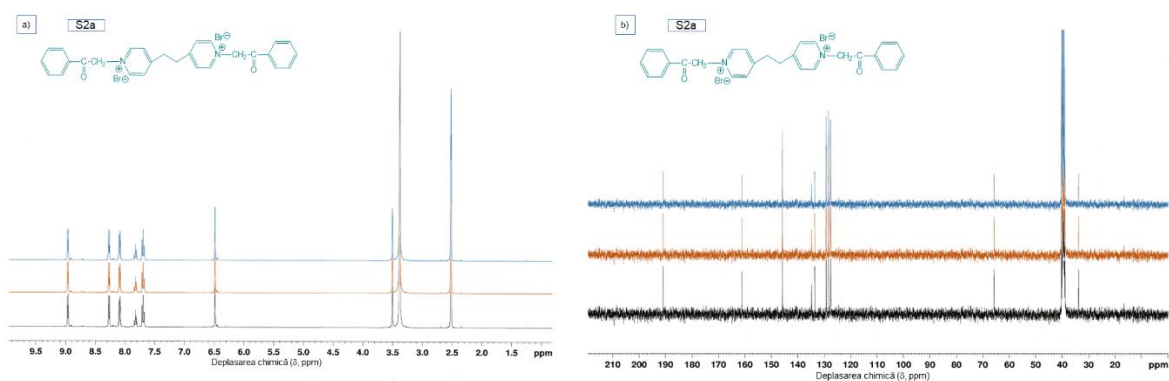
Figure 4.4. Spectrum overlay a) ¹H-RMN, b) ¹³C-RMN for compound S2a: black-classical synthesis, brown-assisted synthesis with US, blue-assisted synthesis with MW.

CHAPTER 5. Generation of symmetrical bis-indolizines by unconventional catalysis

5.2. Specific scientific objectives

The specific scientific objective of the research presented in this chapter was to generate indolizine derivatives by unconventional obtaining methods, belonging to "green chemistry".

5.7. Results and discussion

Optimization of reaction conditions for the biocatalysis process

To optimize the efficiency of the synthesis process, the influence of biocatalytic medium and experimental conditions in the synthesis of indolizine compounds was investigated (Table 5.1). The first experiments were carried out with 1 g of horseradish roots in phosphate buffer solution at pH = 6.0, with continuous stirring, at room temperature and for 168 hours.

Table 5.1. Optimization of reaction conditions for Iz1a compound synthesis

Vegetable source of enzyme catalyst	Plant weight (g)	pH of buffer solution	20 ±3°C	25 ±3°C	37 ±3°C
			Time (Hours)		
Horseradish root	0.5	6.0	>120	>120	>120
	0.5	7.0	>120	>120	>120
	0.5	8.0	>120	>120	>120
	1.0	6.0	>120	>120	>120
	1.0	7.0	>120	>120	>120
	1.0	8.0	>120	>120	>120
	1.5	6.0	117	112	113
	1.5	7.0	114	106	109
	1.5	8.0	119	124	110
	2.0	6.0	96	88	94
	2.0	7.0	87	84	86
	2.0	8.0	93	87	88

By monitoring the reaction with thin-layer chromatography, it was found that the reactants were consumed over time and the final reaction product (Iz1a) was obtained in a reaction time of over 120 hours. Additional optimization experiments were conducted for the synthesis of the compound Iz1a, and the results are presented in Table 5.1. The most promising results were

obtained at pH = 7.0 and with 2 g of plant material when the reaction product was obtained with 84% yield at room temperature.

The synthesis of indolizine derivatives by enzymatic biocatalysis

The investigation of catalytic conditions was extended to 7 plants evaluated in this thesis and also to the use of various reactive halogenated derivatives (Figure 5.6). Indolizine derivatives were also obtained by multicomponent, single-step reactions catalyzed by pure horseradish peroxidase (POD-HRP). This synthesis process resulted in the synthesis of desired compounds as solid powders with yields of 40-76%.

Following biocatalytic processes with enzymes extracted from fresh plant products, as well as with the pure enzyme POD-HRP, appropriate reaction products with moderate to very good yields (45%–86%) were obtained. The proposed reaction mechanism for oxidizing enzyme-catalyzed syntheses involves the intermediate formation of pyridinium cations from pyridine derivatives and reactive halogenated derivatives (Figure 5.7).

Free radical products generated by oxidases are highly reactive species that can, in some cases, alter the heme group of the enzyme [421]. For example, for horseradish peroxidase (HRP), substrates for which this type of reaction has been observed according to literature data are alkyl- and aryl hydrazine, nitromethane or cyclopropanone hydrate. Radicals with low reactivity can be added to vinyl groups in the structure of heme peroxidase, these changes in the protein heme are also generated in some cases by oxidation products formed by peroxidases when oxidizing halide ions. Therefore, the oxidation of bromide by HRP could involve the formation of HOBr and its addition as HOBr to vinyl groups in heme oxidases [423].
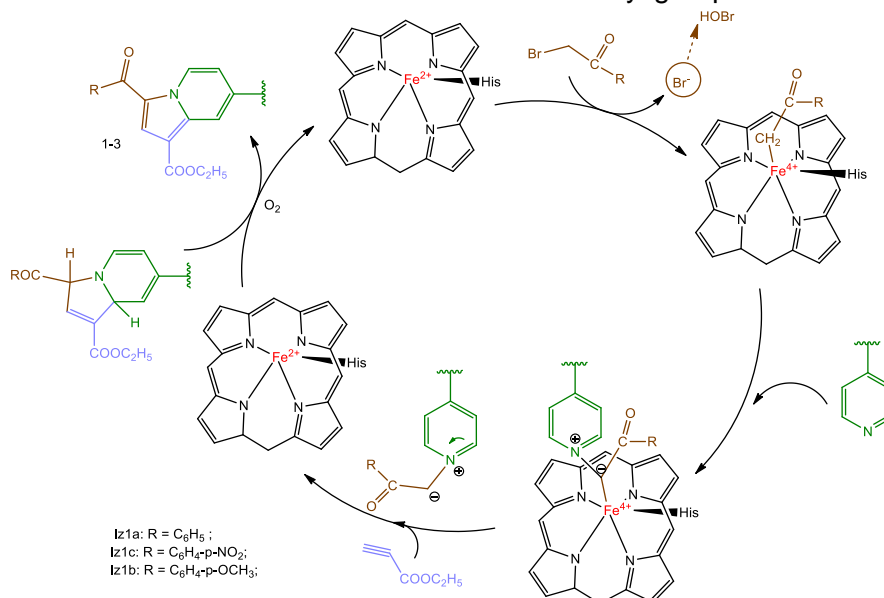
Figure 5.7. Proposed mechanism for the conversion of reactants to intermediate compounds and then to indolizine derivatives, promoted by enzymatic catalysts from plant sources.

Further, the research was expanded by testing six other local plants. The reactions were carried out by cascade biocatalysis, with a complex enzyme system from whole tissues of fresh plants and obtaining reaction products with good yields (45-86%). These methods have been investigated to minimize the number of unwanted by-products and to avoid the use of toxic solvents. After separation and purification of the reaction products, it was found that the synthesized bis-indolizines led to the expected structures (Figure 5.9, Figure 5.10), the results obtained being consistent with those of the control bis-indolizines previously obtained by classical chemical synthesis [375], presented in Chapter 3. Comparing reaction conditions in classical and biocatalyzed synthesis and yields in final products, it was found that the use of multi-enzyme systems to catalyze bis-indolizine reactions was the most effective in terms of *green chemistry* from the studied methods (Table 5.2).

19

Obţinerea şi caracterizarea unor compuşi heteroaromatici cu proprietăţi bioactive utilizând metode clasice sau aparţinând chimiei verzi

DEDIU (BOTEZATU) Andreea Veronica
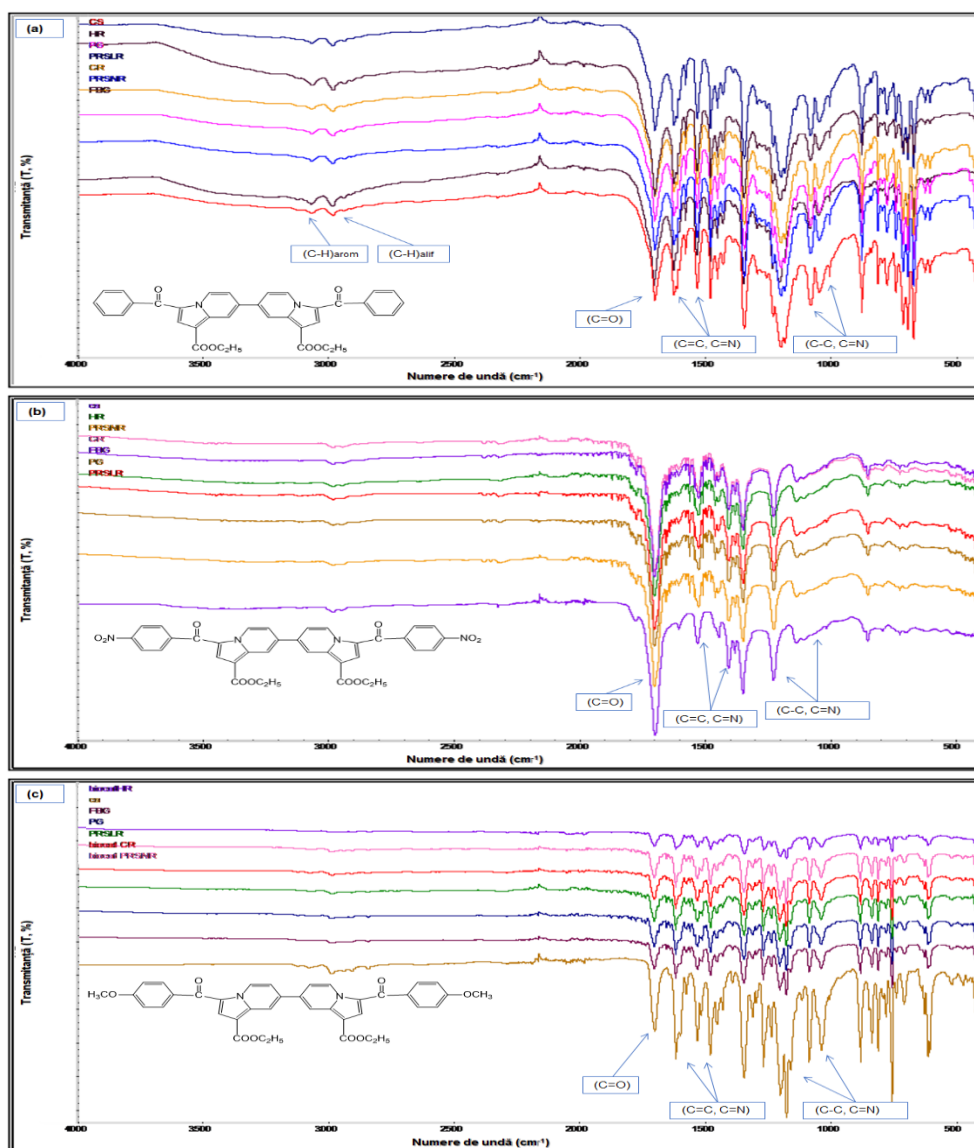
Figure 5.9. FT-IR analysis of compounds: a) Iz1a, b) Iz1b, c) Iz1c obtained by conventional catalysis (CS) and biocatalyzed reactions of plant enzymes: HR-horseradish root, PRSNR-parsnip root, CR- celery root, FBG- bean sprouts, PG- pumpkin germs, PRSLP- parsley root.

(a)

(b)

(c)
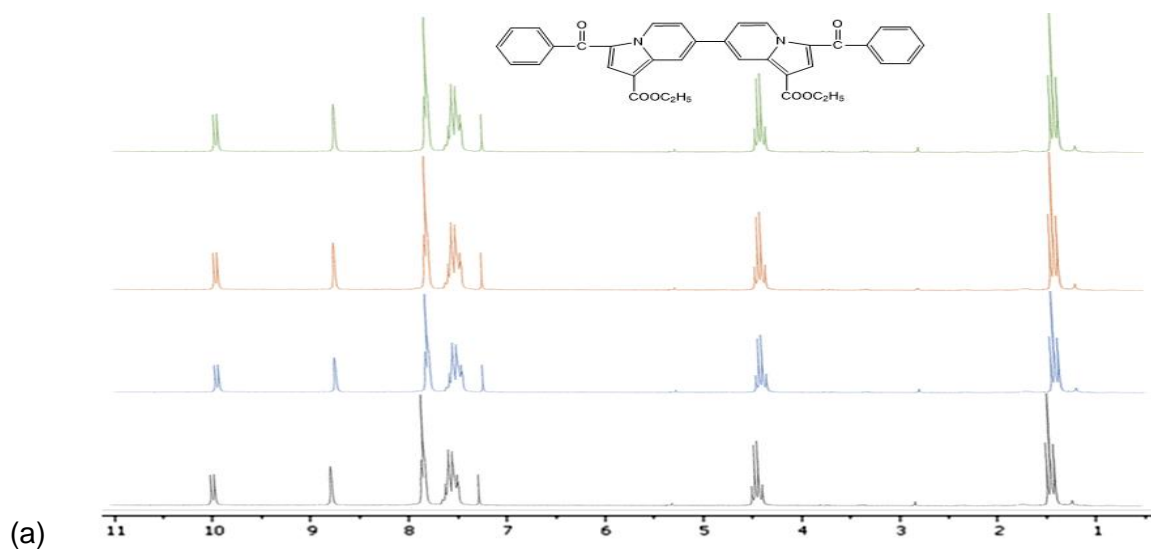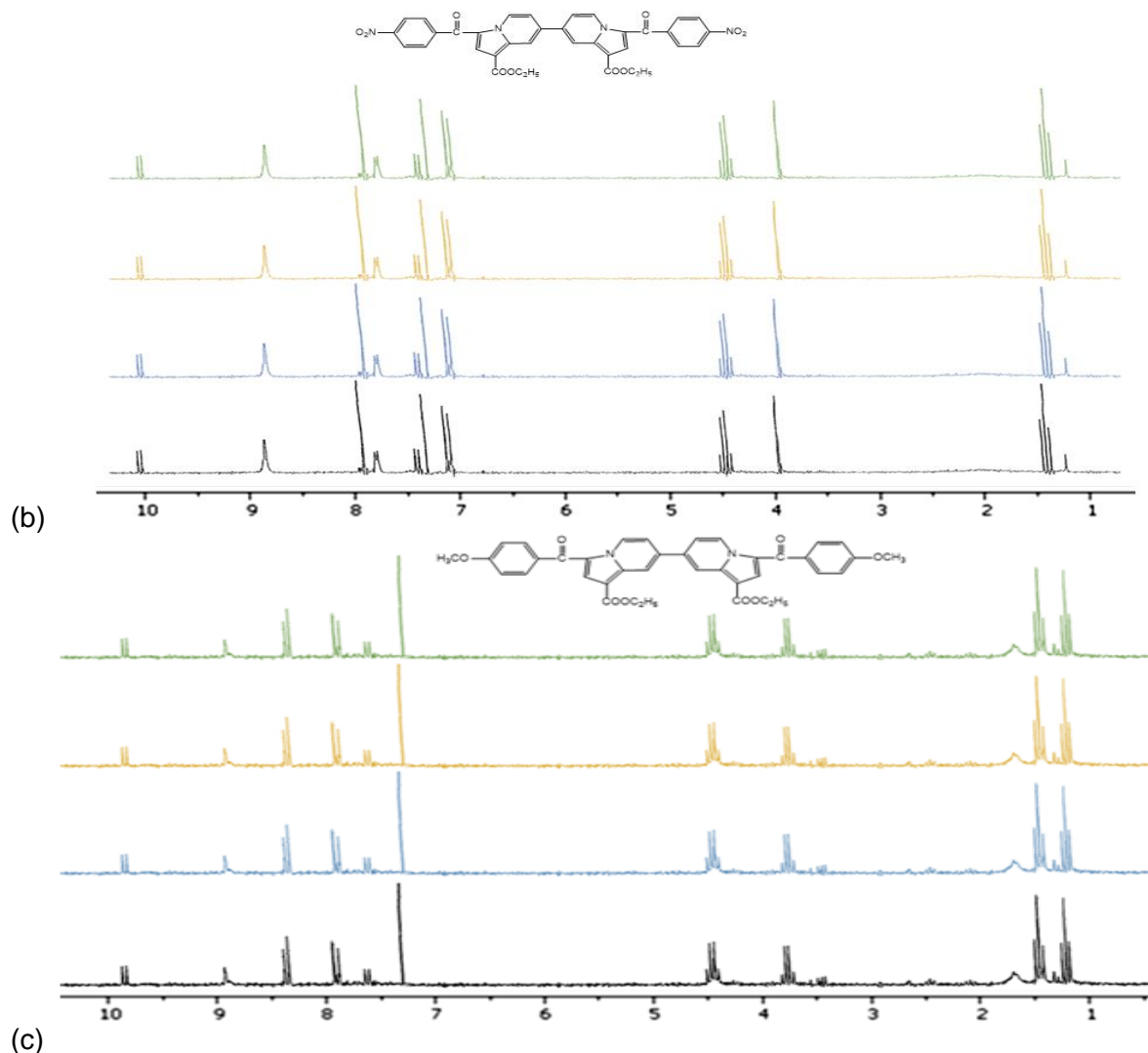
Figure 5.10. ^{1}H RMN analysis of compounds: a) Iz1a, b) Iz1b, c) Iz1c obtained by conventional catalysis (black), biocatalyzed reactions by plant enzymes (blue), pure peroxidase (brown) and with catalytic system I_2/H_2O_2 (green)

CHAPTER 6. Evaluation of cytotoxicity of some studied quaternary pyridinium salts and indolizines

6.1. Specific scientific objectives

The specific scientific objective of this chapter was to assess the toxicity of synthesized compounds. To achieve this objective, the effects of some studied compounds, from the class of quaternary pyridinium salts and the class of indolizines, on the germination of wheat seeds (*Triticum aestivum*) were investigated. Given the considerable increase in the importance of indolizine derivatives, the cytotoxicity of some indolizine derivatives on the model eukaryotic microorganism, *Saccharomyces cerevisiae* yeast, during alcoholic multiplication and fermentation processes has been investigated.

6.5. Results and discussion
6.5.1 Cytotoxicity of some compounds as assessed by *Triticum aestivum* test

Given the broad spectrum of potential applications of ScPy in various fields, the effects of 11 selected ScPy (S1a-e, S2a-e and S2i), with different electronic effects (attractive and electron repellent), on wheat seed germination were investigated, as a first step towards

estimating the potential danger of these chemicals to the environment. The compounds S1a-e, S2a-e and S2i were also selected to see if different functional groups could generate toxic effects, given that, for example, the nitro group in certain chemical molecules has been shown to induce toxicity. According to literature data, during this test, the most sensitive physiological parameters in plant germination and development for *T. aestivum* species were evaluated.

GS values greater than 95 % and close to those obtained for control (C) (Figure 6.5), as well as relative seed germination rates (GRS) ranging from 98.96 % to 100.75 % (Figure 6.6) for seeds treated with quaternary pyridinium salts, demonstrated that the tested ScPy derivatives had no negative influence on seed germination. Furthermore, the values obtained for the radicels relative growth parameter (RRC) were not negatively influenced by the presence of test compounds (Figure 6.7). For samples evaluated by exposure to ScPy at various concentrations, values greater than 100% were obtained, therefore ScPy has been shown not to exhibit cytotoxic effect on seed germination [469]. Germination index values (GI, %), greater than 95% and close to those obtained for the control (Figure 6.8), confirm that the tested ScPy does not exert phytotoxicity [444]. Toxicity studies performed by *Triticum aestivum* assay on quaternary pyridinium salts S1a-e, S2a-e and S2-i at two different concentrations (10^{-5} M and 10^{-6} M), showed no inhibitory effect on seed germination and early stem growth. The evaluation of the most sensitive germination indicators for the evaluation of phytotoxicity of indolizine derivatives was also carried out by the *Triticum aestivum test*. GS values (%), very similar to control samples based on literature data [440,469], demonstrate that the presence of test compounds had no negative influence on wheat seed germination (Figure 6.9). The obtained results are similar to other literature results presented for the *T. aestivum* method in assessing the phytotoxicity of some chemical compounds [440,459,460].

GRS (%) and RRC (%) values greater than 100% for samples treated with indolizine derivatives demonstrate that the presence of test compounds did not cause harmful effects on wheat seed germination (Figures 6.10 to 6.11). The obtained results are similar to other data presented in the literature for similar studies evaluating phytotoxicity by wheat seed germination method [440,469]. The values obtained for the vigor index (IV) between 79.13 ± 0.48% and 96.83 ± 0.95%, higher than 75% and close to the mean value obtained for the control sample (85.80 ± 0.52%) reveal the absence of harmful effects of the tested compounds on wheat seed germination (Figure 6.12).

Figure 6.5. Seed germination (GS, %) of *Triticum aestivum* L. exposed to different concentrations of ScPy (10^{-5}M - light green, and 10^{-6}M – dark green). The values shown represent the average of four replicates for each experimental condition and the SD error bars
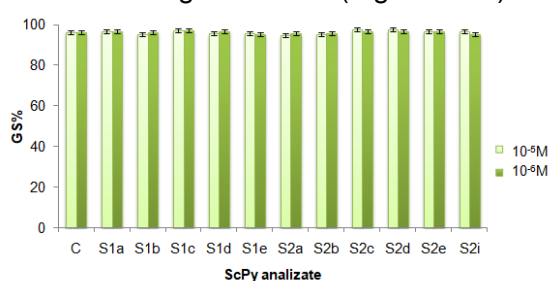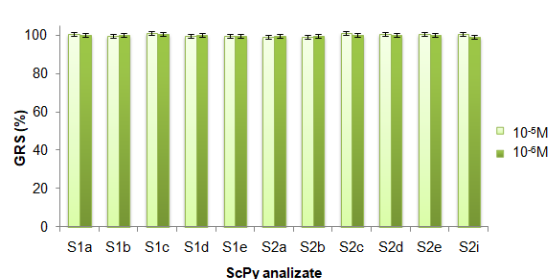
Figure 6.6. Relative seed germination (GRS, %) of *Triticum aestivum* L. exposed to different concentrations of ScPy (10^{-5}M - light green, and 10^{-6}M – dark green). The plotted values represent the average of four repetitions and the error bars with SD
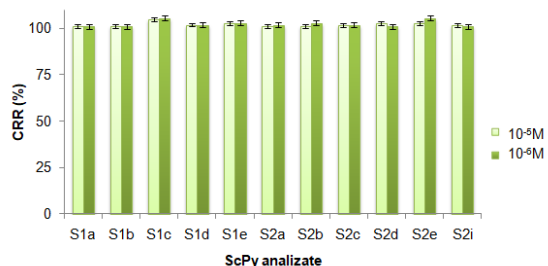
Figure 6.7. Relative radicels increase (CRR, %) of *T. aestivum* exposed to different concentrations of ScPy (10^{-5}M - light green, and 10^{-6}M – dark green). The data represents the average of four repetitions and error bars with SD
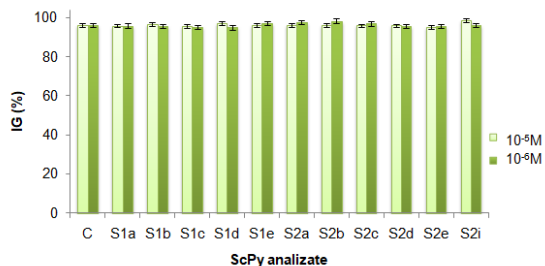
Figure 6.8. Sprouting index for seeds of *T. aestivum* treated with different concentrations of ScPy (10^{-5}M - light green, and 10^{-6}M – dark green). The data represent the mean of four repetitions and the error bars with standard deviation
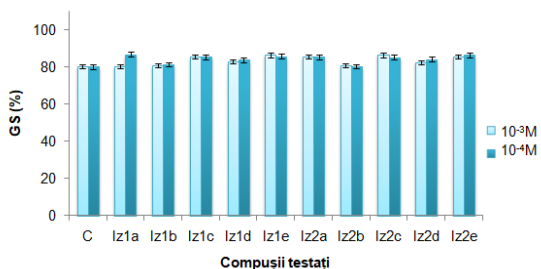
Figure 6.9. Seed germination (GS, %) of *Triticum aestivum* L. exposed to different concentrations of indolizine compounds (10^{-3}M - light blue, and 10^{-4}M – dark blue). The values represent the average of four replicates for each experimental condition with the SD error bars
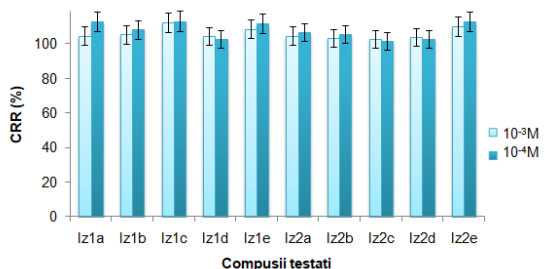
Figure 6.10. Relative radicle increase (CRR, %) of *T. aestivum* exposed to different concentrations of indolizine compounds (10^{-3}M - light blue, and 10^{-4}M – dark blue). The data represent the mean of four repetitions and the error bars with standard deviation

In conclusion, physiological parameters describing the germination process showed that exposure of seeds to compounds evaluated in the germination medium has no toxicological effects on the development and growth of wheat germ and strains compared to controls treated only with water. To evaluate at the cellular level the impact of seed exposure to various indolizine compounds in the germination process, the obtained sprouts were analyzed, by selecting representative germs for each experimental condition, by confocal microscopy. Indolizines Iz1a-e or Iz2a-e at tested concentrations (10^{-3} M, 10^{-4} M) did not exert a cytotoxic effect on plant organisms, their adsorption did not result in damage to the structure of plant tissues or physiological processes such as cell growth and differentiation.
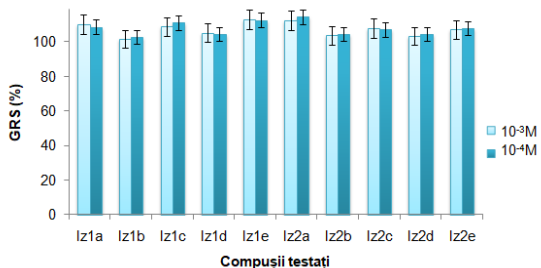
Figure 6.11. Relative seed germination (GRS, %) of *T. aestivum* exposed to different concentrations of indolizine compounds (10^{-3}M - light blue, and 10^{-4}M – dark blue). The plotted values represent the average of four repetitions and the error bars with SD.

Figure 6.12. The vigor indices (IV, %) for seeds of *T. aestivum* exposed to different concentrations of indolizine compounds (10^{-3}M - light blue, and 10^{-4}M – dark blue). The values shown are the mean of four replicates for each experimental condition and the standard deviation error bars
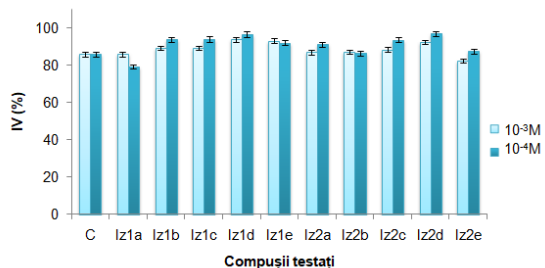
6.5.2. Impact of some indolizine derivatives on *Saccharomyces cerevisiae* yeast growth

Given the considerable increase in the importance of indolizine derivatives, in this doctoral thesis, the cytotoxicity of these compounds on model yeast cells *Saccharomyces cerevisiae* was investigated, during alcoholic multiplication and fermentation processes. In this context, alternative approaches with a view of minimal use of animal tests in scientific experiments were pursued and the cytotoxicity of indolizine derivatives on yeast cells was assessed. The kinetic parameter values determined after 48 hours for samples supplemented with Iz1c compound were close to those of the control sample (Table 6.1).

The dry matter yield obtained for the control sample (12.72% ± 0.16%) showed similar values to the samples to which the analyzed compounds Iz1a, Iz1b and Iz1c at concentrations of 1 µM and 10 µM were added (Figure 6.24). The best dry matter yield was obtained for the medium supplemented with the Iz1a compound at a concentration of 10 µM (15.49% ± 0.13%), followed by samples to which the analyzed chemical compounds were added: 1 µM Iz1b (14.81% ± 0.08%) and 10 µM Iz1c (14.05% ± 0.36%). A lower biomass yield compared to that of the control sample showed the samples to which the compounds Iz1c (12.68% ± 0.31%) and Iz1b (12.21% ± 0.17%) at concentrations of 1 µM and 10 µM respectively were added (Figure 6.24).

Table 6.1. Kinetic parameters determined after 48 hours of cultivation under submerged conditions with agitation and aeration: n = number of generations; µ = growth rate; tg = generation time

Test sample	Concentration	n	μ [h^{-1}]	tg [h]
Control		18,6 ± 0,4	0,38 ± 0,06	2,58 ± 0,26
Iz1a	1 µM	15,4 ± 0,1	0,32 ± 0,12	3,12 ± 0,28
Iz1a	10 µM	13,2 ± 0,3	0,27 ± 0,14	3,63 ± 0,14
Iz1b	1 µM	11,4 ± 0,4	0,24 ± 0,13	4,21 ± 0,16
Iz1b	10 µM	11,8 ± 0,3	0,25 ± 0,17	4,07 ± 0,24
Iz1c	1 µM	19,4 ± 0,1	0,40 ± 0,08	2,47 ± 0,36
Iz1c	10 µM	21,4 ± 0,0	0,44 ± 0,04	2,24 ± 0,28

After the first 24 hours of cultivation, budding for the control sample showed a value of 17.5% ± 0.8%, close to that of the sample supplemented with Iz1c at a concentration of 10 µM (18.08% ± 0.7%). After 48 hours of cultivation, the budding value in the presence of the same concentration of Iz1c (19.90% ± 1.1%) was higher than that of the control sample as opposed to the 1 µM concentration, where the budding value after 24 hours showed the highest value of 21.3% ± 1.2%, and after 48 hours the lowest value of 16.24% ± 1.3%. In the case of indolizine Iz1a, at the minimum concentration used in this experiment, a higher degree of budding of cells was achieved compared to the control and approximately 20 % lower after 48 hours of submerged cultivation. At the maximum concentration tested, the presence of Iz1b produced budding of more than 20% of yeast cells, while at the minimum analyzed concentration values comparable to those of controls were obtained after 48 hours of submerged cultivation (Figure 6.25).
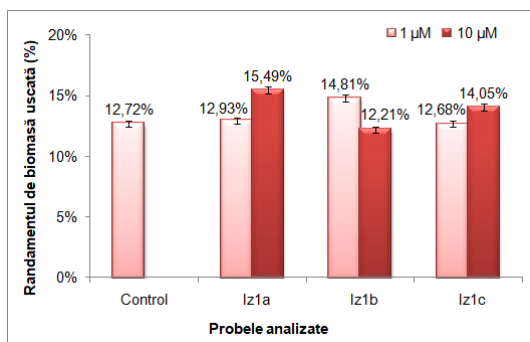
Figure 6.24. Yield of dry biomass for yeast grown in liquid medium supplemented with test compounds. The control sample was not supplemented with indolizine derivatives in the growth medium of yeast cells. The values obtained represent the average of three experimental repetitions for each sample ± SD.
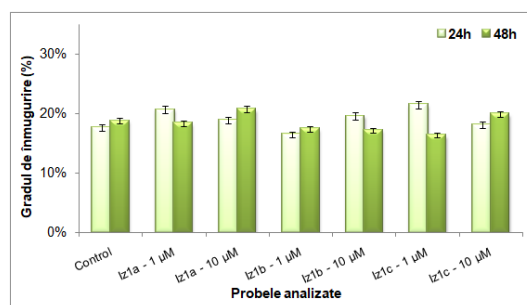
Figure 6.25. The degree of budding of yeast cells of *S. cerevisiae* in the presence of indolizine compounds at different concentrations in the culture medium. The control was considered free of indolizine compounds in the growth medium of yeast cells. The values obtained represent the average of three experimental repetitions for each sample ± SD

Figure 6.26 (a) shows that the presence of Iz1a at 1 µM concentration resulted in a lower degree of autolysis of *S. cerevisiae* yeast cells in the multiplication process (2.27% ± 0.08%, 0.87% ± 0.06%, 1.07% ± 0.07 %) than that of the control sample after 24, 48 and 120 hours of cultivation (1.60% ± 0.03%, 2.34% ± 0.05%, 2.68% ± 0.06%). Also, the presence of Iz1a at 10 µM concentration resulted in a lower degree of autolysis after 24 and 48 hours of cultivation (0.82% ± 0.01%, 1.04% ± 0.02%) compared to the control, and after 120 hours of cultivation, it was observed that the degree of autolysis showed a higher value compared to the control. The presence of Iz1b in the growth medium at both concentrations tested resulted in autolysis values higher after 24 hours by approximately 0.6% compared to the control. After 48 and 120 hours of cultivation, the autolysis values for samples supplemented with Iz1b compound at both tested concentrations showed values very close to those given by the control after 48 and 120 h of cultivation (Figure 6.26 b). Supplementation of the culture medium of S. *cerevisiae* yeast cells with Iz1c at a concentration of 1 µM resulted in lower autolysis values than those shown by the control after 24, 48 and 120 hours of cultivation. Also, the presence of Iz1c at a concentration of 10 µM in culture medium resulted in lower autolysis values (1.09% ± 0.03%, 1.36% ± 0.02%) than those of the control after 48 and 120 hours of cultivation (Figure 6.26 c).

The multiplication dynamics of yeast cells for the control sample were similar to that of samples supplemented with the studied compounds (Figure 6.27), indicating that these compounds do not adversely influence the growth and multiplication process of yeast cells.
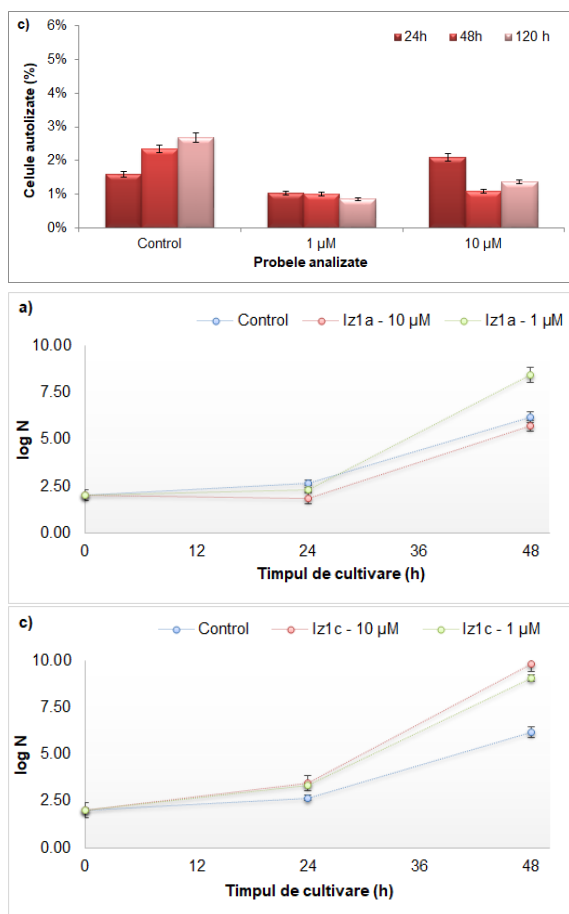
Figure 6.26. Degree of autolysis of yeast cells for culture medium supplemented with compounds a) Iz1a, b) Iz1b, c) Iz1c at different concentrations. The control sample was not supplemented with indolizine compounds in the growth medium of yeast cells. The values obtained represent the average of three experimental repetitions for each sample ± SD

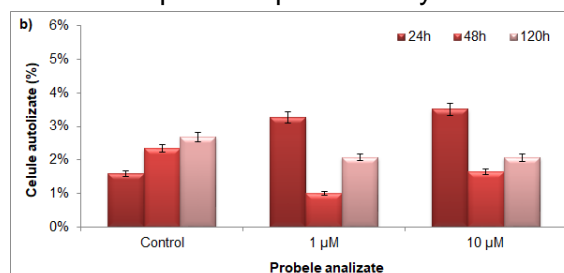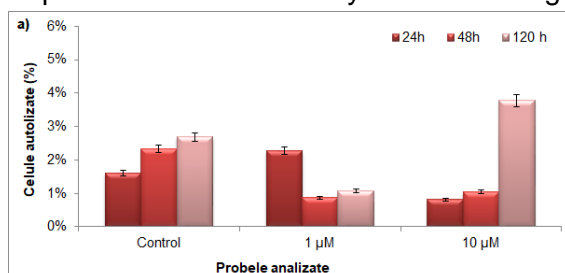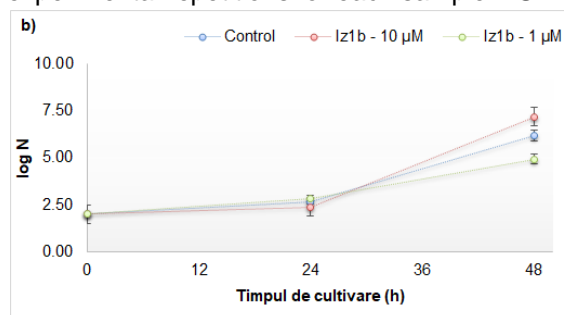**Figure 6.27.** Dynamics of yeast cell multiplication in culture medium supplemented with compounds a) Iz1a, b) Iz1b, c) Iz1c at different concentrations. The values obtained represent the average of three experimental replicates for each sample ± SD

CHAPTER 7. Evaluation of biologically active properties

7.2. Specific scientific objectives

The specific scientific objective of this chapter was to evaluate the biologically active properties of heterocyclic nitrogen compounds (quaternary pyridinium salts, indolizines, pyridinium-indolizine hybrids, metal complexes). To achieve this goal, the antimicrobial, antioxidant, anticancer, antineurodegenerative and anti-inflammatory properties of compounds obtained by classical and unconventional synthesis methods were determined.

7.9. Results and discussion
7.9.1. Determination of antimicrobial properties

The antimicrobial activity of quaternary pyridinium salts (ScPy) is a topical subject, this class of compounds having known germicidal properties [480,503]. Evaluation of the antibacterial activity of S2a-c and S2f-q salts was performed using the TTC test as a qualitative test and the microdilution method as a quantitative method. The class of tetrazolium salts that are widely used in various chemical and biological applications [504,505], contains organic compounds that can form intensely colored azoderivatives known as formazan's [491,506,507]. This property can be used to detect and measure cell viability [507–510].

In this thesis, the antimicrobial effects of some quaternary pyridinium salts (ScPy) containing in their structure various electron substitutes, attractive or repellent, which can influence these evaluated properties.

Evaluation of inhibition percentage of growth of microorganisms by TTC test

The TTC colorimetric test has proven to be an effective colorimetric method for evaluating antibacterial properties [491,507]. The obtained results in this thesis demonstrated the antibacterial potential of ScPy expressed as percentages of inhibition of bacterial cell growth.

After testing ScPy against the pathogenic microorganism *E. coli*, nine compounds demonstrated good antibacterial activity. The presence of vital cells of bacteria was evidenced by an intense red color of formazan obtained in the growth medium by the TTC method. After adding ScPy, a reduction in color intensity to colorless could be observed. From Figure 7.3 the percentage of inhibition of bacterial growth ranged from 3% to 59%, depending on the structure of ScPy. A strong inhibitory effect (59%) against *E. coli* was demonstrated by the compound S2c, followed by S2q (50%), S2g (42%) and S2k (33%). It was also observed that the bacteria's vital cells were inhibited by ScPy S2b, S2i and S2p, with an average percentage of inhibition of less than 20%. A reduced inhibitory potential against the bacterial strain tested was obtained for S2o, with an inhibition percentage of 10%, while S2l had the lowest inhibitory effect (3%). The antibacterial action of ScPy is manifested in a mechanism of destruction of the lipid membrane by dipole-dipole interactions of positively charged quaternary nitrogen with polar head groups of acid phospholipids [503,513]. It has also been previously shown that there is a good relationship between structural descriptors (LogP, polarizability, polar surface (2D) and Van der Waals surface (3D)) and antibacterial properties of these types of ScPy [191].

Minimal inhibitory concentrations (MIC)

The MIC values of ScPy, S2a-c and S2f-q were determined as a quantitative assessment of their antibacterial activity, recording a different sensitivity against Gram-negative bacteria. MIC values ranged from 0.312 to 2.5 mg/mL (Figure 7.4). The lowest MIC value (0.312 mg/mL) was exhibited by S2c, S2g and S2q compounds against *E. coli.* Some differences in antibacterial activities were also observed for tested compounds. Thus, S2i, S2k and S2p compounds showed higher MIC values of 0.625 mg/mL, while S2l and S2o showed the highest CMI value (2.5 mg/mL).

The results obtained by the microdilution method confirm the data determined by the TTC test (Figure 7.3). These results showed a greater antibacterial potential of ScPy studied in this PhD thesis compared to other ScPy against the E*. coli strain* [515].
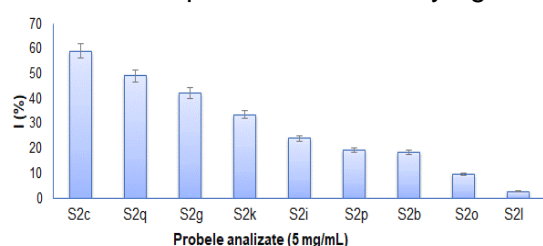
Figure 7.3. Percentages (%) of inhibition of *E. coli* growth by ScPy as determined by the Tetrazolium/Formazan test
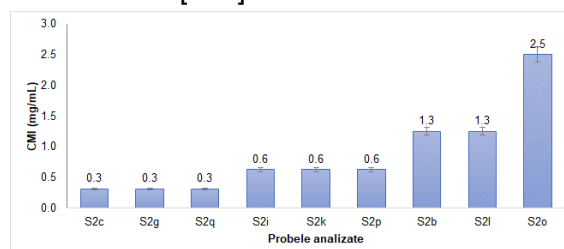
Figure 7.4. Antibacterial activity of ScPy against *E. coli*, expressed as MIC (mg/mL) determined by microdilution method

7.9.2. Determination of antioxidant properties

Oxidative stress is implicated in numerous conditions, such as cancer, diabetes and neurodegenerative diseases [293,295,517,518]. Reactive oxygen species can cause cell damage and subsequent cell death because they oxidize vital cellular components such as lipids, proteins, and DNA (Figure 7.7). Moreover, the human body is exposed throughout life to excitatory amino acids (such as glutamate), whose metabolism produces ROS, thereby increasing toxicity. Antioxidant mechanisms include O_2 removal, elimination of reactive oxygen/nitrogen species or their precursors, inhibition of ROS formation, chelation of metal ions necessary for catalysis of ROS generation and regulation of endogenous antioxidant activity [519–521]. The percentage of DPPH radical inhibition indicative of antioxidant activity was calculated at organic compound concentrations of 48 µg/mL, 188 µg/mL and 750 µg/mL (Figure 7.8). Although activity was assessed for several molecules as shown in Table 7.1,

some compounds showed a large standard deviation due to precipitation in the reaction mixture.

Most molecules showed little or no antioxidant activity when evaluated at a concentration of 48 µg/mL. Increasing the concentration of the analyzed compounds to 750 µg/mL led to a significant increase in the percentage of inhibition. Among the hybrid compounds, the neutral compound Iz3-b showed promising activity, with nearly 60% inhibition at 188 µg/mL, but solubility problems prevented accurate determinations at higher concentrations. The compound Iz-Py-7 showed the highest antioxidant properties (approximately 90% inhibition) at 750 µg/mL. Similar trends were observed for symmetric analogues, with bipyridinium salts showing better activity compared to bis-indolizines (Table 7.1).
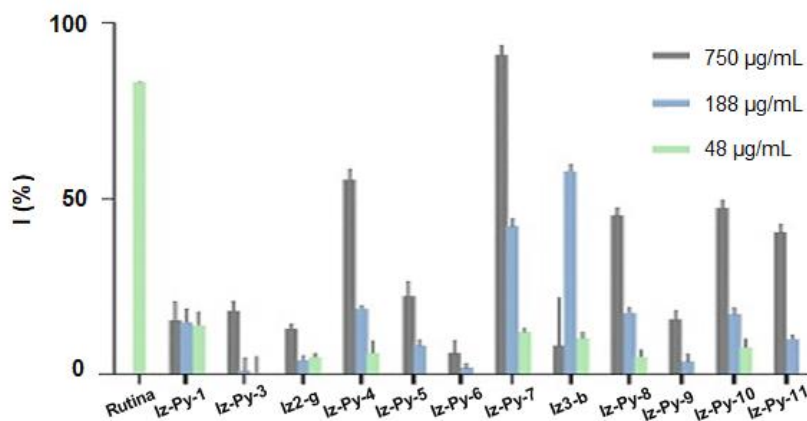
Figure 7.8. Antioxidant activity (%) determined using the DPPH method at test substance concentrations of 48 µg/mL (green), 188 µg/mL (blue), or 750 µg/mL (grey), routine was used as a positive control. All analyses were carried out in triplicate and each value corresponds to the mean value ± SD.

7.9.3. Determination of anticancer properties

Cytotoxic activity on cancer cell lines

The cytotoxic activity of the La-Nd-DPY complex was evaluated on various cell lines representative of different human cancers, such as A2780 and A2780cisR for ovarian cancer, cisplatin-sensitive and cisplatin-resistant, respectively, PC3 cells for prostate cancer, and MCF7 cells for breast cancer. Cisplatin has been included as a positive reference standard in comparative determination, as it is a drug containing a metal (platinum) and is clinically approved for cancer chemotherapy [537,538]. The effect of the compounds on cell viability was assessed by the MTT assay after incubation for 24 hours and 48 hours. La-Nd-DPY demonstrated constant high cytotoxic activity for all cell lines after 48 hours of exposure. At shorter incubation times (24 h), the cytotoxic profile was particularly different for A2780cisR ovarian cancer cells and prostate cancer cells (Figure 7.10).

Among ScPy and symmetrical indolizine compounds, higher cytotoxicity of S2-e, Iz2-e and Iz1-c compounds was noted. Cisplatin after both incubation periods was found to be less cytotoxic on cell lines than mixed Ln complex (La-Nd-DPY) in all studied cancer cell types (Figure 7.11). The mixed Ln complex has shown a high cytotoxic action on cisplatin-resistant cells and PC3 cells, which are known for their extremely aggressive behavior [539]. These results indicated that neither pro-ligand S1-a nor lanthanide salts are the active species responsible for the observed cytotoxicity of the mixed lanthanide complex.
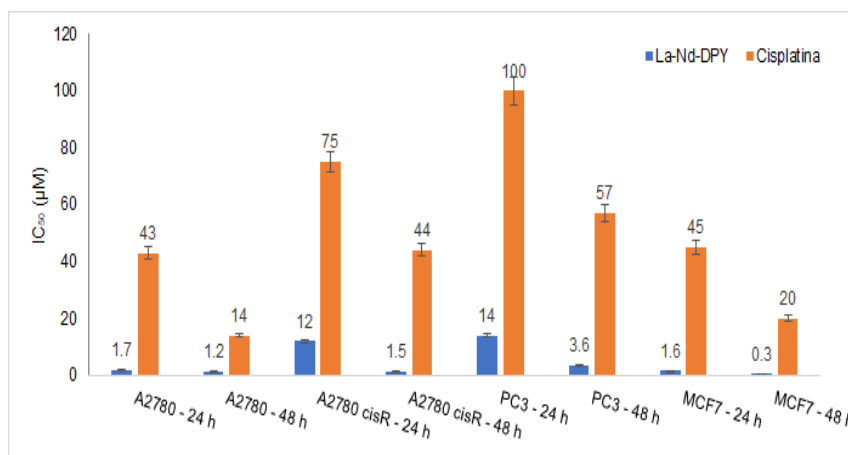
Figure 7.11. IC_{50} values (µM) obtained for La-Nd-DPY complex and cisplatin on different cancer cell types after 24 and 48 hours of incubation. The data shall be the mean of at least two independent experiments in hexaplicate each ± SD

Cytotoxic activity on tumor spheroids

Following the evaluation of cytotoxicity on human cancer cell lines, the interaction of the La-Nd-DPY mixed complex on an advanced three-dimensional cancer cell model of multicellular tumor spheroids derived from the PC3 prostate cancer cell line was evaluated. This type of three-dimensional culture method highlights the in vivo microenvironment of tumor cells, with cultured cells growing into spheres that promote cell-to-cell and cell-ECM (extracellular matrix) interactions, and which are lacking in conventional 2D culture. PC3 tumor spheroids were cultured and grown for 3 days, after which they were incubated in the presence of the La-Nd-DPY complex for 48 hours. Images of PC3 spheroids exposed to different concentrations of the mixed lanthanide complex are shown in Figure 7.13.

Spheroid size and shape were affected by exposure to higher concentrations of the analyzed complex (La-Nd-DPY) according to microscopic images (Figure 7.13), this result is confirmed by decreased growth of PC3 spheroids by exposure to mixed Ln complex (Figure 7.14.a). There was a decrease in the size of incubated spheroids with the higher concentration (50 µM) of the analyzed compound, although there was already a noticeable delay in spheroid growth compared to controls, starting at a concentration of only 5 µM. The results obtained from the viability tests shown in Figure 7.14.b show that, unlike conventional monolayer cultures, in the case of 3D spheroids the complex shows lower cytotoxicity (values ~80% of control viability at higher concentrations).
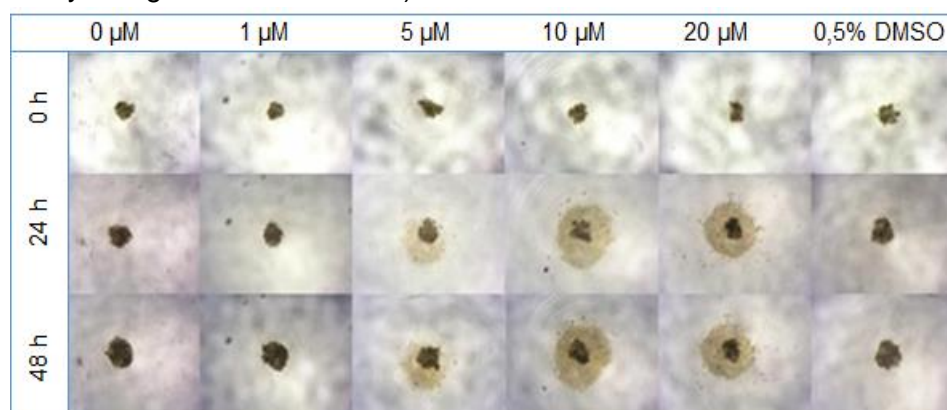
Figure 7.13. Representative microscopic images of PC3 spheroids before (0 h) and after (24 and 48 h) exposure to different concentrations of the mixed Ln complex. The reference control are spheroids incubated with culture medium only (control-0µM) or 0.5 % DMSO

This result is similar to other data presented in literature studies, with 3D culture systems frequently being more refractory to cancer treatments due to limited drug penetration and activation of multiple resistance mechanisms [540]. Spheroid models can mimic metabolic and proliferative gradients of tumors *in vivo*, with subsequent changes in cell phenotype and status, exhibiting multicellular chemoresistance.

Production of ROS

The potential induction of intracellular ROS formation by La-Nd-DPY and cisplatin in A2780 and PC3 cells was analyzed using a fluorescent compound, H_2DCFDA, which can detect hydrogen peroxide, hydroxyl radicals or peroxynitrite. ROS formation was present for the mixed complex in a way directly proportional to the concentration for both cell lines. Regarding cisplatin, its cytotoxicity has been correlated with the generation of mitochondrial ROS that can generate harmful processes and influence metabolic functions, which can ultimately lead to cell death [530,540]. However, under the same experimental conditions, no production of ROS, detectable in the presence of cisplatin, was observed, probably due to the short exposure time (3 hours) (Figure 7.15).
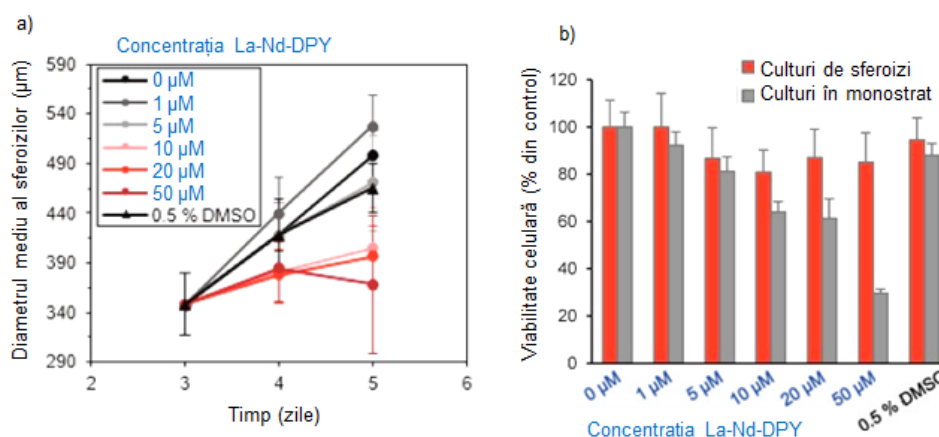
Figure 7.14. Effect of exposure to La-Nd-DPY complex on PC3 spheroid growth (a) represented by mean spheroid diameter (in µm) as a function of number of days of cultivation and cell viability after 48 hours (b) assessed by APH assay in parallel with monolayer cultured cells. Controls are spheroids or cells cultured in monolayer by incubation with culture medium alone or 0,5 % DMSO. The data presented are the average of the experiments performed in hexaplicate ± SD
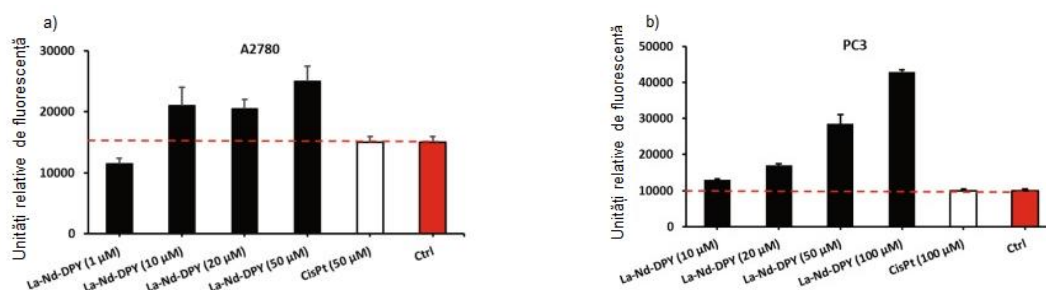
Figure 7.15. Production of ROS by A2780(a) and PC3(b) cells after 3-hour exposure to La-Nd-DPY and cisplatin (cisPt) detected with H_2DCFDA. The results are expressed in relative units of fluorescence (mean of four replicates ± SD). Control samples (Ctrl) consist of cells incubated only in culture medium.

Evaluation of apoptosis
Caspase activation

Apoptotic cell death is mediated by caspases, a family of cysteine proteases important for maintaining homeostasis by regulating inflammation and cell lysis [541]. To evaluate the influence of mixed Ln complex on cellular apoptosis, the active form of caspases 3 and 7 was quantified in cell lines A2780 and PC3 [542]. The complex studied, La-Nd-DPY, could not

activate caspase-3/7 in these cell lines, and the values detected were like those obtained for control cells incubated only in the culture medium (Figure 7.16).

DNA fragmentation

To confirm the obtained results with the caspase activation method, a Hoechst staining test of nuclei was performed to determine the percentage of apoptotic cells in a population of PC3 cells in the presence and absence of the La-Nd-DPY complex. Morphological hallmarks of apoptosis include DNA condensation, chromatin fragmentation or apoptotic fragment formation, and the appearance of apoptotic markers in evaluated cultures.

Correlating the inability of this prostate cancer cell line to activate caspase-3/7 observed in the previous method, no statistically significant increase in apoptosis levels was observed in a cell population after 24- or 48-hour exposure to IC_{50} concentrations of the evaluated compound (Figure 7.17). Therefore, cell death observed in the cytotoxicity test is not caused by apoptosis and other mechanisms of cell death exist under these conditions.
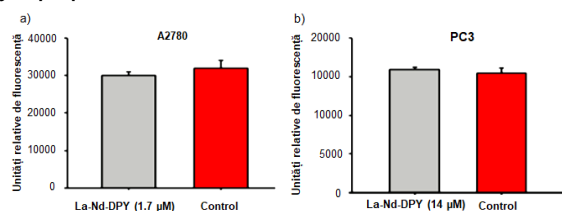
Figure 7.16. Caspase-3/7 activity in A2780(a) cells and PC3(b) cells after exposure for 24 hours to a concentration corresponding to the IC50 value obtained for the same cell line. Data were obtained from three examples per condition and were expressed as a mean ± SD from two independent tests in relative units of fluorescence
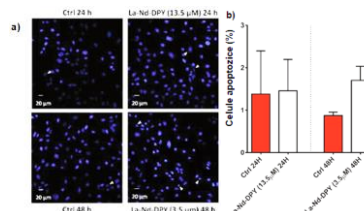
Figure 7.17. a) Representative microscopic analysis of PC3 cells stained with Hoechst 33,342 (A) in the absence (control) or presence of La-Nd-DPY complex for 24 hours or 48 hours; b) Quantification of the number of apoptotic PC3 cultured cells (%).

7.9.4. Evaluation of antineurodegenerative activity

Cholinesterase inhibition

Cholinesterase activity was assessed using the Ellman spectrophotometric method [543]. Several compounds were evaluated in this method against electric eel acetylcholinesterase (AChE) and butyrylcholinesterase (eqBChE), and compounds that showed remarkable activity on them were further tested against human enzymes (hAChE and hBChE). The objective of this method was to select molecules that could significantly inhibit cholinesterase. To achieve this objective, a selection of the action of compounds at a concentration of 4 µM against eeAChE and eqBChE was first carried out (Figure 7.18). Only molecules that inhibited at least 50% of ChE activity at this micromolar concentration were then evaluated over a higher concentration range to accurately calculate IC_{50} values. Data obtained by this method are collected in Table 7.2 (Figure 7.19 for IC_{50} curves).

The already mentioned high UV-Vis absorbance of the molecules Iz1-f, Iz-Py-1, Iz-Py-2 and Iz-Py-3, together with their low solubility in water, prevented their study in a wide range of concentrations, and the promising effects obtained for a selected concentration of 4 µM, especially for Iz-Py-1 and Iz-Py-2 against eeAChE, could not be confirmed (Figure 7.18.a). Similarly, unloaded indolizine-pyridine (Iz2-g, Iz3-a and Iz3-b) are inactive against both enzymes (Figure 7.18.b and c). Most corresponding symmetrical cation pyridinium-indolizine hybrids were active at 4 µM, unlike that observed for most bis-indolizines (Table 7.3) which easily form aggregates in aqueous solutions. The generally better solubility of pyridinium-indolizine hybrids allowed them to be assessed over a wider concentration range. Cationic hybrids showed IC_{50} with micromolar values, with slight selectivity for eeAChE compared to

eqBChE (Table 7.2), except for the compound Iz-Py-7 and its analogue Iz-Py-10, which showed the highest selectivity (being 10 times more active than eeAChE compared to eqBChE). For comparison, the evaluation of symmetric analogues (Table 7.3) was performed using eeAChE with an enzyme activity of 0.5 U. The evaluated compounds showed IC$_{50}$ values in the 2-5 µM range. The series of compounds Iz3a-b and Iz-Py-8-11, which contain the 3-p-methoxybenzoyl group, demonstrated higher activity against the two enzymes compared to their Iz2-f analogues, Iz-Py-4-7. This effect may be related to the better flexibility of the propylene bridge compared to the shorter ethylene bridge between the pyridyl nuclei.

Table 7.2. IC$_{50}$ (µM) concentration values for inhibition of ChE *

Analysed samples	Iz2-g	Iz-Py-4	Iz-Py-5	Iz-Py-6	Iz-Py-7	Iz3-a	Iz3-b
ee AChE	-	4.4 ± 0.5	-	2.0 ± 0.4	5.4 ± 0.1	-	-
eq. BChE	-	17.5 ± 8.2	-	8.8 ± 3.5	55.4 ± 2.3	-	-
hAChE	nd	6.6 ± 1.1	nd	8.0 ± 0.9	37.1 ± 4.1	nd	nd
hBChE	nd	nd	nd	nd	nd	nd	nd
Analysed samples	**Iz-Py-8**	**Iz-Py-9**		**Iz-Py-10**	**Iz-Py-11**	**Donepezil**	
ee AChE	2.6 ± 0.6	> 10 µM**		7.9 ± 0.6	2.7 ± 0.6	0.052 ± 0.007	
eq. BChE	7.5 ± 3.4	4.8 ± 1.3		72.1 ± 15.9	7.3 ± 1.2	6.0 ± 1.7	
hAChE	3.3 ± 0.7	nd		4.0 ± 0.9	9.4 ± 2.5	0.029 ± 0.005	
hBChE	38.9 ± 14.0	nd		> 100 µM	nd	9.2 ± 5.6	

*IC$_{50}$ values (µM) are averaged ± standard deviation of three independent determinations per condition; molecules indicated as inactive (-) showed no significant activity during a first selection at a concentration of 4 µM. Donepezil was used as a control (Figure 7.19 and Figure 7.20 for IC$_{50}$ curves). ** Formation of aggregates at higher concentrations in the presence of eeAChE.
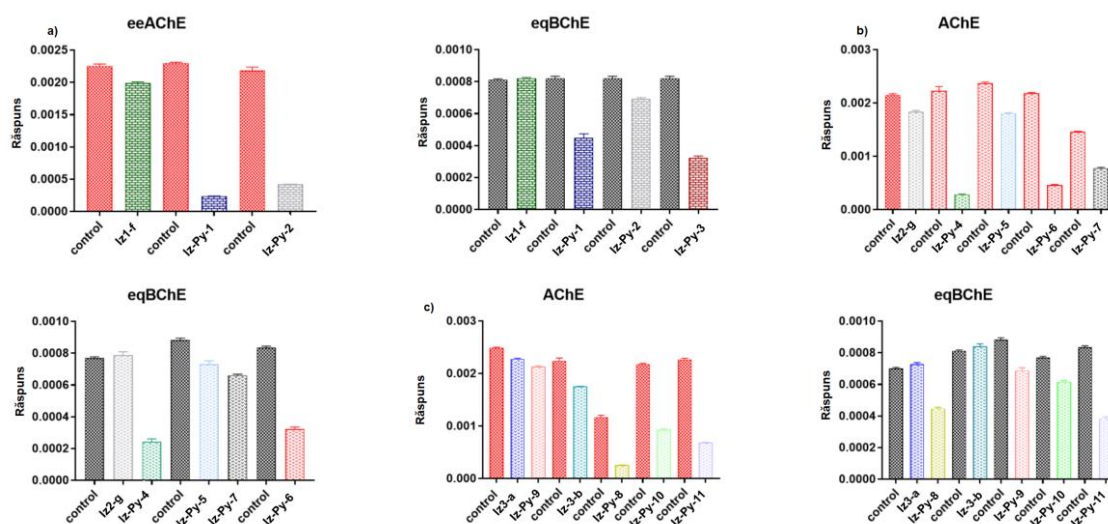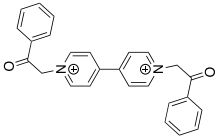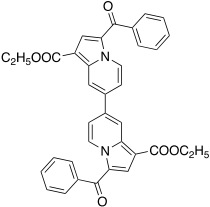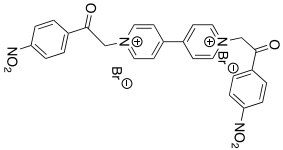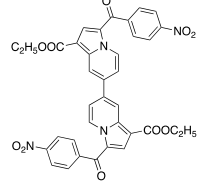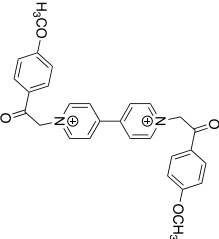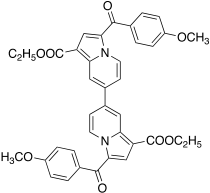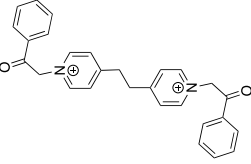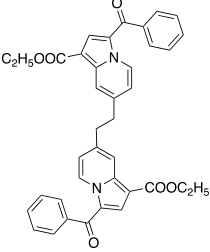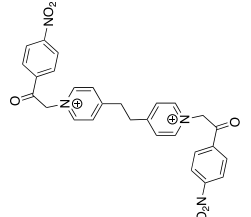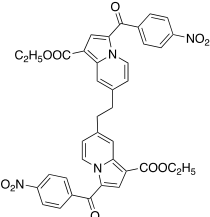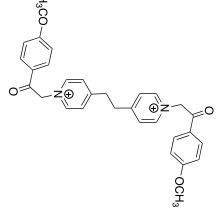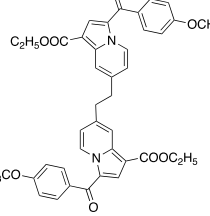
Figure 7.18. Preliminary assessments of the activity of the studied compounds (4 µM) on eeAChE and eqBChE. The error bars are the standard deviation obtained from three independent experiments carried out in at least three copies.

The compounds Iz3a-b and Iz-Py-8-11, which contain the 3-p-methoxybenzoyl group as a substitute, demonstrated higher activity against the two enzymes compared to their Iz2-f analogues, Iz-Py-4-7. This effect may be related to the better flexibility of the propylene bridge compared to the shorter ethylene bridge. In terms of inhibition of eeAChE, the pyridinium-indolizine hybrid Iz-Py-5 was the only inactive hybrid compound. This hybrid has in its structure the voluminous lipophilic group N-dimethoxybenzyl together with the substitute 3-p-methoxybenzoyl. Its analogue Iz-Py-9 demonstrated higher activities against both enzymes, however, a more detailed analysis of Prism curves and calculations (Figure 7.19) showed that

its solubility limited to concentrations greater than 10 µM in the presence of eeAChE leads to a decrease in the value of the R^2 coefficient when compared to the other molecules tested.

Table 7.3. Assessment of AChE activity inhibition potential

Analyzed compound	IC_{50} AchE (µM)	Chemical structure	Analyzed compound	IC_{50} AchE (µM)	Chemical structure
S1a	4.4 ± 0.4		Iz1a	3.7 ± 0.9	
S1b	Inactive (>20)		Iz1b	Inactive (>20)	
S1c	2.0 ± 0.3		Iz1c	2.4 ± 0.3	
S2a	5.7 ± 1.2		Iz2a	Inactive (>20)	
S2b	5.3 ± 2.2		Iz2b	Inactive (>50)	
S2c	Inactive (>50)		Iz2c	Inactive (>20)	

The compound Iz-Py-11, an analogue of Iz-Py-9, in which 3-p-methoxybenzoyl was replaced by the methyloxycarbonyl group of smaller size, showed good activity against both eeAChE (IC_{50} = 2.7 µM) and eqBChE (IC_{50} = 7.3 µM) without any apparent limitation of solubility. Due to the high cost of human cholinesterase, only a few active molecules were selected for further evaluation (Table 7.2 and Figure 7.20 for IC_{50}). For most compounds tested, the IC_{50} values against hAChE remained in the same micromolar range, except for the

compound Iz-Py-7 which lost its cholinesterase inhibiting activity on human enzymes, with IC_{50} > 30 µM for hAChE. Two molecules, Iz-Py-8 and Iz-Py-10, differing only in the nature of the substituent at position 3 of the indolizine core, were also tested against hBChE. The effectiveness of the compound Iz-Py-8, which previously showed a micromolar IC_{50} value significant compared to eqBChE, in the case of human enzyme the value decreased strongly (IC_{50} / 5) compared to hBChE. The compound Iz-Py-10 was not active (IC_{50} > 100 µM) confirming previously observed selectivity for AChE over BChE.

Docking calculations were then performed to compare the possible binding mechanisms of Iz-Py-8 and Iz-Py-10 compounds at the active sites of the two human ChE. While both are active as AChE inhibitors (fish or human), these compounds exhibited different behavior on BChE (equine or human) (**Chapter 8**).

Inhibition of amyloid fibrils

To monitor the effect of molecules on the process of amyloid fibril formation, the T-based fluorescence test (ThT) is generally used, since it is very sensitive to β-folded structures of fibrils [545]. By binding to fibrils, ThT displays redshifted emission, allowing selective detection of structures rich in β sheets, such as fibrils. Two models of amyloid peptides were used, both derived from the tau protein sequence (Figure 7.22).
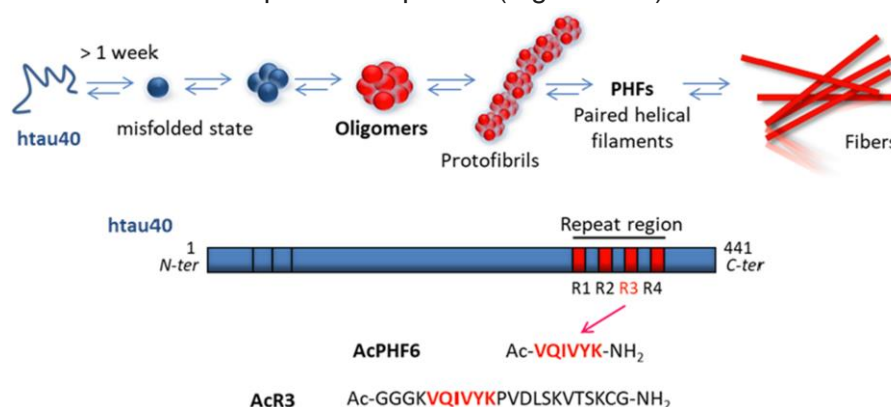
Figure 7.22. The process of formation of tau-т- fibrils (in β-folded structures: red) and the sequences of the two tau models used in this study.

The AcPHF6 model is a short peptide of 6 amino acids corresponding to the nucleus of tau fibrils [546]. Its fibril formation process is much faster than tau protein or amyloid peptides, which can take days and is well suited for the first selection of a set of molecules by ThT fluorescence tests [500]. Studies were conducted in phosphate buffer, and the ThT fluorescence signal was recorded in the absence and presence of Iz-Py and Iz molecules at a concentration of 100 µM (corresponding to a ratio of 1/1 to amyloid peptide). For the AcR3 model, heparin was added as a fibrillation inducer and 10 µM heparin corresponding to a 0.1/1 ratio to this amyloid peptide was used. The results reported in Figure 7.23 are expressed as a percentage inhibition of ThT fluorescence. Control wells were used to evaluate any possible intrinsic fluorescence emission of hybrids. No fluorescence additional to that of free ThT was detected for these controls.

As can be seen in Figure 7.23.a, most hybrid compounds showed activity in the AcPHF6 model. The compounds Iz2-g and Iz3-b were significantly less effective. The length of the bridge between pyridine nuclei does not appear to play an important role, since similar activities were observed for both compounds analyzed with two or three carbon atoms, nor did the nature of the substituents in the structure of each hybrid. To investigate this process further, the four most active compounds Iz-Py-4,5,6 and 7, as well as Iz1-f, were evaluated on the longer peptide model AcR3. The efficiency of the inhibition process was found to be divided by at least a factor of two (Figure 7.23).
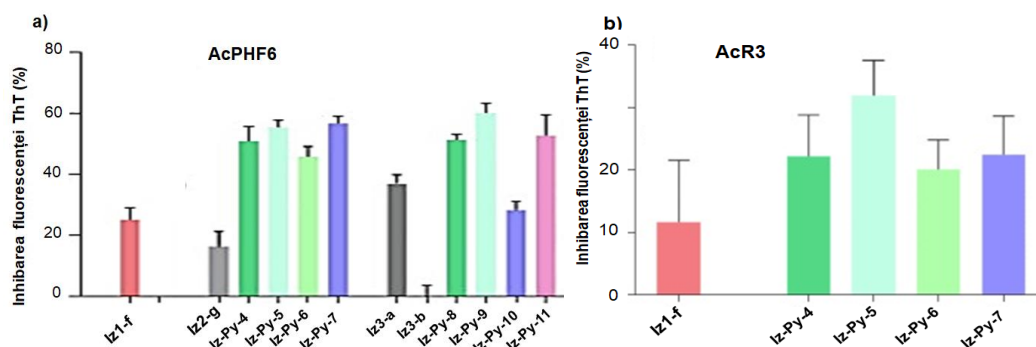
Figure 7.23. ThT tests on AcPHF6(a) and AcR3(b) models of amyloid fibrils ($\lambda_{excitare}$ = 440 nm, λ_{emisie} = 480 nm). The results are expressed as % ThT fluorescence inhibition using a compound/model ratio of 1/1 (concentration 100 μM). The error bars are the average of three independent experiments conducted in triplicate.

It was noted that fluorescence inhibition in ThT assays does not necessarily represent inhibition of amyloid fibril formation, and ThT displacement related to the tested compounds may also occur. Consequently, a solution of AcR3 fibrils was prepared in the presence of ThT and ThT signals were recorded before and immediately after the addition of compounds of the Iz-Py-4,5,6 and 7 series (Figure 7.24.a, dotted lines). No decrease in the ThT signal to 480 nm was observed, suggesting that the compounds are unable to replace the bound dye. The same observation was obtained for compound Iz1-f. To verify that the recorded signal is still from bound ThT, it was verified that the fluorescence of the compounds did not increase significantly in the presence of preformed fibrils at the working wavelengths (Figure 7.24.a, continuous lines). However, a slight increase and redshift of the fluorescence signal were observed in Figure 7.24.a (dotted lines) when adding the charged molecules Iz-Py-4-6 is probably due to this additional, even weak, fluorescence and suggests that Iz-Py-4-6 interacts strongly with fibrils. This is confirmed by the high fluorescence emission in the presence of fibrils when excited to maximum absorbance, while not showing fluorescence in their absence (Figure 7.24.b). The compound Iz1-f was evaluated by the ThT test (Figure 7.24). The strong absorption of Iz-Py-1 and Iz-Py-2 compounds around 415 nm and, in addition, the strong fluorescence of Iz-Py-1 and Iz-Py-3 in the wavelength range of bound ThT fluorescence emission did not allow their assessment [547] (Figures 7.21 and 7.26). The compound Iz-Py-7, which has in its structure two ester groups on the indolizine core, is the exception to this observation. The analogues Iz-Py-9 and Iz-Py-11 exhibited the same behavior (Figure 7.25): Iz-Py-11 with two ester groups showed no significant emission in the presence of AcR3 fibrils, unlike Iz-Py-9, suggesting the importance of the benzoyl substituent for higher interaction with fibrils.
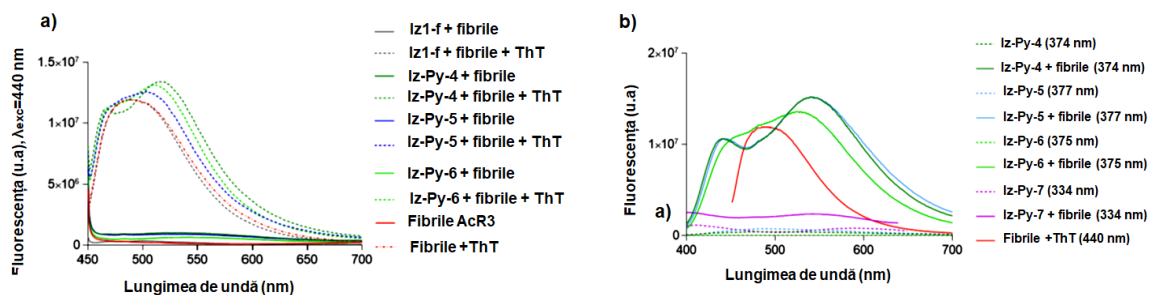
Figure 7.24. (a) Evaluation of the displacement of the fluorescence maximum of ThT. The excitation wavelength was λ=440 nm. The compound/ThT ratio was 10/1 (100/10 μM) and AcR3 fibrils were prepared from 100 μM peptide in the absence (continuous lines) or in the presence of ThT (dotted lines). (b) Fluorescence emission of compounds (100 μM) individually (dotted lines) or in the presence of 100 μM preformed fibrils (solid lines). The excitation wavelength corresponds to their maximum

absorbance (value given in parentheses); ThT in the presence of fibrils is used for comparative evaluation
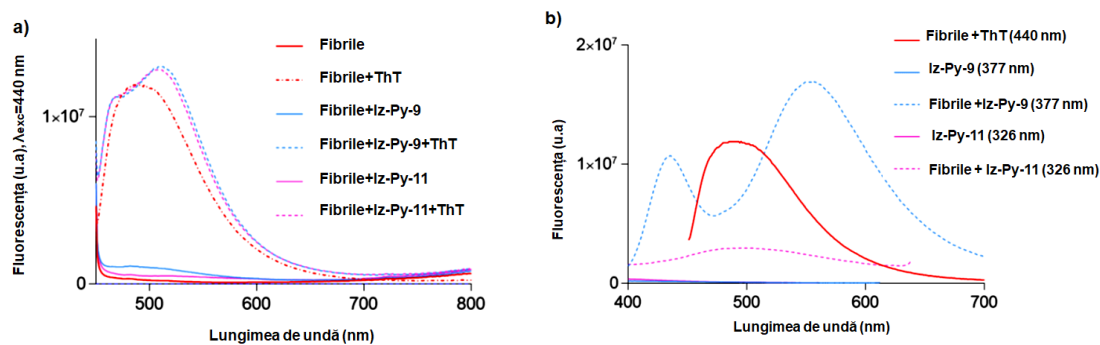
Figure 7.25. Interaction of Iz-Py-9 and Iz-Py-11 with AcR3 fibrils. (a) ThT test, $\lambda_{excitation}$ = 440 nm. Composite ratio/ThT = 1/1 (100 µM), AcR3 fibrils being prepared from 100 µM peptide, 10 µM heparin in the absence (continuous lines) or in the presence (dotted lines) of 100 µM ThT. (b) Fluorescence emission for Iz-Py-9 and Iz-Py-11 compounds (100 µM) individually and in the presence of 100 µM of preformed fibrils (prepared in the absence of ThT). The excitation wavelength corresponds to their maximum absorbance.

   To study the interaction of hybrid molecules, circular dichroism spectroscopy (CD) was used, which provides structural information about amyloid peptides during the aggregation process. CD spectra of the AcR3 peptide were recorded in a phosphate buffer in the presence of heparin as a fibrillation inducer. They showed the typical profile of a peptide with a large fraction of β-folded structures, characterized by a wide negative shoulder around 218 nm (Figure 7.28, red color) in less than 24 hours at 37°C. No significant difference was observed when compounds Iz1-f and Iz-Py1-3 were added over the fibrillation mixture (Figure 7.28.a), demonstrating that these compounds did not prevent the formation of β-folded structures. These results tend to show that Iz1-f and Iz-Py1-3 do not inhibit fibril formation or at least the formation of structures rich in β-folded sheets.
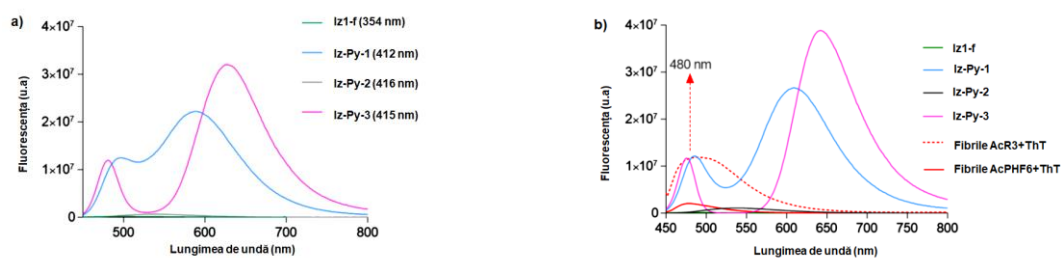
Figure 7.26. Fluorescence spectra. (a) The spectra were recorded at a concentration of 20 µM in a phosphate buffer of 50 mM in the presence of 0.1 % DMSO. The excitation wavelengths correspond to the maximum absorbance (values in parentheses); (b) The spectra were recorded at a concentration of 100 µM in a phosphate buffer of 50 mM in the presence of 0.5 % DMSO. The excitation wavelength was 440 nm, which is used for the ThT test. To compare the fluorescence profiles of ThT dye (10 µM) in the presence of AcR3 and AcPHF6 fibrils (100 µM), they are represented in red. The fluorescence intensity of Iz-Py-1 and Iz-Py-3 compounds at 480 nm is highlighted.
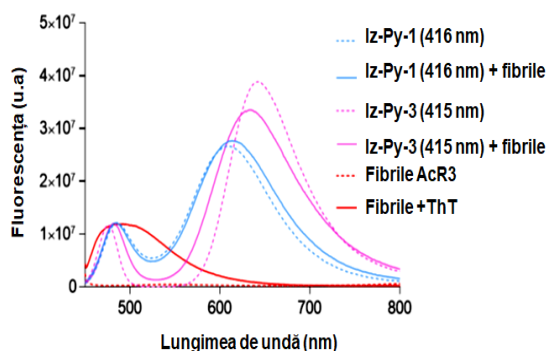
Figure 7.27. Fluorescence spectra for Iz-Py-1 and Iz-Py-3 with AcR3 fibrils. Spectra were recorded at a concentration of 100 µM of the compound in 50 mM phosphate buffer in the presence of 0.5% DMSO, individually or in the presence of 100 µM of preformed AcR3 fibrils. The excitation wavelength corresponds to their maximum absorbance (value between parentheses). To compare the fluorescence profile of ThT dye (100 µM) in the presence of ACR3, it is shown in red
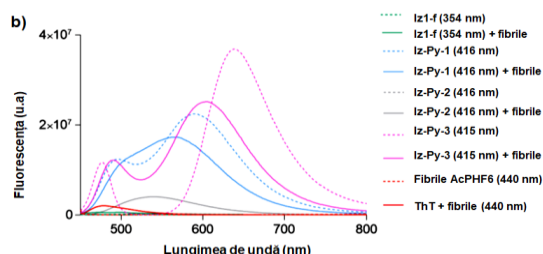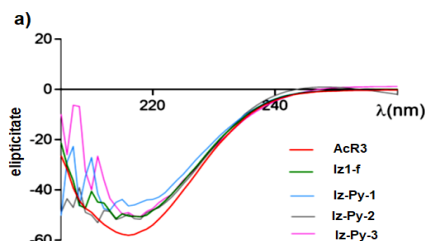
Figure 7.28. (a) CD spectra were obtained after 24 hours of incubation at 37 °C of AcR3 at 100 µM individually (red) or in the presence of 100 µM Iz1-f and Iz-Py1-3 (green, blue, grey and pink). Heparin 10 µM was used as a fibrillation inducer. (b) Fluorescence emission of Iz1-f and Iz-Py1-3 series (100 µM) for each compound separately (dotted lines) and in the presence of 100 µM of preformed AcPHF6 fibrils (solid lines). The excitation wavelength corresponds to their maximum absorbance (value given in parentheses); For comparison, 10 µM ThT was used in the presence of fibrils (continuous red line)

CHAPTER 8. Analysis of compounds synthesized by *in silico* studies (molecular modelling)

8.2. Specific scientific objectives

The specific scientific objective of the research presented in this chapter was to evaluate in *silico* N-heterocyclic compounds against Alzheimer's disease by determining intra-molecular interactions as well as binding affinity to the target molecule. To accomplish this goal, docking studies with the most relevant molecules were conducted to understand the factors involved in cholinesterase inhibition, as well as the influence of chemical structures on key molecule binding modes involved in AD.

8.5. Results and discussion

A set of ADMET descriptors has been determined for hybrid molecules and obtained data are collected in Table 8.1.

Table 8.1. ADMET molecular descriptors calculated for a series of hybrid molecules.

The analyzed compound	The number of binding acceptor sites of H	Molecular weight (g/mol)	LogP (LogD)	PSA ($Å^2$)	BBB crossing
Iz-1-f	5	370.4	3.78 (3.77)	60.6	yes
Iz-Py-1	4	385.4	-0.16 (-0.16)	51.6	yes
Iz-Py-2	9	430.4	-0.22 (-0.22)	94.8	no

The analyzed compound	The number of binding acceptor sites of H	Molecular weight (g/mol)	LogP (LogD)	PSA (Å^2)	BBB crossing
Iz-Py-3	6	415.4	-0.32 (-0.32)	60.9	yes
Iz2-f	7	414.4	4.15 (3.96)	69.9	yes
Iz2-g	5	338.3	2.86 (3.14)	69.9	yes
Iz-Py-4	6	429.5	0.21 (0.21)	60.9	yes
Iz-Py-5	10	565.6	1.62 (1.62)	79.3	no
Iz-Py-6	8	473.5	-0.42 (-0.42)	81.1	no
Iz-Py-7	4	353.4	-1.09	60.9	yes
Iz3-a	7	428.5	4.60 (4.36)	69.9	yes
Iz3-b	5	352.4	3.30 (3.53)	69.9	yes
Iz-Py-8	6	443.5	0.65 (0.65)	60.9	yes
Iz-Py-9	10	579.6	2.06 (2.06)	79.3	no
Iz-Py-10	4	367.4	-0.64 (-0.64)	60.9	yes
Iz-Py-11	8	503.5	0.77 (0.77)	79.3	no

To perform a comparative study between the hybrid compounds in Table 8.1 and other synthesized compounds, the descriptors were also calculated for some symmetrical bis-pyridinium salts and bis-indolizines (S1a-c, S2a-c and Iz1a-c and Iz2a-c respectively). All calculations were performed using *Marvin* software and collected in Table 8.2.

Table 8.2. ADMET molecular descriptors for symmetrical bis-pyridinium salts and bis-indolizines

The analyzed compound	The number of binding acceptor sites of H	Molecular weight (MW)	LogP (=LogD)
S1a	4	394.4	-4.24
S1b	14	484.4	-4.36
S1c	8	454.5	-4.55
S2a	4	422.5	-3.35
S2b	14	512.5	-3.47
S2c	8	482.5	-3.66
Iz1a	8	584.6	6.37
Iz1b	18	674.6	6.25
Iz1c	12	644.6	6.06
Iz2a	8	612.6	7.26
Iz2b	18	702.6	7.14
Iz2c	12	672.7	6.95

Pyridil-indolizines (Iz1-f, Iz2-f, Iz2-g, Iz3-a and Iz3-b) are not protonated or are only partially protonated at 7.4 pH (calculated pKa of 4.6 for Iz1-f and 5.6 for the other compounds), resulting in a large increase in lipophilicity reflected by high LogP values. Alkylation of the pyridine ring leads to the generation of monocationic molecules over a wide pH range, thereby conferring ADMET descriptor values compatible with potential CNS drugs [596].

In the series of hybrid molecules derived from 1,2-di(4-pyridyl)ethane and 1,3-bis(4-pyridyl)propane, it was found that the change of the more hydrophobic p-methoxybenzoyl group on the indolizine nucleus by the methyloxycarbonyl group has no effect on PSA, but significantly decreases LogP values (from 0.65 for Iz-Py-8 to -0.64 for Iz-Py-10, or 2.06 for Iz-Py-9 to 0.77 for Iz-Py-11). Increasing the chain length between the two pyridine nuclei does not affect PSA but leads to an increase in lipophilicity (LogP being between -0.32 for Iz-Py-3 and 0.65 for Iz-Py-8).

The BBB penetration capability was estimated using *the Swiss ADME* web service. The results predicted that some molecules exhibit high PSA and/or LogP values (Iz-Py-5, Iz-Py-6, Iz-Py-9, Iz-Py-11), i.e., those compounds containing large lipophilic substituents are not favorable to BBB penetration. The symmetric bis-pyridinium dications (S1a-c, S2a-c) are too polar (strongly negative logP). It has also been observed that bis-indolizines (Iz1a-c, Iz2a-c) are too lipophilic (LogP > 6), with high PSA values. Their calculated high lipophilicity is experimentally correlated with low solubility in water and the formation of aggregates. However, the involvement of an active BBB penetration mechanism cannot be excluded.

Docking calculations **were performed** to compare possible binding modes of Iz-Py-8 and Iz-Py-10 compounds (Figure 8.3) at the active sites of the two human cholinesterase, hAChE and hBChE. While both compounds were found to be active as AChE inhibitors (electric eel or human), they exhibited different behavior on BChE (equine or human). It is difficult to design a good inhibitor that is active on both hAChE and hBChE because these two enzymes differ considerably in size (the binding site of hAChE is much smaller than that of hBChE) and composition (residues W286, V294, Y124, Y337, F297 for hAChE and A277, P285, Q119, A328 and V288 respectively for hBChE).

The compounds Iz-Py-8 and Iz-Py-10 showed *Glide* docking scores of -11.3 and -9.3 kcal/mol, respectively, in hAChE and -9.1 kcal/mol and -8.5 kcal/mol in hBChE, respectively. These theoretical affinity models are consistent with the experimental IC_{50} values presented in Chapter 7, with the Iz-Py-8 compound being more active than Iz-Py-10 on both enzymes. In the hAChE active site (Figure 8.4), the optimized spatial orientation of the Iz-Py-8 compound was identified with the pyridinium fragment facing towards the bottom of the catalytic site, close to E202 and catalytic serine S203 (Figure 8.4.b).

This binding mode has been fully preserved among the 20 best positions of the compound Iz-Py-8, probably determined by stabilizing interaction with negatively charged E202. The compound Iz-Py-8 was not in a suitable position for enzymatic hydrolysis with hAChE. The Iz-Py-10 compound with a methylester group was oriented with the pyridinium fragment towards the grid box input (*x, y, z*) and the methylester group at position 3 in the catalytic process area at the bottom, allowing possible hydrolysis (Figure 8.4.b). The indolizine fragment is surrounded by W86, Y337, F338 residues and the pyridinium fragment establishes π- stacking interactions with W286. Due to its smaller size, the Iz-Py-10 compound showed more heterogeneity between binding positions. These data are consistent with similar activity observed for both Iz-Py-8 and Iz-Py-10 on hAChE.

At the binding site of hBChE, the Iz-Py-8 compound adopted an optimized conformation oriented with the pyridinium fragment inserted at the bottom of the catalytic site, close to the H438 catalytic subunit. The charge is stabilized by the hydroxyl groups in tyrosine Y332,

tyrosine Y440 and three carbonyl groups of residues A328, G78 and H438 (Figure 8.4.d). The W82 residue provides a favorable π interaction with the pyridinium fragment.

The methyl ester is located less than 5 Å catalytic S198 and it is assumed that this compound may adopt a tight binding mode to butyrylcholine (the natural substrate). This binding mode was highly conserved among the twenty best positions of the compound Iz-Py-8. The optimized conformation of the compound Iz-Py-10 showed its pyridinium fragment oriented towards the entrance to the *grid box*, where it is stabilized by oxygen from the carbonyl group of the A328 residue (Figure 8.4.c). The methyl ester at position 1 is in a very good position for hydrolysis by subunit S198. The compounds Iz-Py-8 and Iz-Py-10 adopted a protected orientation of their pyridinium fragments at the active site of hBChE, but an inverse positioning in hAChE, Iz-Py-8 appears with the pyridinium fragment towards the active site, while Iz-Py-10 has the same fragment oriented towards the entrance to the *grid box*.

The compounds interact with the AlaW286neighboring amino acid in hAChE due to the $\pi\iota$-cation electrostatic interaction between the benzoyl substituent in the structure of the compound Iz-Py-8 and the pyridinium fragment in the structure of the compound Iz-Py-10. As regards the two ester groups in the structure of the compound Iz-Py-10, it was noted that in the case of both enzymes, a methyl ester is in a favourable position for hydrolysis.
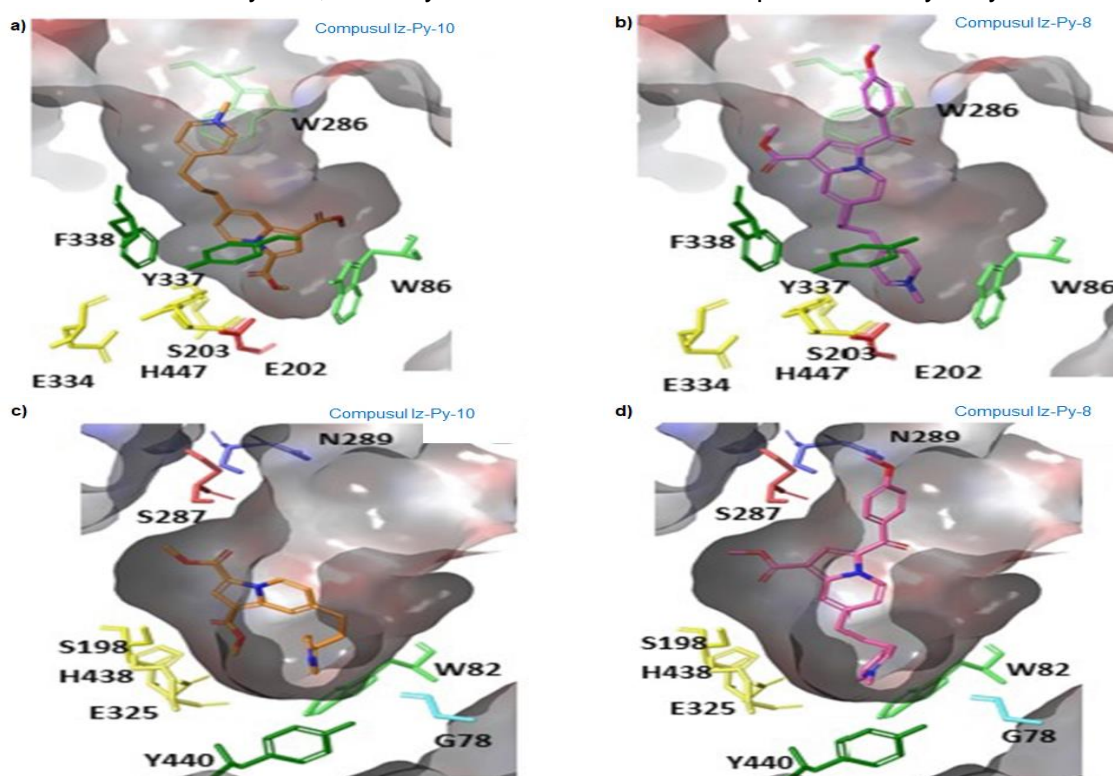
Figure 8.4. In a) and b) the binding sites of hAChE with Iz-Py-10 and Iz-Py-8 docked compounds are illustrated. In c) and d) respectively, the optimized docking positions of the compounds Iz-Py-10 and Iz-Py-8 in the active site of hBChE are represented. Catalytic residues are shown in yellow

CHAPTER 9. General conclusions and elements of originality

9.1. General conclusions and elements of originality

Various procedures have been shown in the literature for the synthesis of indolizines that include single or multiple reaction steps. The main routes of synthesis of indolizines include the Tschitschibabin reaction, cycloaddition reactions, intramolecular cyclization, cycloisomerization from 2-pyridine derivatives and pyridotriazole cycloaddition with alkynes. Newer and more environmentally friendly methods such as microwave-assisted reactions,

ultrasound, reactions on a solid support, without solvents, without metal catalysts and reactions in the aqueous medium have been proposed especially in recent years by the literature through "green" syntheses of quaternary pyridinium salts and indolizines compounds.

In this doctoral thesis, the synthesis of N-heterocyclic compounds (quaternary pyridinium salts, indolizines derivatives, pyridinium-indolizine hybrids, metal complex) was achieved by conventional methods starting from three bipyridine compounds (4,4'-bipyridyl, 1,2-di(4-pyridyl)ethane and 1,3-bis(4-pyridyl)propane). Quaternary pyridinium salts obtained (S1a-e and S2a-q) by conventional synthesis showed high yields (85-95% ± 1%) and were characterized by elemental analysis and spectral methods, IR, ^1H NMR and ^{13}C NMR. Through classical synthesis, processes were obtained bisindolizines (Iz1a-e, Iz2a-e) and mono-indolizines with variable yields (12-85%), and were characterized by elemental analysis, IR, ^1H NMR and ^{13}C NMR.

Several new N- pyridinium-indolizine (Iz-Py) hybrids with structural diversity were obtained by varying the initial bipyridines and N-alkyl substituents with good yields (50-100%). Two synthesis strategies were pursued based on the formation of the indolizine core by 1,3-dipole cycloaddition of alkynes with generated ylides *in situ* from appropriately substituted pyridinium salts. The compounds showed high purity and were characterized by spectrophotometric, chromatographic, and elemental analyses.

A new mixed lanthanide (III) complex of La-Nd-DPY was prepared by reacting the La (III) and Nd (III) sulfates with the bis-quaternary salt of bipyridinium S1a. The characterization of the possible structure for the new mixed Ln complex was achieved by several modern analysis techniques (MS, SEM, PXRD). A modern electrochemical method, cyclic voltammetry, was used in the study of the redox potential of the La-Nd-DPY complex, which turned out to be within a biologically relevant range.

The synthesis processes by *green* methods (MW and US) proceeded with very good yields (77-98%) and in a much shorter time (5-15 min) than the classical method.

The structure of the synthesized compounds was confirmed by determining the melting points, IR, NMR, and elemental analyses and comparing the data obtained with those of the control compounds obtained by classical synthesis. A series of quaternary pyridinium salts, based on the structure of 1,2-di(4-pyridyl) ethane, were obtained using for the first time two different *green* methods, such as microwave irradiation (MW) and ultrasound (US). By using unconventional methods in the synthesis processes of organic compounds with important biological properties, the consumption of reagents was considerably reduced.

Although studies with less toxic syntheses of indolizine compounds including methods without metal catalysts are presented in the literature, synthesis by biocatalysis with plant enzymes in aqueous buffer has not been reported to date in other studies.

Single-step processes leading to the generation of bis-indolizine symmetric compounds have been developed for the first time through new enzyme biocatalysis approaches. The unconventional synthesis of bis-indolizines with moderate to excellent yields (40-86%) was achieved by multicomponent reactions, starting from bipyridine heterocyclic compounds, reactive halogenated derivatives and activated alkynes. A set of local plants was evaluated for enzymatic activity in "one pot" biocatalysis of fluorescent indolizine compounds. Most of the evaluated plants demonstrated a rich content of oxidoreductase enzymes (POD: 0,56-1,08 mmol purpurogaline·g^{-1} fresh vegetable weight·min^{-1}, PPO: 27,19-48,95 PPO units /mg fresh vegetable weight, CAT: 3,27-21,71 µmol O_2·g^{-1} fresh vegetable weight·min^{-1}). Horseradish root (*Armoracia rusticana*) was selected as the most promising source of biocatalysts among the evaluated plants, and the yields obtained were higher than in the conventional synthesis method.

Indolizine compounds could be obtained by catalyzed reactions using the I_2 / H_2O_2 system, this being an unconventional new synthesis method used for the first time in the synthesis of bis-indolizines. The structures of bis-indolizine derivatives have been confirmed by NMR spectrometry, elemental analysis, as well as FT-IR spectrometry.

The tested ScPy were found to have no toxic action on plants, activity assessed by their effect on wheat seed germination. The use of simple seed germination tests demonstrated the absence of toxic effects of ScPy (S1a-e and S2a-e) and indolizines (Iz1a-e and Iz2a-e) on plant germination and thus on the environment. Exposure of wheat seeds to various concentrations of ScPy (10^{-5}M; 10^{-6}M) or indolizines (10^{-3}M; 10^{-4}M) showed no harmful effects on the process of germination and growth of sprouts. The most sensitive physiological parameters demonstrated that the indolizine compounds, at the evaluated concentrations, showed no harmful effects on the germination and growth of wheat germ, which is also confirmed by microscopic analyses with confocal laser scanning.

The cytotoxicity of some indolizine compounds **on the growth of the yeast model microorganism** *Saccharomyces cerevisiae* MIUG 3.6 was also evaluated. By adding indolizine derivatives to the fermentation medium of the yeast strain *S. cerevisiae* MIUG 3.6, a stimulation of alcoholic fermentation was found for all analyzed samples by supplementing the fermentation media with indolizine compounds compared to the yeast cell fermentation control sample (in the absence of tested compounds). Various parameters (number of generations, growth rate, generation time, dry matter yield, grade of budding yeast cells and degree of yeast autolysis, fermentation intensity), describing yeast growth, suggest that culture medium supplemented with different concentrations of bis-indolizines (10 µM and 1 µM) did not exert toxic effects on yeast strain growth, under submerged and shaking aerobic cultivation conditions. In this thesis, the toxicity of quaternary bipyridinium salts and indolizines compounds on plant germination as well as on the growth of the yeast model microorganism *Saccharomyces cerevisiae* in multiplication and fermentation processes was carried out for the first time.

Evaluation of antimicrobial activity demonstrated that most ScPy of the S2a-c and S2f-q series had good activity against the pathogenic microorganism *E. coli.* The most active ScPy against *E. coli* were S2c, S2g and S2q, with a MIC value of 0.312 mg/mL. Of the nine bacteria and fungi tested, *Alternaria* spp. showed the highest sensitivity to symmetric compounds assessed at 5 mg/mL (diameter of the inhibition zone was a maximum of 27 mm), while *Penicillium expansum* showed a medium sensitivity (inhibition zone up to 12 mm diameter).

The cytotoxic activity of La-Nd-DPY on cancer cell lines of ovarian (A2780), mammary (MCF7) and prostate (PC3) origin and PC3-cell-derived multicellular tumor spheroids was evaluated by 3-(4,5-dimethylthiazole), MTT, and acid phosphatase (APH) methods. Compared to cisplatin, this new complex showed improved toxicity, with IC_{50} values at least 10 times higher, even at 24 hours of exposure. Cytotoxic effects appear to be mediated by the generation of reactive oxygen species (ROS) but not by apoptosis, confirmed by activation of caspase 3/7 and Hoechst staining tests of nuclei. The mechanism of cell death observed in cytotoxicity tests is likely due to other cell lysis pathways that may be investigated in future research.

In this doctoral thesis, several bis-pyridinium salts and pyridinium-indolizine hybrids were synthesized and evaluated. The molecules were tested against processes distinctive to AD, i.e., antioxidant properties, inhibition of AChE and BChE, and interference with amyloid fibrillation using tau peptide models (τ). No hybrid indolizine compounds showed significant activity on the three targets simultaneously, i.e., antioxidant activity (inhibition of DPPH %>50 to 48 µg/mL), inhibition of hChE (IC_{50} < 10 µM) and inhibition of amyloid fibril formation. The

Iz-Py-4, 5, 6, 7 and Iz-Py-8, 9, 10,11 series demonstrated reduced antioxidant activity and moderate inhibition of amyloid fibril formation. However, most cationic molecules in these two series were active on both eeAchE and hChE within a micromolar concentration range.

Several molecules also inhibited eqBChE but did not inhibit the human enzyme hBChE. The Iz-Py-1, Iz-Py-2, and Iz-Py-3 series showed significantly different behavior from the other two series of compounds. Both the limitation of solubility (molecules are prone to aggregation in aqueous solution) and spectral properties did not allow their study either as cholinesterase inhibitors or as fibril inhibitors. However, in the context of amyloid fibril, fluorescence and CD experiments have shown that if these molecules do not interfere in the fibrillation process, the positively charged compounds Iz-Py-1, Iz-Py-2 and Iz-Py-3, and especially the derivative substituted with the nitro group, can be new fluorescent dyes in the formation of amyloid fibril. The method of inhibiting thermal denaturation of human albumin observed a promising anti-inflammatory potential of ScPy S1a-c and S2a-c, close to diclofenac sodium, a known anti-inflammatory. Alkylation of the pyridine ring leads to the generation of monocationic molecules over a wide pH range, generating ADMET descriptor values compatible with potential CNS drugs.

Increasing the length of the chain between the two pyridine fragments does not influence PSA values but leads to an increase in lipophilicity. Compounds containing large lipophilic substituents are not favorable for penetration of the blood-brain barrier. Simulation by comparative molecular modeling of the docked compounds Iz-Py-8 and Iz-Py-10 in hAChE and hBChE, revealed in the binding mechanism the importance of the substituent to C-3 (p-methoxybenzoyl or methyloxycarbonyl, respectively) in the indolizines structure. It was found that the Iz-Py-8 hybrid with a larger molecule fits better into the active site of the two enzymes, compared to the Iz-Py-10 compound which showed a greater degree of freedom.

The presented data highlight the role of compounds obtained through synthesis processes of "green chemistry" in the research of biological properties.

Synthetic organic compounds represent a fruitful field of research to detect unknown molecules with novel structures and properties that research developments have refined for targeted biological roles.

This PhD thesis also led to the identification and structural characterization of novel molecules, which could contribute to the complex process of discovering potential drugs for treating a wide range of conditions. These results demonstrated the importance of N-heterocyclic compounds and constitute the premise for research into new compounds, reported in this doctoral thesis, that could be promising agents in future research as low- or non-toxically anti-inflammatory, antimicrobial, and anticancer agents.

CHAPTER 10. Dissemination of results

Articles published in specialized journals indexed by ISI (WOS) during doctoral studies (cumulative FI = 105.6)

Articles published in ISI-indexed specialist journals (WOS) from the doctoral thesis (cumulative IF = 25,9)

1. **Botezatu Dediu**, A.V.; Bahrim, G.E.; Ungureanu, C.V.; Busuioc, A.C.; Furdui, B.; Dinica, R.M. Green "one-Pot" Fluorescent Bis-Indolizine Synthesis with Whole-Cell Plant Biocatalysis. *Green Process. Synth.* **2023**, *12*, https://doi.org/10.1515/gps-2023-0046, **FI = 4,3**.

2. **Dediu Botezatu, A.V**.; Apetrei, R.-M.; Costea (Nour), I.F.; Barbu, V.; Grigore-Gurgu, L.; Botez, F.; Dinica, R.M.; Furdui, B.; Cârâc, G. Synthesis and Characterization of Novel Chitosan Derivatives (Containing Dipyridinium Quaternary Salts) with Antimicrobial Potential. *Carbohydr. Res.* **2023**, 108964, doi: https://doi.org/10.1016/j.carres.2023.108964, **FI = 3,1**.

3. Baussanne, I.; Firstova, O.; **Dediu Botezatu, A.**; Larosa, C.; Furdui, B.; Ghinea, I.O.; Thomas, A.; Chierici, S.; Dinica, R.; Demeunynck, M. Interest of Novel N-Alkylpyridinium-Indolizine Hybrids in the Field of Alzheimer's Disease: Synthesis, Characterization and Evaluation of Antioxidant Activity, Cholinesterase Inhibition, and Amyloid Fibrillation Interference. *Bioorg. Chem.* **2021**, *116*, 105390, https://doi.org/10.1016/j.bioorg.2021.105390, **FI = 5,3.**

4. **Botezatu (Dediu), A.V.;** Horincar, G.; Ghinea, I.O.; Furdui, B.; Bahrim, G.-E.; Barbu, V.; Balanescu, F.; Favier, L.; Dinica, R.-M. *Whole-Cells of Yarrowia lipolytica Applied in "One Pot" Indolizine Biosynthesis*, *Catalysts* **2020**, *10*, 629. https://doi.org/10.3390/catal10060629, **FI = 4,1.**

5. Tăbăcaru, A.; **Botezatu Dediu, A.V.;** Dinică, R.M.; Cârâc, G.; Basliu, V.; Paula Cabral Campello, M.; Silva, F., Pinto; C.I.G, Guerreiro, J.F., Martins, M., Mendes, F., Marques, F. (**2020**) *Biological properties of a new mixed lanthanide(III) complex incorporating a dypiridinium ylide, Inorganica Chim. Acta*, **506** (III), 119517. https://doi.org/10.1016/j.ica.2020.119517, **FI = 2,8.**

6. Tăbăcaru, A.; **Dediu Botezatu, A.V**.; Horincar, G.; Furdui, B.; Dinică, R.M. *Green Accelerated Synthesis, Antimicrobial Activity and Seed Germination Test of Quaternary Ammonium Salts of 1,2-bis(4-pyridyl)ethane*, *Molecules* **2019**, *24*, 2424. https://doi.org/10.3390/molecules24132424, **FI = 4,6**

7. Carac, A.; Boscencu, R.; **Dediu, A.V**.; Bungau, S.G.; Dinica, R.M. Solvent Effects on the Spectral and Electrochemical Properties of Some Pyridinium Quaternary Compounds. *Rev. Chim.* **2017**, *68*, https://doi.org/10.37358/RC.17.7.5688, **FI = 1,7.**

Books/Chapters in books from the doctoral thesis:

1. Bianca Furdui, **Andreea V. Dediu (Botezatu)**, Rodica M. Dinica, Copper Catalysis in Organic Synthesis, editat de Gopinathan Anilkumar, Salim Saranya; **Capitolul 2**, *Cu-Catalyst in Reactions Involving Pyridinium and Indolizinium Moieties*; pg7-22; John Wiley & Sons, **2021**; ISBN 3527347372, 9783527347377; https://books.google.ro/books?id=0KTsDwAAQBAJ

2. Chia-Hung Kuo and Chwen-Jen Shieh (Eds.), Biocatalytic Process Optimization, Pages: 296, Published: January **2021** (*This book is a printed edition of the Special Issue Biocatalytic Process Optimization that was published in Catalysts*), ISBN 978-3-03943-915-7 (Hbk); ISBN 978-3-03943-916-4 (PDF), pg 203-219, https://doi.org/10.3390/books978-3-03943-916-4.

Articles published in ISI-indexed specialist journals (WOS) through collaboration (cumulative IF = 79,7)

1. *El Moujahed, S.; Dinica, R.M.; Abou Oualid, H.; Cudalbeanu, M.;* **Botezatu-Dediu, A.V.**; *Cazanevscaia Busuioc, A.; Ouazzani Chahdi, F.; Kandri Rodi, Y.; Errachidi, F. „Sustainable Biomass as Green and Efficient Crosslinkers of Collagen: Case of by-Products from Six Pomegranate Varieties with Global Commercial Interest in Morocco". J. Environ. Manage.* **2023**, *335, 117613, doi:10.1016/j.jenvman.2023.117613*, **IF = 8,7**.

2. *Busuioc, A.C.; Costea, G.V.;* **Botezatu, A.V.D**.; *Furdui, B.; Dinica, R.M. „Cucumis Metuliferus L. Fruits Extract with Antioxidant, Anti-Inflammatory, and Antidiabetic Properties as Source of Ursolic Acid". Separations* **2023**, *10, doi:10.3390/separations10050274,* **IF = 3,34**.

3. *Bălănescu, F.;* **Botezatu, A.V**.; *Marques, F.; Busuioc, A.; Marincaş, O.; Vînătoru, C.; Cârâc, G.; Furdui, B.; Dinica, R.M.; „Bridging the Chemical Profile and Biological Activities of a New Variety of Agastache Foeniculum (Pursh) Kuntze EXtracts and Essential Oil". Int. J. Mol. Sci.* **2023**, *24, 828, doi:10.3390/ijms24010828,* **IF = 6,2**.

4. *Zongo, E.; Busuioc, A.; Meda, R.N.-T.;* **Botezatu, A.V.;** *Mihaila, M.D.; Mocanu, A.-M.; Avramescu, S.M.; Koama, B.K.; Kam, S.E.; Belem, H.; „Exploration of the Antioxidant and Anti-Inflammatory Potential of Cassia Sieberiana DC and Piliostigma Thonningii*

*(Schumach.) Milne-Redh, Traditionally Used in the Treatment of Hepatitis in the Hauts-Bassins Region of Burkina Faso". Pharmaceuticals **2023**, 16, 133, doi:10.3390/ph16010133, IF = 5,2.*

5. *Souleymane, H.D.; Djibo, A.K.; Seyni, S.H.; Zakaria, O.; **Botezatu, A.V.**; Dinica, R.M.; Ibrahim Maman Laouali, A.; Kouakou, N.D.V. „Phytochemical Characterization and In Vitro Evaluation of the Anti-Sickle Cell Activity of Aqueous and Ethanolic Extracts of Two Medicinal Plants from Niger: Flueggea Virosa (Roxb. Ex Willd.) Royle and Kigelia Africana (Lam.) Benth". Plants **2023**, 12, 3522, doi:10.3390/plants12203522, IF = 4,5.*

6. *Lanciu Dorofte, A.; Dima, C.; Ceoromila, A.; **Botezatu, A**.; Dinica, R.; Bleoanca, I.; Borda, D. „Controlled Release of β-CD-Encapsulated Thyme Essential Oil from Whey Protein Edible Packaging". Coatings **2023**, 13, 1–18, doi:10.3390/coatings13030508, IF = 3,4.*

7. *Musat, V.; Crintea (Capatana), L.; Anghel, E.-M.; Stanica, N.; Atkinson, I.; Culita, D.C.; Baroiu, L.; Tigau, N.; Ceoromila, A.C.; **Botezatu (Dediu), A.-V**.; et al„ Ag-Decorated Iron Oxides-Silica Magnetic Nanocomposites with Antimicrobial and Photocatalytic Activity". Nanomaterials **2022**, 12, doi:10.3390/nano12244452, IF = 5,71.*

8. *Nechita, P.; Roman, M.; Cantaragiu Ceoromila, A.; **Botezatu, A.V.** „Improving Barrier Properties of Xylan-Coated Food Packaging Papers with Alkyl Ketene Dimer". Sustainability **2022**, 14, doi:10.3390/su142316255, IF = 3,88.*

9. *Silihe, K.K.; Zingue, S.; Sipping, M.T.K.; Cazanevscaia, A.B.; **Botezatu, A.V.D**.; Njamen, D.; Dinica, R.M. „The Antioxidant Potential of Ficus Umbellata Vahl (Moraceae) That Accelerates In Vitro and the In Vivo Anti-Inflammatory Protective Effects". Appl. Sci. **2022**, 12, doi:10.3390/app12189070, IF = 2,83.*

10. *Rusu, L.; Grigoras, C.-G.; Simion, A.-I.; Suceveanu, E.-M.; **Botezatu, A.V.D**.; Harja, M. „Biosorptive Removal of Ethacridine Lactate from Aqueous Solutions by Saccharomyces Pastorianus Residual Biomass/Calcium Alginate Composite Beads: Fixed-Bed Column Study". Materials (Basel). **2022**, 15, doi:10.3390/ma15134657, IF = 3,74.*

11. *Tanase (Butnariu), L.-A.; Nistor, O.-V.; Andronoiu, D.-G.; Mocanu, G.-D.; **Botezatu Dediu, A.V.**; Botez, E. „Different Types of Meatballs Enriched with Wild Thyme/Lemon Balm Aqueous Extract-Complex Characterization". Molecules **2022**, 27, doi:10.3390/molecules27123920, IF = 4,92.*

12. *Balanescu, F.; Busuioc, A.C.; **Botezatu, A.V.D.**; Gosav, S.; Avramescu, S.M.; Furdui, B.; Dinica, R.M. „Comparative Study of Natural Antioxidants from Glycine Max, Anethum Graveolensand Pimpinella Anisum Seed and Sprout Extracts Obtained by Ultrasound-Assisted Extraction". Separations **2022**, 9, 152, doi:10.3390/separations9060152, IF = 3,34.*

13. *Ngenge Tamfu, A.; Roland, N.; Munvera Mfifen, A.; Kucukaydin, S.; Gaye, M.; **Botezatu, A**.V.; Emin Duru, M.; Mihaela Dinica, R. „Phenolic Composition, Antioxidant and Enzyme Inhibitory Activities of Parkia Biglobosa (Jacq.) Benth., Tithonia Diversifolia (Hemsl) A. Gray, and Crossopteryx Febrifuga (Afzel.) Benth". Arab. J. Chem. **2022**, 15, 103675, doi:10.1016/j.arabjc.2021.103675, IF = 6,21.*

14. *El Moujahed, S.; Errachidi, F.; Abou Oualid, H.; **Botezatu-Dediu, A.V.**; Ouazzani Chahdi, F.; Kandri Rodi, Y.; Dinica, R.M. „Extraction of Insoluble Fibrous Collagen for Characterization and Crosslinking with Phenolic Compounds from Pomegranate Byproducts for Leather Tanning Applications". RSC Adv. **2022**, 12, 4175–4186, doi:10.1039/d1ra08059h, IF = 4,03.*

15. *Ngenge Tamfu, A.; Mfifen Munvera, A.; **Dediu Botezatu, A.V.;** Talla, E.; Ceylan, O.; Tagatsing Fotsing, M.; Tanyi Mbafor, J.; Shaheen, F.; Mihaela Dinica, R. „Synthesis of Benzoyl Esters of β-Amyrin and Lupeol and Evaluation of Their Antibiofilm and Antidiabetic Activities". Results Chem. **2022**, 4, 100322, doi:10.1016/j.rechem.2022.100322, IF = 2,3.*

16. *Dinica, R.M.; Sandu, C.; Dediu **Botezatu, A.V**.; Busuioc, A.C.; Balanescu, F.; Mihaila, M.D.I.; Dumitru, C.N.; Furdui, B.; Iancu, A.V. „Allantoin from Valuable Romanian Animal and Plant Sources with Promising Anti-Inflammatory Activity as a Nutricosmetic Ingredient". Sustainability **2021**, 13, 10170, doi:10.3390/su131810170, **IF = 3,25**.*

17. *Rusu, L.; Grigoraş, C.G.; Suceveanu, E.M.; Simion, A.I.; **Botezatu, A.V.D**.; Istrate, B.; Doroftei, I. „Eco-Friendly Biosorbents Based on Microbial Biomass and Natural Polymers: Synthesis, Characterization and Application for the Removal of Drugs and Dyes from Aqueous Solutions". Materials (Basel). **2021**, 14, doi:10.3390/ma14174810, **IF = 3,74**.*

18. *Busuioc, A.C.; **Botezatu, A.V.D**.; Furdui, B.; Vinatoru, C.; Maggi, F.; Caprioli, G.; Dinica, R.M. „Comparative Study of the Chemical Compositions and Antioxidant Activities of Fresh Juices from Romanian Cucurbitaceae Varieties". Molecules **2020**, 25, doi:10.3390/molecules25225468, **IF = 4,41**.*

Participation in project research-development teams/research grants:

1. **Project Director,** Andreea V. DEDIU BOTEZATU **(PN-III-P1-1.1-MC2019-1608 within Mobility projects for researchers' competition** 2019): PhD thesis preparation in the Department of Molecular Pharmaceutical Chemistry, Rhone Alpes University, Grenoble, France, November 2019 -December 2019.

2. Member of Erasmus project KA220-HED, Cooperation Partnership, number 2022-1-TR01-KA220-HED-000089361, 7171, „Green Chemistry Applications on Selected Medicinal and Aromatic Plants in the Artvin Region", financed by the European Union.

3. Member of ADER project 5.2.1, nr. 521/18.07.2023, „Conservarea și valorificarea patrimoniului genetic al speciilor aromatice și medicinale pretabile a fi cultivate pe teritoriul României", MADR, Coordonator de proiect BRGV Buzău.

4. **Andreea V. DEDIU BOTEZATU,** member of the target group within the project "Proactive Health Without Borders" 2SOFT/4.1/104, Joint Operational Programme Romania–Republic of Moldova 2014- 2020 – ENI -2nd Call for proposals Prioritatea 4.1 – Sprijin pentru dezvoltarea serviciilor de sănătate și a accesului la sănătate.

5. Target group member, **Andreea-Veronica Dediu Botezatu**, Program 1-Development of the national research and development system, Subprogram 1.2 – Institutional performance – RDI excellence financing projects, Project code 14PFE/17.10.2018, 2018, Project title: Excelență, performanță și competitivitate în activități CDI la Universitatea "Dunărea de Jos" din Galați, EXPERT.

6. Member, **Andreea-Veronica Dediu Botezatu**, Project title: "Strategii inovative și durabile de obținere a acoperirilor pe bază de hemiceluloză cu proprietăți adecvate hartiei de ambalaj activ pentru alimente", PN-III-P4-PCE2021-0714, 2021.

Participation in international summer schools:

1. **Andreea Veronica Dediu Botezatu**, Dunarea de Jos University of Galati, has Attended the Web edition of the International School of Chemistry for everyday life, 2020 September 1-6, Camerino Italy.

2. **Andreea Veronica DEDIU BOTEZATU**, participated in International Summer School, FOOD SAFETY AND HEALTHY LIVING, FSHL – 2020, held online, July 5-8, 2020.

AWARDS

1. **First prize**, 11th Ediţion of the Scientific Conference of the Doctoral Schools of „Dunărea de Jos" University, Galaţi,18-19 June **2023**.

2. **Third prize**, 11ᵗʰ Edition of the Scientific Conference of the Doctoral Schools of „Dunărea de Jos" University, Galați,18-19 June **2023**.

3. Diploma of Excellence Assist.PhD. **Botezatu Andreea Veronica**, for excellent results in research activity at "Dunarea de Jos" University of Galati, CNFIS-FDI-2021-0443, CEREX **2022**

4. **First prize**, 10ᵗʰ Edition of the Scientific Conference of the Doctoral Schools of „Dunărea de Jos" University, Galați,18-19 June **2022**.

5. Diploma of Excellence Assist.PhD. **Botezatu Andreea Veronica**, for excellent results in research activity at "Dunarea de Jos" University of Galati, CNFIS-FDI-2021-0443, CEREX **2021**

6. **First prize**, 9th Edition of the Scientific Conference of the Doctoral Schools of „Dunărea de Jos" University, 10th and 11th of June **2021**.

7. **Second prize-** 9th Edition of the Scientific Conference of the Doctoral Schools of „Dunărea de Jos" University, 10th and 11th of June **2021**.

8. **First prize** in the Danube Growth Initiative competition within the BLUACT project - BLUegrowth cities in ACTion, **2020**

9. **Award for the MOST ACTIVE PhD STUDENT**, **Andreea Veronica DEDIU BOTEZATU**, during International Summer School, FOOD SAFETY AND HEALTHY LIVING, FSHL – **2020**, July 5-8, 2020.

10. **AWARD - THE MOST ACTIVE TEAM OF STUDENTS**, **PhD Students from "Dunarea de Jos" University of Galati,** Romania during International Summer School FOOD SAFETY AND HEALTHY LIVING FSHL – 2020, held online, Romania, July 5-8, **2020.**

11. **First prize**, Eighth Edition of the Scientific Conference of the Doctoral Schools of „Dunărea de Jos" University, Galați,18-19 June **2020**.

12. **Second prize**, Seventh edition of the Scientific Conference of the Doctoral Schools of „Dunărea de Jos" University, Galați, 13-14 June **2019**.

13. PN-III-P1-1.1-PRECISI-2020-48235, coordinated by UEFISCDI - Award for the article with the title „Biological properties of a new mixed lanthanide (III) complex incorporating a dypiridinium ylide".

14. PN-III-P1-1.1-PRECISI-2021-65925, coordinated by UEFISCDI - Award for the article with the title „Allantoin from Valuable Romanian Animal and Plant Sources with Promising Anti-Inflammatory Activity as a Nutricosmetic Ingredient".

15. PN-III-P1-1.1-PRECISI-2021-66903, coordinated by UEFISCDI - Award for the article with the title „Interest of novel N-alkylpyridinium-indolizine hybrids in the field of Alzheimer's disease: Synthesis, characterization and evaluation of antioxidant activity, cholinesterase inhibition, and amyloid fibrillation interference".

16. PN-III-P1-1.1-PRECISI-2020-50800, coordinated by UEFISCDI - Award for the article with the title „Whole-Cells of Yarrowia lipolytica Applied in "One Pot" Indolizine Biosynthesis".

Conference participation with oral presentations/posters:

1. International Scientific Symposium „Modern Trends In The Agricultural Higher Education" October 5-6, 2023, „Technical University" of Moldova (UTM).

2. „Scientific Conference of Doctoral Schools SCDS-UDJG Perspectives and challenges in doctoral research 11th Edition", „Dunarea de Jos" University of Galati, 8-9 of June 2023.

3. „Modern approaches of the environment-climate change interconnectivity, ENVIROCLIM 2" 2nd edition, September 20-23, 2023, Galați.

4. „6ᵗʰ Edition of International Conference on Chemical Engineering, ICCE," 05-07.10.2022, Iasi, Romania.

5. „A XXXVI-a Conferinţă Naţională De Chimie – CNChim", 2022, Călimăneşti – Căciulata, Romania.

6. „Young Researchers' International Conference on Chemistry and Chemical Engineering (YRICCCE III)", Cluj-Napoca, June 04 – 05, 2021.

7. „Scientific Conference of Doctoral Schools SCDS-UDJG 2021, The Ninth Edition," Galaţi, 10th-11th of June 2021.

8. „International Conference on Innovative Research EUROINVENT", 20-21 Mai 2021, Iasi.

9. „EurOAliment", 7-8 octombrie 2021, Galati.

10. „Symposium 'Ecology and Protection Of Ecosystems' The XIIIth Edition", 4–5 of November 2021 Bacau, Romania.

11. „Scientific Conference of Doctoral Schools-UDJG 2020 The Eighth Edition, Perspectives and challenges in doctoral research", Galaţi, 18th-19th of June 2020.

12. „Conferința Facultății de Chimie, IasiChem 2019", 31 octombrie - 01 noiembrie 2019.

13. „55èmes Rencontres Internationales de Chimie Thérapeutique", 2019, Nantes, France - July 3-5, 2019.

14. „The 2nd International Symposium on Catalysis and Specialty Chemicals ISCSC-2018", October 1-3, 2018; Tlemcen – Algeria.

15. „4th European Organic Chemistry congress", March 01-03, 2018, London, UK.

16. „4ème Colloque Franco-Roumain de Chimie Médicinale", 05-07 Octobre 2017, Universitatea Al. I. Cuza, Iași.

17. „Conferința Internațională AGRI-FOOD 2017, Agriculture and Food for the XXI century", 2017, Sibiu România.

18. „Conferința Școlii Doctorale 2017-Perspectives and challenges in doctoral research", Galaţi, 2017, România.

19. „ a 8-a ediţie a Simpozionului Internaţional Euroaliment 2017 – Mutatis mutandis in Food", Galaţi, România.

20. „Journées Scientifiques du Médicament Epigenetic: Toward New Therapeutic Targets "June 1st 2017, Grenoble, France.

21. „a 8-a ediţie a Conferinţei Molecular Modeling in Chemistry and Biochemistry", Cluj-Napoca, 2016.

SELECTED BIBLIOGRAPHY

Hao, W.; Liu, Y. C-H Bond Halogenation Catalyzed or Mediated by Copper: An Overview. *Beilstein J. Org. Chem.* **2015**, *11*, 2132–2144, doi:10.3762/bjoc.11.230.

Sadowski, B.; Klajn, J.; Gryko, D.T. Recent Advances in the Synthesis of Indolizines and Their π-Expanded Analogues. *Org. Biomol. Chem.* **2016**, *14*, 7804–7828, doi:10.1039/c6ob00985a.

Liao, Y.; Huang, B.; Huang, X.; Cai, M. Heterogeneous Copper-Catalyzed Cascade Three-Component Reaction Towards Imidazo[1,2-A]pyridines: Efficient and Practical One-Pot Synthesis of Alpidem. *ChemistrySelect* **2019**, *4*, 2320–2326, doi:10.1002/slct.201900128.

Munir, I.; Zahoor, A.F.; Rasool, N.; Naqvi, S.A.R.; Zia, K.M.; Ahmad, R. Synthetic Applications and Methodology Development of Chan–Lam Coupling: A Review. *Mol. Divers.* **2019**, *23*, 215–259, doi:10.1007/s11030-018-9870-z.

Verma, C.; Quraishi, M.A.; Ebenso, E.E. Microwave and Ultrasound Irradiations for the Synthesis of Environmentally Sustainable Corrosion Inhibitors: An Overview. *Sustain. Chem. Pharm.* **2018**, *10*, 134–147, doi:10.1016/j.scp.2018.11.001.

Dinică, R.; Furdui, B.; Bahrim, G.; Demeunynck, M. Précurseurs de Nouveaux Hétérocycles D`intéret Biologique. *Rev. Roum. Chim.* **2008**, *53*, 21–24.

Furdui, B.; Dinica, R.M.; Tabacaru, A.; Pettinari, C. Synthesis and Physico-Chemical Properties of a Novel Series of Aromatic Electron Acceptors Based on N-Heterocycles. *Tetrahedron* **2012**, *68*, 6164–6168, doi:10.1016/j.tet.2012.05.077.

Dinica, R.M.; Pettinari, C. Synthesis of Substituted 7,7'-bis-Indolizines via 1,3-Dipolar Cycloaddition under Microwave Irradiation. *Heterocycl. Commun.* **2001**, *7*, doi:10.1515/HC.2001.7.4.381.

Furdui, B.; Parfene, G.; Ghinea, I.O.; Dinica, R.M.; Bahrim, G.; Demeunynck, M. Synthesis and

in Vitro Antimicrobial Evaluation of New N-Heterocyclic Diquaternary Pyridinium Compounds. *Molecules* **2014**, *19*, 11572–11585, doi:10.3390/molecules190811572.

Dinica, R.M.; Druta, I.I.; Pettinari, C. The Synthesis of Substituted 7,7′-Bis-Indolizines via 1,3-Dipolar Cycloaddition under Microwave Irradiation. *Synlett* **2000**, *2000*, 1013–1015, doi:10.1055/s-2000-6657.

Vlahovici, A.; Druţa, I.; Andrei, M.; Cotlet, M.; Dinica, R. Photophysics of Some Indolizines, Derivatives from Bipyridyl, in Various Media. *J. Lumin.* **1999**, *82*, 155–162, doi:10.1016/S0022-2313(99)00027-7.

Bonte, S.; Ghinea, I.O.; Dinica, R.; Baussanne, I.; Demeunynck, M. Investigation of the Pyridinium Ylide-Alkyne Cycloaddition as a Fluorogenic Coupling Reaction. *Molecules* **2016**, *21*, 1–15, doi:10.3390/molecules21030332.

Furdui, B.; Dinica, R.; Druta, I.I.; Demeunynck, M. Improved Synthesis of Cationic Pyridinium-Substituted Indolizines. *Synthesis (Stuttg).* **2006**, 2640–2642, doi:10.1055/s-2006-942482.

Furdui, B.; Dinică, R.; Demeunynck, M.; Druţă, I.; Vlahovici, A. New Reactive Pyridinium-Indolizines Fluorophores. *Rev. Roum. Chim.* **2007**, *52*, 633–637.

Smith, B. *Infrared Spectral Interpretation*; 1st Edition; CRC Press: Boca Raton, **1998**; ISBN 9780203750841.

Coates, J. Interpretation of Infrared Spectra, A Practical Approach. In *Encyclopedia of Analytical Chemistry*; Meyers, R.A., Ed.; John Wiley& Sons Ltd: Chichester, **2000**; pp. 1–304 ISBN 9780203750841.

Jacobsen, N.E. Interpretation of Proton (1 H) NMR Spectra. In *NMR Spectroscopy Explained*; Wiley, **2007**; pp. 39–73 ISBN 9780470173350.

Jacobsen, N.E. Carbon-13 (13C) NMR Spectroscopy. In *NMR Spectroscopy Explained*; John Wiley & Sons, Ltd, **2007**; pp. 135–154 ISBN 9780470173350.

Balci, M. *Basic 1H- and 13C-NMR Spectroscopy*; Balci, M.B.T.-B. 1H-and 13C-N.S., Ed.; Elsevier: Amsterdam, 2005; ISBN 9780444518118.

Balci, M. 13C Chemical Shifts of Organic Compounds. In *Basic 1H- and 13C-NMR Spectroscopy*; Balci, M.B.T.-B. 1H-and 13C-N.S., Ed.; Elsevier: Amsterdam, **2005**; pp. 293–324 ISBN 978-0-444-51811-8.

Cârâc, A.; Boscencu, R.; Dinică, R.M.; Guerreiro, J.F.; Silva, F.; Marques, F.; Campello, M.P.C.; Moise, C.; Brîncoveanu, O.; Enăchescu, M.; et al. Synthesis, Characterization and Antitumor Activity of Two New Dipyridinium Ylide Based lanthanide(III) Complexes. *Inorganica Chim. Acta* **2018**, *480*, 83–90, doi:10.1016/j.ica.2018.05.003.

Druta, Ioan I.; Dinica, R.M.; Bacu, E.; Humelnicu, I. Synthesis of 7,7'-Bisindolizines by the Reaction of 4,4'-Bipyridinium-Ylides with Activated Alkynes. *Tetrahedron* **1998**, *54*, 10811–10818.

Silverstein, R.W.; Bassler, G.C. Spectrometric Identification of Organic Compounds. *J. Chem. Educ.* **1962**, *39*, 546–553, doi:10.1021/ed039p546.

Nakamoto, K. *Infrared and Raman Spectra of Inorganic and Coordination Compounds, Part B: Applications in Coordination, Organometallic, and Bioinorganic Chemistry*; John Wiley & Sons, **2009**; ISBN 0470405872.

Aljuhani, A.; Rezki, N.; Al-Sodies, S.; Messali, M.; Elshafei, G.M.S.; Hagar, M.; Aouad, M.R. Dicationic Bis-Pyridinium Hydrazone-Based Amphiphiles Encompassing Fluorinated Counteranions: Synthesis, Characterization, TGA-DSC, and DFT Investigations. *Molecules* **2022**, *27*, doi:10.3390/molecules27082492.

Naik, V.M.; Mallur, N.B. Synthesis and Characterization of lanthanide(III) Nitrate Complexes with Terdentate ONO Donor Hydrazone Derived from 2-Benzimidazolyl Mercaptoaceto Hydrazide and O-Hydroxy Aromatic Aldehyde. *E-Journal Chem.* **2011**, *8*, 1900–1910, doi:10.1155/2011/743948.

Liu, S.; Yang, L.W.; Rettig, S.J.; Orvig, C. Bulky Ortho 3-Methoxy Groups on N4O3 Amine Phenol Ligands Producing Six-Coordinate Bis(ligand)lanthanide Complex Cations [Ln(H3L)2]3+ (Ln = Pr, Gd; H3L = Tris(((2-Hydroxy-3-Methoxybenzyl)amino)ethyl)amine). *Inorg. Chem.* **1993**, *32*, 2773–2778, doi:10.1021/ic00064a031.

Dehnicke, K.; Greiner, A. Unusual Complex Chemistry of Rare-Earth Elements: Large Ionic Radii - Small Coordination Numbers. *Angew. Chemie - Int. Ed.* **2003**, *42*, 1340–1354, doi:10.1002/anie.200390346.

Cotton, S.A. Establishing Coordination Numbers for the Lanthanides in Simple Complexes. *Comptes Rendus Chim.* **2005**, *8*, 129–145, doi:10.1016/j.crci.2004.07.002.

Na, B.; Zhang, X.-J.; Shi, W.; Zhang, Y.-Q.; Wang, B.-W.; Gao, C.; Gao, S.; Cheng, P. Six-Coordinate Lanthanide Complexes: Slow Relaxation of Magnetization in the Dysprosium(III) Complex. *Chem. - A Eur. J.* **2014**, *20*, 15975–15980, doi:10.1002/chem.201404573.

Das, A.; Banik, B.K. *Microwave-Assisted Synthesis of N-Heterocycles*; Elsevier Inc., **2021**; ISBN 9780128228951.

Garella, D.; Borretto, E.; Di Stilo, A.; Martina, K.; Cravotto, G.; Cintas, P. Microwave-Assisted

Synthesis of N-Heterocycles in Medicinal Chemistry. *Medchemcomm* **2013**, *4*, 1323, doi:10.1039/c3md00152k.

Torres, E.; Ayala, M. Biocatalysis Based on Heme Peroxidases: Peroxidases as Potential Industrial Biocatalysts. *Biocatal. Based Heme Peroxidases Peroxidases as Potential Ind. Biocatal.* **2010**, 1–358, doi:10.1007/978-3-642-12627-7.

Eduardo, T.; Marcela, A. *Biocatalysis Based on Heme Peroxidases*; Torres, E., Ayala, M., Eds.; Springer Berlin Heidelberg: Berlin, Heidelberg, **2010**; Vol. 53; ISBN 978-3-642-12626-0.

Khanmohammadi, M.; Dastjerdi, M.B.; Ai, A.; Ahmadi, A.; Godarzi, A.; Rahimi, A.; Ai, J. Horseradish Peroxidase-Catalyzed Hydrogelation for Biomedical Applications. *Biomater. Sci.* **2018**, *6*, 1286–1298, doi:10.1039/c8bm00056e.

Guo, J.; Liu, Y.; Zha, J.; Han, H.; Chen, Y.; Jia, Z. Enhancing the Peroxidase-Mimicking Activity of Hemin by Covalent Immobilization in Polymer Nanogels. *Polym. Chem.* **2021**, *12*, 858–866, doi:10.1039/d0py01465f.

Botezatu (Dediu), A.V.; Horincar, G.; Ghinea, I.O.; Furdui, B.; Bahrim, G.-E.E.; Barbu, V.; Balanescu, F.; Favier, L.; Dinica, R.-M.M.; Botezatu, A.V.; et al. Whole-Cells of Yarrowia Lipolytica Applied in "one Pot" Indolizine Biosynthesis. *Catalysts* **2020**, *10*, 1–16, doi:10.3390/catal10060629.

Luo, Y.; Liang, J.; Zeng, G.; Chen, M.; Mo, D.; Li, G.; Zhang, D. Seed Germination Test for Toxicity Evaluation of Compost: Its Roles, Problems and Prospects. *Waste Manag.* **2018**, *71*, 109–114, doi:10.1016/j.wasman.2017.09.023.

Tiquia, S.M.; Tam, N.F.Y.; Hodgkiss, I.J. Effects of Composting on Phytotoxicity of Spent Pig-Manure Sawdust Litter. *Environ. Pollut.* **1996**, *93*, 249–256, doi:10.1016/S0269-7491(96)00052-8.

Li, R.; He, J.; Xie, H.; Wang, W.; Bose, S.K.; Sun, Y.; Hu, J.; Yin, H. Effects of Chitosan Nanoparticles on Seed Germination and Seedling Growth of Wheat (Triticum Aestivum L.). *Int. J. Biol. Macromol.* **2019**, *126*, 91–100, doi:10.1016/j.ijbiomac.2018.12.118.

Tabacaru, Aurel, A.V.D.B.; Horincar, G.; Furdui, B.; Dinica, R.M. Green Accelerated Synthesis , Antimicrobial Activity. *Molecules* **2019**.

Alptüzün, V.; Parlar, S.; Taşli, H.; Erciyas, E. Synthesis and Antimicrobial Activity of Some Pyridinium Salts. *Molecules* **2009**, *14*, 5203–5215, doi:10.3390/molecules14125203.

Liang, Z.; Zhu, M.; Yang, Y.W.; Gao, H. Antimicrobial Activities of Polymeric Quaternary Ammonium Salts from Poly(glycidyl Methacrylate)s. *Polym. Adv. Technol.* **2014**, *25*, 117–122, doi:10.1002/pat.3212.

Yamane, N.; Oiwa, T.; Kiyota, T.; Saitoh, H.; Sonoda, T.; Tosaka, M.; Nakashima, M.; Fukunaga, H.; Masaki, T.; Miyagawa, K. Multicenter Evaluation of a Colorimetric Microplate Antimycobacterial Susceptibility Test: Comparative Study with the NCCLS M24-P. *Rinsho Byori.* **1996**, *44*, 456–464.

Ol'Khovik, V.K.; Matveienko, Y. V.; Vasilevskii, D.A.; Kalechits, G. V.; Zheldakova, R.A. Synthesis, Antimicrobial and Antifungal Activity of Double Quaternary Ammonium Salts of Biphenyls. *Russ. J. Gen. Chem.* **2013**, *83*, 329–335, doi:10.1134/S1070363213020163.

Abate, G.; Aseffa, A.; Selassie, A.; Goshu, S.; Fekade, B.; WoldeMeskal, D.; Miörner, H. Direct Colorimetric Assay for Rapid Detection of Rifampin-Resistant Mycobacterium Tuberculosis. *J. Clin. Microbiol.* **2004**, *42*, 871–873, doi:10.1128/JCM.42.2.871-873.2004.

Moussa, S.H.; Tayel, A.A.; Al-Hassan, A.A.; Farouk, A. Tetrazolium/Formazan Test as an Efficient Method to Determine Fungal Chitosan Antimicrobial Activity. *J. Mycol.* **2013**, *2013*, 1–7, doi:10.1155/2013/753692.

Klančnik, A.; Piskernik, S.; Jeršek, B.; Možina, S.S. Evaluation of Diffusion and Dilution Methods to Determine the Antibacterial Activity of Plant Extracts. *J. Microbiol. Methods* **2010**, *81*, 121–126, doi:10.1016/j.mimet.2010.02.004.

Altman, F.P. *Tetrazolium Salts and Formazans*; Gustav Fischer Verlag · Stuttgart, **1976**; Vol. 9; ISBN 3437104535.

Thom, S.M.; Horobin, R.W.; Seidler, E.; Barer, M.R. Factors Affecting the Selection and Use of Tetrazolium Salts as Cytochemical Indicators of Microbial Viability and Activity. *J. Appl. Bacteriol.* **1993**, *74*, 433–443, doi:10.1111/j.1365-2672.1993.tb05151.x.

Caviedes, L.; Delgado, J.; Gilman, R.H. Tetrazolium Microplate Assay as a Rapid and Inexpensive Colorimetric Method for Determination of Antibiotic Susceptibility of Mycobacterium Tuberculosis. *J. Clin. Microbiol.* **2002**, *40*, 1873–1874, doi:10.1128/JCM.40.5.1873-1874.2002.

Chanawanno, K.; Thuptimdang, P.; Chantrapromma, S.; Fun, H.-K. New Tunable Pyridinium Benzenesulfonate Amphiphiles as Anti-MRSA Quaternary Ammonium Compounds (QACs). *J. Mol. Struct.* **2022**, *1254*, 132389, doi:https://doi.org/10.1016/j.molstruc.2022.132389.

Li, L.; Zhao, Y.; Zhou, H.; Ning, A.; Zhang, F.; Zhao (Kent), Z. Synthesis of Pyridinium N-Chloramines for Antibacterial Applications. *Tetrahedron Lett.* **2017**, *58*, 321–325, doi:10.1016/j.tetlet.2016.12.021.

Ezelarab, H.A.A.A.; Abbas, S.H.; Abourehab, M.A.S.S.; Badr, M.; Sureram, S.; Hongmanee, P.; Kittakoop, P.; Abuo-Rahma, G.E.-D.D.A.; Hassan, H.A. Novel Antimicrobial Ciprofloxacin-Pyridinium

Quaternary Ammonium Salts with Improved Physicochemical Properties and DNA Gyrase Inhibitory Activity. *Med. Chem. Res.* **2021**, *30*, 2168–2183, doi:10.1007/s00044-021-02798-3.

Mundhe, P.; Kidwai, S.; Saini, S.M.; Singh, H.R.; Singh, R.; Chandrashekharappa, S. Design, Synthesis, Characterization, and Anti-Tubercular Activity of Novel Ethyl-3-Benzoyl-6, 8-Difluoroindolizine-1-Carboxylate Analogues: Molecular Target Identification and Molecular Docking Studies. *J. Mol. Struct.* **2023**, *1284*, 135359, doi:10.1016/j.molstruc.2023.135359.

Gilbert, P.; Al-taae, A. Antimicrobial Activity of Some Alkyltrimethylammonium Bromides. *Lett. Appl. Microbiol.* **1985**, *1*, 101–104, doi:10.1111/j.1472-765X.1985.tb01498.x.

Vereshchagin, A.N.; Gordeeva, A.M.; Frolov, N.A.; Proshin, P.I.; Hansford, K.A.; Egorov, M.P. Synthesis and Microbiological Properties of Novel Bis-Quaternary Ammonium Compounds Based on Biphenyl Spacer. *European J. Org. Chem.* **2019**, *2019*, 4123–4127, doi:10.1002/ejoc.201900319.

Gupta, D.; Bhatia, D.; Dave, V.; Sutariya, V.; Gupta, S.V. Salts of Therapeutic Agents: Chemical, Physicochemical, and Biological Considerations. *Molecules* **2018**, *23*, 1–15, doi:10.3390/molecules23071719.

Lenoir, S.; Pagnoulle, C.; Detrembleur, C.; Galleni, M.; Jérôme, R. New Antibacterial Cationic Surfactants Prepared by Atom Transfer Radical Polymerization. *J. Polym. Sci. Part A Polym. Chem.* **2006**, *44*, 1214–1224, doi:10.1002/pola.21229.

Mohammed, M.; Tahar, B.; Aïcha, D.; Eddine, H.D. Antibacterial Activity of Quaternary Ammonium Salt from Diethylaminoethyl Methacrylate. *E-Journal Chem.* **2010**, *7*, 61–67, doi:10.1155/2010/637549.

Marini, M.; Bondi, M.; Iseppi, R.; Toselli, M.; Pilati, F. Preparation and Antibacterial Activity of Hybrid Materials Containing Quaternary Ammonium Salts via Sol-Gel Process. *Eur. Polym. J.* **2007**, *43*, 3621–3628, doi:10.1016/j.eurpolymj.2007.06.002.

Luo, M.; Zhou, L.; Huang, Z.; Li, B.; Nice, E.C.; Xu, J.; Huang, C. Antioxidant Therapy in Cancer: Rationale and Progress. *Antioxidants* **2022**, *11*, 1–19, doi:10.3390/antiox11061128.

Gilgun-Sherki, Y.; Melamed, E.; Offen, D. Oxidative Stress Induced-Neurodegenerative Diseases: The Need for Antioxidants That Penetrate the Blood Brain Barrier. *Neuropharmacology* **2001**, *40*, 959–975, doi:10.1016/S0028-3908(01)00019-3.

Kim, T.Y.; Leem, E.; Lee, J.M.; Kim, S.R. Control of Reactive Oxygen Species for the Prevention of Parkinson's Disease: The Possible Application of Flavonoids. *Antioxidants* **2020**, *9*, 1–28, doi:10.3390/antiox9070583.

Mendiratta, M.; Gupta, S. Exploring the Role of Phytochemicals and Antioxidants on Antihyperglycemic Potentials of Indian Medicinal Plants. **2017**.

Gulcin, İ. *Antioxidants and Antioxidant Methods: An Updated Overview*; **2020**; Vol. 94; ISBN 0123456789.

Dontha, S. A Review on Antioxidant Methods. *Asian J. Pharm. Clin. Res.* **2016**, *9*, 14–32, doi:10.22159/ajpcr.2016.v9s2.13092.

Lauridsen, C. From Oxidative Stress to Inflammation: Redox Balance and Immune System. *Poult. Sci.* **2019**, *98*, 4240–4246, doi:10.3382/ps/pey407.

Tsuji, A. Small Molecular Drug Transfer across the Blood-Brain Barrier via Carrier-Mediated Transport Systems. *NeuroRx* **2005**, *2*, 54–62, doi:10.1602/neurorx.2.1.54.

Al-Sodies, S.; Rezki, N.; Albelwi, F.F.; Messali, M.; Aouad, M.R.; Bardaweel, S.K.; Hagar, M. Novel Dipyridinium Lipophile-Based Ionic Liquids Tethering Hydrazone Linkage: Design, Synthesis and Antitumorigenic Study. *Int. J. Mol. Sci.* **2021**, *22*, 10487, doi:10.3390/ijms221910487.

Wang, Z.M.; Lin, H.K.; Zhu, S.R.; Liu, T.F.; Chen, Y.T. Spectroscopy, Cytotoxicity and DNA-Binding of the lanthanum(III) Complex of an L-Valine Derivative of 1,10-Phenanthroline. *J. Inorg. Biochem.* **2002**, *89*, 97–106, doi:10.1016/S0162-0134(01)00395-6.

Tai, S.; Sun, Y.; Squires, J.M.; Zhang, H.; Oh, W.K.; Liang, C.Z.; Huang, J. PC3 Is a Cell Line Characteristic of Prostatic Small Cell Carcinoma. *Prostate* **2011**, *71*, 1668–1679, doi:10.1002/pros.21383.

Mittler, F.; Obeïd, P.; Rulina, A. V.; Haguet, V.; Gidrol, X.; Balakirev, M.Y. High-Content Monitoring of Drug Effects in a 3D Spheroid Model. *Front. Oncol.* **2017**, *7*, doi:10.3389/fonc.2017.00293.

Marullo, R.; Werner, E.; Degtyareva, N.; Moore, B.; Altavilla, G.; Ramalingam, S.S.; Doetsch, P.W. Cisplatin Induces a Mitochondrial-Ros Response That Contributes to Cytotoxicity Depending on Mitochondrial Redox Status and Bioenergetic Functions. *PLoS One* **2013**, *8*, 1–15, doi:10.1371/journal.pone.0081162.

McIlwain, D.R.; Berger, T.; Mak, T.W. Caspase Functions in Cell Death and Disease. *Cold Spring Harb. Perspect. Biol.* **2015**, *7*, doi:10.1101/cshperspect.a026716.

Brentnall, M.; Rodriguez-Menocal, L.; De Guevara, R.L.; Cepero, E.; Boise, L.H. Caspase-9, Caspase-3 and Caspase-7 Have Distinct Roles during Intrinsic Apoptosis. *BMC Cell Biol.* **2013**, *14*, doi:10.1186/1471-2121-14-32.

Ellman, G.L.; Courtney, K.D.; Andres, V.; Featherstone, R.M. A New and Rapid Colorimetric

Determination of Acetylcholinesterase Activity. *Biochem. Pharmacol.* **1961**, *7*, 88–95, doi:10.1016/0006-2952(61)90145-9.

Kapková, P.; Alptüzün, V.; Frey, P.; Erciyas, E.; Holzgrabe, U. Search for Dual Function Inhibitors for Alzheimer's Disease: Synthesis and Biological Activity of Acetylcholinesterase Inhibitors of Pyridinium-Type and Their Aβ Fibril Formation Inhibition Capacity. *Bioorganic Med. Chem.* **2006**, *14*, 472–478, doi:10.1016/j.bmc.2005.08.034.

Goux, W.J.; Kopplin, L.; Nguyen, A.D.; Leak, K.; Rutkofsky, M.; Shanmuganandam, V.D.; Sharma, D.; Inouye, H.; Kirschner, D.A. The Formation of Straight and Twisted Filaments from Short Tau Peptides. *J. Biol. Chem.* **2004**, *279*, 26868–26875, doi:10.1074/jbc.M402379200.

Lunven, L.; Bonnet, H.; Yahiaoui, S.; Yi, W.; Da Costa, L.; Peuchmaur, M.; Boumendjel, A.; Chierici, S. Disruption of Fibers from the Tau Model AcPHF6 by Naturally Occurring Aurones and Synthetic Analogues. *ACS Chem. Neurosci.* **2016**, *7*, 995–1003, doi:10.1021/acschemneuro.6b00102.

Gade Malmos, K.; Blancas-Mejia, L.M.; Weber, B.; Buchner, J.; Ramirez-Alvarado, M.; Naiki, H.; Otzen, D. ThT 101: A Primer on the Use of Thioflavin T to Investigate Amyloid Formation. *Amyloid* **2017**, *24*, 1–16, doi:10.1080/13506129.2017.1304905.